



Paszkowski, M., Budzyń, B., Mazur, S., Sláma, J., Shumlyanskyy, L., Środoń, J., Dhuime, B., Kędzior, A., Liivamägi, S., & Pisarzowska, A. (2019). Detrital zircon U-Pb and Hf constraints on provenance and timing of deposition of the Mesoproterozoic to Cambrian sedimentary cover of the East European Craton, Belarus. *Precambrian Research*, 331, [105352]. <https://doi.org/10.1016/j.precamres.2019.105352>

Peer reviewed version

License (if available):
CC BY-NC-ND

Link to published version (if available):
[10.1016/j.precamres.2019.105352](https://doi.org/10.1016/j.precamres.2019.105352)

[Link to publication record in Explore Bristol Research](#)
PDF-document

This is the accepted author manuscript (AAM). The final published version (version of record) is available online via Elsevier at <https://doi.org/10.1016/j.precamres.2019.105352>. Please refer to any applicable terms of use of the publisher.

University of Bristol - Explore Bristol Research

General rights

This document is made available in accordance with publisher policies. Please cite only the published version using the reference above. Full terms of use are available:
<http://www.bristol.ac.uk/red/research-policy/pure/user-guides/ebr-terms/>

Detrital zircon U-Pb and Hf constraints on provenance and timing of deposition of the Mesoproterozoic to Cambrian sedimentary cover of the East European Craton, Belarus

Mariusz Paszkowski^{1,*}, Bartosz Budzyń^{1,*}, Stanisław Mazur¹, Jiří Sláma², Leonid Shumlyanskyy^{3,4}, Jan Środoń¹, Bruno Dhuime^{5,6}, Artur Kędzior¹, Sirle Liivamägi¹, Agnieszka Pisarzowska^{1,7}

¹ *Institute of Geological Sciences, Polish Academy of Sciences (ING PAN), Research Centre in Kraków, Senacka 1, PL–31002 Kraków, Poland*

² *The Czech Academy of Sciences, Institute of Geology, Rozvojová 269, Prague 6 16500, Czech Republic*

³ *M.P. Semenenko Institute of Geochemistry, Mineralogy and Ore Formation, Palladina ave., 34, 03142, Kyiv, Ukraine*

⁴ *School of Earth and Planetary Sciences, Curtin University, Perth, GPO Box U1987, WA 6845, Australia*

⁵ *Bristol Isotope Group, School of Earth Sciences, University of Bristol, Wills Memorial Building, Queen's Road, Bristol BS8 1RJ, UK*

⁶ *CNRS-UMR5243, Géosciences Montpellier, Université de Montpellier, 34095 Montpellier Cedex 05, France*

⁷ *Faculty of Earth Sciences, University of Silesia, Będzińska 60, 41-200, Sosnowiec, Poland*

* Corresponding authors e-mails: ndpaszko@cyf-kr.edu.pl, ndbudzyn@cyf-kr.edu.pl

Abstract

The sedimentary cover of the East European Craton (EEC) is unique because of its low degree of diagenetic alteration that allows preservation of the original “source to sink” relationships. The present study provides U-Pb and Hf zircon data for the entire Proterozoic sedimentary section of the EEC based on samples from five boreholes in Belarus within the Volyn-Orsha Basin, one of the most important sedimentary basins of the craton. Twenty-one samples of mudstones and sandstones were selected for detrital zircon U-Pb geochronology, supplemented by the Hf isotope analyses of zircons from 6 samples representing different U-

Pb age spectra and bulk rock XRD mineralogy of all mudstone samples collected from the studied boreholes. Five clastic successions in the Volyn-Orsha Basin are characterized by different sources of detrital material: (1) The Mesoproterozoic Pinsk Suite with a narrow population of c. 2.0 Ga zircons, (2) The Orsha Suite with a broad 1.3–3.2 Ga zircon age distribution, (3) Glacial sediments of the Vilchitsy Series with an age spectra similar to the Orsha Suite, except for a c. 1.0 and 1.2 Ga cluster, (4) The Volyn and Valdai Series, including lowermost Cambrian, with a narrow trimodal population of 0.5, 1.5, and 1.8 Ga zircons, and (5) lower Cambrian (?) sediments with a diffused zircon age spectrum, including a 500–700 Ma cluster. Maximum depositional ages were constrained for the Vilchitsy Series at 977 ± 6 Ma and for the Volyn Series at $579\text{--}545 \pm 4$ Ma. Combined Hf zircon data indicate four episodes of new continental crust generation at 3.3, 2.8, 2.1–2.3 and 1.8 Ga, suggestive of source terrains within the crust of the present-day EEC. These sources experienced subsequent reworking of crust at c. 1.8 Ga and 550–600 Ma. Only a lower Cambrian sample lacks any trend or clustering within the Hf data probably due to mixing of zircons from exotic and local sources. Paleogeographic models, explaining these provenance signals, in terms of intracratonic erosion and sediment transport until to the beginning of Cambrian are presented.

Key-words: Baltica, Ediacaran, Hf isotopes, maximum depositional ages, Rodinia, zircon geochronology

1. Introduction

The East European Craton (EEC) is the coherent mass of the Precambrian continental crust that occupies the north-eastern half of the present-day European continent (Fig. 1). The EEC was assembled at c. 1.8–1.7 Ga through multiple terrane collisions and it has never been dismembered since then (Bogdanova et al., 1996, 2008). The sedimentary cover of the major

part of the EEC is unique because of its low degree of diagenetic alteration (Goryl et al., 2018; Liivamägi et al., 2018; Pehr et al., 2018) that assures preservation of the original sediment characteristics, indicative of the paleoenvironment and life on the planet at this fundamental evolutionary event. Having been deposited on a stable craton, the Precambrian sediments of the EEC keep record of the “source to sink” relationships from the time preceding the Ediacaran fragmentation of the Rodinia supercontinent.

The Proterozoic sedimentary cover of the EEC has been extensively drilled and studied since the 1950’s when detailed lithological descriptions, petrographic observations and lithostratigraphic subdivisions of the sedimentary sequence were established (review in Makhnach et al., 2001). More recently the Neoproterozoic flood basalt ages were constrained by zircon U-Pb dating (Shumlyanskyy et al., 2016 and references therein). The youngest, post-eruptive sediments are widespread on the craton (Russia, Baltic States, Belarus, Ukraine, Moldova and Poland; Rozanov and Łydka, 1987), whereas older sediments are preserved only locally, mostly in Belarus and Russia. Their ages remain unconstrained by biostratigraphy due to the absence of fossils. U-Pb geochronological constraints are also lacking in Belarus.

In this contribution, a provenance study for the entire Proterozoic sedimentary column of the EEC was undertaken, using samples from five boreholes in Belarus, selected to represent the main sedimentary basin on the craton (Figs. 1, 2). The U-Pb geochronology of detrital zircon was supplemented by Hf isotope analysis of representative zircon groups and the bulk rock XRD mineralogy of the host rocks. Such a combined analytical approach is aimed at constraining changes in provenance and sources of sediments, particularly at the time of Rodinia break-up and the birth of Baltica, during the Ediacaran/Cambrian transition (e.g.,

Torsvik et al., 1992, 1996). In addition to the provenance information, the U-Pb zircon data is used to constrain maximum depositional ages, which offers a potentially more accurate age determination compared to the previously used general lithostratigraphy and acritarch-based biostratigraphy (Makhnach et al., 2001).

2. Geological background

2.1. Crystalline basement

The main lithotectonic units of the crystalline basement of Belarus are composed of medium- to high-grade metamorphic rocks of Paleoproterozoic age (Bogdanova et al., 2001; Claesson et al., 2001; Shumlyanskyy, 2014). They run NE–SW, parallel to the c. 1.8 Ga old tectonic suture between Sarmatia and Fennoscandia (Elming et al., 1998; Bogdanova et al., 2008; Lubnina et al., 2009) (Fig. 1a). The crystalline basement of Belarus on both sides of the suture was already deeply eroded and peneplained by the end of Paleoproterozoic. However, subsequent differentiated subsidence produced the Volyn-Orsha Aulacogen and Prypyat Trough, prominent cratonic basins reaching several kilometres in depth (e.g., Bogdanova et al., 2008).

2.2. Volcano-sedimentary cover

The volcano-sedimentary cover in Belarus (Fig. 1a) includes a large variety of lithostratigraphic units ranging in age from Mesoproterozoic to recent and are variable in the extent and thickness – from a few dozens of meters on the domal uplifts up to several kilometres in the cratonic basins, aulacogens, and troughs (Makhnach et al., 2001). The lithostratigraphic subdivision of the pre-Ordovician rocks used in this study (Figs. 2, 3) and their description below was compiled from data published by Chumakov and Semikhatov

(1981), Rundqvist and Mitrofanov (1993), Makhnach et al. (2005) and Paczeńska (2010), including their stratigraphic age assignments (Fig. 3).

2.2.1. Belarus Series

The oldest rocks studied belong to the Belarus Series that fills the Volyn-Orsha Aulacogen (Fig. 1) and is subdivided into the Rogachev, Pinsk, Orsha and Lapichi Suites (Fig. 3). The weighted average $^{207}\text{Pb}/^{206}\text{Pb}$ age of the youngest group of detrital zircons found in the Polissya Series (Ukrainian equivalent of the Belarus Series) defines a maximum depositional age of 1228 ± 15 Ma (Shumlyanskyy et al., 2015). This age is older than previously obtained mica and feldspar K-Ar ages of 700–815 Ma and K-Ar whole-rock ages of 880–980 Ma (Makhnach et al., 1976; Chebanenko et al., 1990) as well as whole-rock K-Ar age of 1055 Ma by Nechaev (1974).

The Pinsk Suite in the study area (Fig. 3) rests unconformably on Paleoproterozoic crystalline basement and reaches 460 m in thickness. It is mainly composed of fine-grained sandstones/coarse-grained siltstones with interbeds of oligomictic to mesomictic medium-grained sandstones (quartz arenites are minor component), argillaceous siltstones and clays. Rocks are weakly to moderately cemented by either clay minerals or rarely by dolomite. The sediments are generally variegated, reddish with abundant reduction greyish spots, bands, and interlayers. The sedimentary sequence is characterized by the rhythmic appearance of fining upward sequences, each starting with an erosional surface.

The Orsha Suite with a well-developed basal horizon reaches 620 m in thickness and overlies the eroded surface of the Pinsk Suite or, in peripheral areas of the Volyn-Orsha linear depocenter, rests directly on the Paleoproterozoic crystalline basement. The Orsha Suite is

composed of predominantly red-coloured, loose, quartz arenites of well-rounded and well-sorted framework with finely dispersed kaolinite. In the top part of the unit, quartz-cemented sediments occur. Siltstones and argillites are rare. The sediments are usually horizontally or cross-bedded. The Orsha Suite does not contain any organic remnants or trace fossils and its monotonous composition makes correlations difficult.

The Lapichi Suite is absent from the studied wells (Fig. 2), but elsewhere it reaches 82 m in thickness (Fig. 3) and occurs only locally in central Belarus. This unit is represented mainly by mesomictic to oligomictic sandstones, siltstones, clays, dolomites, syngenetic dolomitic breccias, rarely conglomerates. The rocks are red and variably coloured. The dolomites form 0.4 to 3 m thick beds of chemical and organic (microphytolitic and stromatolitic) origin (Makhnach et al., 2001).

2.2.2. *Vilchitsy Series*

The Vilchitsy Series sediments are present mainly within the Volyn-Orsha Aulacogen, although small outliers are also known from the adjacent areas (Ukrainian Brody Suite). The Vilchitsy Series is up to 728 m thick terrigenous succession composed of tillites (unsorted massive argillites-siltstones-sandstones with dispersed fine sand to pebble-sized clasts), sandstones, fine-bedded argillites-siltstones and clays. Sandstones and sands are mainly poorly sorted, oligomictic, often cross-bedded, whereas siltstones and clays are horizontally laminated (varved clays) and contain numerous larger clasts.

In the southern part of the Orsha Basin the Vilchitsy Series is subdivided into two terrigenous suites (Fig. 3): (i) lower – the Blon Suite, interpreted as moraine sediments comprising local material, dominated by Orsha quartz arenite erratics, with a very small proportion of exotic

rocks, and (ii) the regionally more extensive Glusk Suite containing 3–4 tillite beds with a thickness of 26–64 m each, alternated with the horizons of sandstones, siltstones, and clays. The Vilchitsy Series is classified as Vendian, but its precise age is unknown (Chumakov, 2015). According to Chumakov (2010), the first (Blon) and second (Glusk) glacial levels of the Vilchitsy Series/Lapland Horizon probably correspond to the global Marinoan and Gaskiers glacial event, respectively.

2.2.3. *Ediacaran Volyn Series*

The Volyn Series sediments cover most of Belarus, also extending into western Ukraine (upper Drevlyane Horizon), eastern Poland (Sławatycze Series) and Lithuania (Merkys Formation). In the south-western Belarus, the thickness of the Volyn Series reaches 300–440 m, but it does not exceed 100 m in other parts of the country. In Belarus, the Volyn Series is subdivided into three suites (Fig. 3).

The lower, *Gorbashi Suite*, 6 to 30 m thick, occurs in north-western Ukraine and south-western Belarus. This unit of predominantly red colour is composed of unevenly-grained and coarse-grained sandstones with interlayers of pebble-sized conglomerates and rarely siltstones. Dating of detrital zircons isolated from conglomerate matrix revealed the presence of a single population of 1422 ± 19 Ma igneous zircons (Shumlyanskyy et al., 2015).

The Rataychitsy Suite and its local equivalents (Lukomsk and Kletsk; Fig. 3) occur as a sequence of volcanic and volcano-sedimentary rocks termed “Volyn flood basalt province” (VFBP; Kuzmenkova et al., 2011; Shumlyanskyy, 2012; Shumlyanskyy et al., 2016). These rocks are widely distributed in Belarus with a maximum thickness of 340 m in the Brest Basin, and decreasing to 100 m elsewhere proportionally to the distance from the area of

volcanic activity. While volcanic rocks (basalts and tuffs with locally occurring felsic volcanic rocks) prevail in the Brest Basin, pyroclastic rocks occur in the surrounding NE areas, passing into terrigenous sediments with an admixture of ash in distal areas. According to Shumlyanskyy et al. (2016), volcanic rocks of the VFBP were emplaced at 573 ± 14 Ma (lower basalts) and 571 ± 13 Ma (rhyolitic dacite), while Compston et al. (1995) dated tuff from SE Poland at 551 ± 4 Ma.

The Rataychitsy Suite is overlaid by the *Girsk Suite* (Brest Basin) or *Lyožno Suite* (Orsha Basin) and *Vidibor Suite* (Pripyat Trough, Eastern part of the Polissya Saddle). The Girsk Suite is composed of red-coloured uneven-grained arkoses and polymictic sandstones with numerous interlayers of pebble-sized conglomerates, and argillaceous siltstones. The rocks contain abundant volcanomictic and pyroclastic material. The coarse-grained sediments are cemented by clay minerals, often with admixture of iron oxides and hydroxides or ferrous dolomite. The Lyožno Suite is composed of grey-coloured finer sediments (clays, argillaceous siltstones) with interlayers and lenses of arkosic sandstones in the lower part of the succession.

2.2.4. *Ediacaran Valdai Series*

The Valdai Series transgressively overlays the older sedimentary rocks and crystalline basement. In NE Belarus it occurs as extensive cover, whereas in SW Belarus it is limited to isolated areas. The Valdai Series is composed of terrigenous deposits that occur as four large sedimentary cycles: the Nizov, Selsk, and Tshernitse Suites, collectively defined as the Redkino Horizon, and the youngest Kotlin Suite (Fig. 3).

The Redkino Horizon is up to 168 m thick. The lower part of each sedimentary cycle starts with unevenly-grained sandstones and conglomerates, passing upwards into arkosic medium-fine-grained sandstones with argillaceous and dolomitic cement of interstitial and basal types. To the top, they grade to heteroliths (interbedded sandstones and siltstones), and then into thin-layered micaceous and argillaceous siltstones and argillites. The Nizov Suite is enriched in volcanic material, probably derived from the underlying Volyn Series. The Selsk Suite contains a horizon of brown argillites. The upper part of this suite also contains a horizon of grey argillaceous siltstones enriched in organic matter. The Tshernitse Suite is enriched in thin laminae of heavy minerals. The transition to overlying Kotlin Suite is gradual and the subdivision is based on biostratigraphy.

The Kotlin Suite is characterised by highly variable thickness from a maximum of 220 m in the Orsha Basin to 50–140 m elsewhere. In the Orsha Basin, the Kotlin Suite shows clear tripartition being dominated by sand, argillaceous siltstones and clay in the lower, middle and upper part, respectively. In the western part of Belarus, the domination of coarse-grained terrigenous deposits with argillaceous siltstone interbeds is explained by the facial variability in the marginal parts of the basin and/or deep erosion that left only the lower, coarse-grained basal part of the suite with the total present thickness of 10–100 m.

2.2.5. Cambrian sediments

The thickness of lower and middle Cambrian sediments varies from more than 520 m in the southwest part of Belarus to 160 m (only lower Cambrian) in the northwest part. Cambrian rocks comprise clays, siltstones, and sandstones relatively poor in organic remains. The amount of fine-grained sediments (clays) gradually increases upward in the section and westwards, in the direction of deeper parts of the Cambrian sedimentary basin. Cambrian

sediments overlie the Ediacaran rocks with an unconformity that is consistent with biostratigraphic data.

3. Sample selection and analytical methods

Quantitative XRD analyses of bulk rocks is an independent source of information to characterise provenance. Such analyses were performed on all mudstone samples collected from the boreholes. The XRD patterns of random samples, wet-ground with ZnO internal standard to assure high reproducibility of intensities (Środoń et al., 2001), were recorded in 5–65 °2 θ range with 0.02 °2 θ step on Xtra diffractometer, equipped with Cu tube and solid-state detector. After mineral identification, quantitative mineral analysis was performed using in-house Q-Min software (M. Szczerba, unpublished).

Twenty-one samples of mudstones and sandstones from five boreholes in Belarus were selected for zircon geochronology (Fig. 2; Table 1). Analytical strategy included selecting c. 40 most euhedral grains with sharp edges (named group A) and c. 100 grains representing random detrital population for provenance analysis (named group B). Maximum depositional ages were calculated using from 2 to 5 youngest zircons following Dickinson and Gehrels (2009). These are presented as concordia ages calculated from the youngest zircons with <2.0% discordance. The Pb/U and Pb isotopic ratios in zircons were measured using a Thermo Scientific Element 2 sector field ICP-MS coupled to a 193 nm ArF excimer laser (Teledyne Cetac Analyte Excite laser) at the Institute of Geology of the Czech Academy of Sciences, Prague, Czech Republic. Analytical details are presented in Supplementary Data (SD1 and SD2).

Hf isotopes were measured in zircons from 6 selected samples representing different U-Pb age spectra in order to shed more light on their provenance. The analyses were performed at the University of Bristol (Bristol Isotope Group) using a ThermoFinnigan Neptune plus multicollector inductively-coupled plasma mass spectrometer (MC-ICP-MS) coupled with a Photon-Machine Analyte G2 Excimer laser (193 nm wavelength). The new crust evolution curve of Dhuime et al. (2011) and chondritic values from Bouvier et al. (2008) were used for model age and initial ϵ_{Hf} calculations. See Supplementary Data (SD1 and SD3) for more details.

4. Results

4.1. Mineral composition

The largest difference in mineral composition was observed between pre-Volyn, Volyn and post-Volyn Series rocks. The pre-Volyn rocks contain >60% quartz, while the fraction of quartz in the sum of primary minerals exceeds 70% and plagioclase is lacking (Table S1; Fig. 4). Orthoclase and microcline, if present, occur in similar proportions (ratio of 0.7–1.4) and micas are minor components. The Orsha Suite differs from the rest of the pre-Volyn Series by extremely mature composition, exclusively quartz, kaolinite and hematite.

The Volyn Series is characterized by a quartz content <25% (38–48% of primary minerals), very high orthoclase/microcline ratio (3–10), high hematite and dioctahedral 2:1 clays, the presence of specific basaltic minerals (calcic plagioclase, occasionally pyroxene, zeolites, saponite, chlorite or mixed layer chlorite-smectite), trioctahedral mica, and the lack of muscovite. The lower part of the Volyn Series in the Vilchitsy borehole, some Volyn samples in the Pinsk borehole and the central part of the Volyn Series in the Kobryn borehole lack microcline, trioctahedral mica and kaolinite, which identifies pure, unweathered volcanic

material (tuffs in the Vilchitsy and Pinsk boreholes, tuffs and basalts in the Kobryn borehole). Tuffs differ from basalts by the much higher quartz and K-feldspar content and lack of pyroxene. Non-stoichiometric dolomite is characteristic of the Volyn Series.

Above the Volyn Series the mineral composition is different (Fig. 4): the low quartz content is slowly increasing, the high orthoclase/microcline ratio is preserved (except of the Kobryn borehole), hematite and the specific basaltic minerals are decreasing abruptly, while $2M_1$ mica and the sum of authigenic minerals are increasing. Na-plagioclase, trioctahedral mica and kaolinite reach the maximum values in Redkino and they are decreasing in the younger rocks, while the dioctahedral 2:1 clays increase from the Redkino minimum. Among authigenic minerals, berthierine and apatite exceed 3% from the Volyn Series to Cambrian, while siderite and dolomite are only present in the Kotlin Suite and in the Cambrian rocks.

4.2. LA-ICP-MS U-Pb zircon geochronology

The majority of zircon crystals of the group A in each sample have oscillatory zoning with some crystals containing euhedral inherited cores (Fig. 5). Homogeneous and patchy zoned crystals are less common. Zircons of the group B are predominantly oscillatory zoned with minor crystals having patchy or complex zoning. The Th/U ratio in the majority of the analysed zircon grains is well above 0.1 (mostly between c. 0.1–4.3) indicating that zircons probably crystallized in magmatic rocks (Hoskin and Black, 2000; Kelly and Harley, 2005; Rubatto, 2017). Because of the large amount of data, the following section presents U-Pb results for both A and B groups together. Inclusion of the euhedral population does not affect data presentation, i.e. there is no significant shift towards younger ages, except for a few samples (see discussion below). U-Pb data are filtered to remove analyses that are >10%

discordant. A full set of analytical results is provided in Table S2. Additional details concerning U-Pb results for groups A and B are presented in Supplementary Data (SD4).

4.2.1. Pre-Volyn rocks

The zircons from the Vilch-2 and Vilch-4 samples representing the Pinsk Suite (Figs. 2, 3) are dominated by Paleoproterozoic c. 2.00 Ga zircons (minor populations at 1.70–1.80 Ga and 2.10–2.15 Ga for Vilch-2; 1.75–1.84 Ga and 2.10 Ga for Vilch-4; Fig. 6), and contain several Archean grains (up to c. 2.90 Ga). Both samples are characterised, in contrast to all other analysed samples, by the limited proportion of euhedral grains. Concerning the latter along with uncertain geological significance of a few younger ages (c. 588 Ma, 980 Ma and 617 Ma, 954 Ma), a maximum depositional age for the Pinsk Suite is not calculated.

In contrast to the Pinsk Suite, samples from the Orsha Suite and Vilchitsy Series bear record of multiple events. Zircons from the Vilch-5B (Orsha Suite) yielded U-Pb ages nearly continuously distributed between 1.29 and 3.19 Ga with local maxima at 1.80 Ga, 1.90 Ga, 2.10 Ga and a dominant peak at 2.00 Ga (Fig. 6). The tillite samples Vilch-6A and Vilch-7A (Vilchitsy Series) contain zircons with U-Pb ages nearly continuously ranging from c. 941 Ma to 2.15 Ga with dominant age peaks at 2.00 Ga for the Vilch-6A, and 945 Ma to 2.20 Ga for the Vilch-7A. In all samples from the Orsha Suite and Vilchitsy Series a few Archean ages up to c. 3.20 Ga were identified. The maximum depositional ages of 977 ± 6 Ma ($n = 2$, MSWD = 1.12) and 1056 ± 4 Ma ($n = 4$; MSWD = 1.9) have been constrained for samples Vilch-6A and Vilch-7A, respectively.

4.2.2. Volyn rocks

The Volyn Series rocks are represented by three samples of the Rataychitsy Suite (lower part of the Volyn Series) and four samples of the Girsk/Lyozno Suites (upper part of the Volyn Series; Fig. 2). The zircons from the lower part (samples Pinsk-45A, Pinsk-46A) show nearly identical U-Pb age pattern with a dominant peak at c. 1.50 Ga with two smaller peaks at c. 590 Ma and 1.80 Ga, whereas in the Kob-10 sample the youngest c. 580 Ma peak dominates over 1.50 and 1.80 Ga (Fig. 6). The maximum depositional ages for both the Pinsk-45A and 46A samples are constrained to 579 ± 4 Ma ($n = 4$, MSWD = 0.18; and $n = 3$, MSWD = 2.2, respectively). For the Kob-10 sample, the PDP plot is shifted towards youngest ages due to c. 580 Ma dominance in group A zircons (for more details see Supplementary Data SD4). A maximum depositional age of 569 ± 4 Ma ($n = 4$, MSWD = 0.72) is 10 Ma younger staying slightly out of the error range (Fig. 6).

The samples from the upper part of the Volyn Series included brown, soft tuffite Kob-27A, arkose/wacke Kob-32A, tuffite Kob-34A and arkose Kob-34B. Zircons from these samples demonstrate a dominant U-Pb age peak at c. 1.50 Ga, along with smaller peaks at 1.80 Ga and 550–570 Ma (except of sample Kob-34B with c. 1.50 Ga and 0.60 Ga peaks roughly of the same size). Maximum depositional ages demonstrate decreasing trend up the profile, from 560 ± 5 Ma (Kob-27A; $n = 3$, MSWD = 2.3), and 567 ± 4 Ma (Kob-32A; $n = 3$, MSWD = 0.102) to ages 545 ± 4 Ma (Kob-34A; $n = 3$, MSWD = 3.7) and 550 ± 4 Ma (Kob-34B; $n = 5$, MSWD = 0.045) staying within the error range (Fig. 6).

4.2.3. Valdai Series rocks

The Valdai Series rocks are represented by 4 samples from the Redkino Horizon (Nizov, Selsk and Tshernitse Suites) and 3 samples from the Kotlin Suite (Fig. 2). The zircon ages

mainly range between c. 1.50 and 1.90 Ga, but without a younger group at c. 550–570 Ma that is present in the older Volyn Series rocks.

Zircons from the Nizov Suite (sample Bog-33A) yielded a dominant age peak at c. 1.50–1.70 Ga with two maxima at c. 1.58 and 1.64 Ga. Another large peak is identified at c. 1.83 Ga, with an additional minor age group at c. 1.91 Ga. Two zircons have older ages of 2.32 and 2.84 Ga. The age pattern of the Selsk Suite (sample Lep-12A) exhibits a dominant age peak at c. 1.84 Ga and smaller peaks at 1.47 and 1.59 Ga and contains only one zircon grain of older age at 2.37 Ga. The zircons from the Tshernitse Suite show an age pattern with a dominant peak at c. 1.50 Ga (minor age clusters at c. 1.62 and 1.83 Ga) in sample Bog-43A and c. 1.84 Ga (smaller peaks at 1.47 and 1.59 Ga; similarly to the age pattern recognised in the Selsk Suite) in sample Lep-20B. Both samples from the Tshernitse Suite contain grains of the older age, i.e. 2.18 Ga in Bog-43A and 2.05–2.32 Ga in Lep-20B.

The samples from the Kotlin Suite (Lep-28A, Bog-51A and Kob-40A) show a similar age pattern to those from the Redkino Horizon with a dominant age peak at c. 1.50–1.54 Ga and smaller peaks at c. 1.80–1.84 Ga. Additionally, the Bog-51A sample reflects also a small peak at c. 1.62 Ga. The older zircon single ages are between 1.96 and 2.75 Ga (Lep-28A and Bog-51A) or c. 3.28 Ga (Kob-40A).

4.2.4. Palaeozoic rocks

The lower Cambrian glauconite-bearing quartz arenite (sample Kob-54) contains most homogeneous age record in this study with a single peak at c. 1.49 Ga. Only five analyses yielded ages staying out of the main cluster, from c. 1.60 to 1.94 Ga. In contrast, the second lower Cambrian sample (Kob-57), a coarse-grained sandstone, contains a nearly continuous

spectrum of ages ranging from c. 542 to 3.41 Ga with dominant peaks at c. 550 and 620 Ma, and smaller older peaks at c. 2.04, 2.10, 2.66 and 2.71 Ga. Two zircons yielded a maximum depositional age of 543 ± 4 Ma (MSWD = 0.91) staying within the error range of the Precambrian–Cambrian boundary.

4.3. Hf isotopes

Zircons from tillite Vilch-6A (Vilchitsy Series) analysed for Hf isotopes have U/Pb or Pb/Pb dates ranging between 683–3185 Ma and they display a wide range of initial ϵ_{Hf} values from -10.6 to 6.1 (Table 2; Fig. 7a). According to their pattern on the measured date versus ϵ_{Hf} plot, all zircons in this sample can be tentatively attributed to three groups (Fig. 7a). The first (oldest) group includes zircons with ages between 3.19 and 2.50 Ga, and ϵ_{Hf} from 2.5 to -6.5 ($n = 6$). These zircons plot along c. 3.3 Ga crust evolution line with $^{176}\text{Lu}/^{177}\text{Hf} = 0.019$; however, due to limited data points, they may also plot along a large number of evolution lines with different slopes corresponding to different $^{176}\text{Lu}/^{177}\text{Hf}$ ratios, and any scenario from felsic to mafic (0.009 and 0.022, respectively; Gardiner et al., 2018) crustal evolution is possible. The second, poorer defined group comprises zircons with ages ranging from 2.17 to 1.42 Ga, and ϵ_{Hf} from 5.2 to -10.2 ($n = 14$). The youngest group is well-defined and comprises zircons ranging in age from 1.53 to 0.68 Ga and ϵ_{Hf} from 6.1 to -2.8 ($n = 8$), most of them being juvenile. These zircons plot along a line of slope $^{176}\text{Lu}/^{177}\text{Hf}$ c. 0.016, which corresponds nearly to the average continental crust. The “new crust” model age (Dhuime et al., 2011) for this group is c. 1.8 Ga, which probably corresponds to a discrete crust-forming event.

Zircons from tuffite Pinsk-46A (Rataychitsy Suite) range in age from c. 1860 to 575 Ma, and initial ϵ_{Hf} from +4 to -13.9 (Table 2; Fig. 7b). These zircons belong to three age groups: the

oldest group (age 1.75–1.87 Ga, ϵ_{Hf} from 3.4 to -1.5; $n = 9$), the intermediate group (age c. 1.50 Ga, ϵ_{Hf} from -2.8 to -5.5; $n = 13$), and the youngest group (age 590–575 Ma, ϵ_{Hf} from -10.2 to -13.9; $n = 4$). All these zircons, irrespective of their age, plot along an evolution line with $^{176}\text{Lu}/^{177}\text{Hf}$ of c. 0.015 indicating average continental crust source, and with the new crust model age of c. 2.3 Ga.

Zircons from the arkose Kob-34B sample (Girsk Suite) were selected from three separate age groups: the oldest group (c. 1.75–1.85 Ga) comprises predominantly chondritic to slightly juvenile zircon with ϵ_{Hf} varying from 4.4 to -1.4 ($n = 9$), the intermediate group of zircons (1.46–1.57 Ga) have ϵ_{Hf} ranging from -1.6 to -4.1 ($n = 12$), and the youngest group have a narrow age interval (548–571 Ma with one date 708 Ma) and wide range of ϵ_{Hf} values – from -0.6 to -18.4 ($n = 9$; Fig. 7c; Table 2). Interestingly, the oldest and intermediate groups in the Rataychitsy and Girsk Suites coincide in age and ϵ_{Hf} se. The data from the Kob-34B sample also plot along an evolution line of slope $^{176}\text{Lu}/^{177}\text{Hf}$ 0.013, which intercepts the new crust evolution line at c. 2.2 Ga.

Zircons from quartz arenite/subarkose sample Bog-33A (Nizov Suite) form a coherent group that ranges in age from 1.93 to 1.49 Ga and initial ϵ_{Hf} from 5.8 to -4.3 ($n = 24$; Table 2; Fig. 7d). This group plots along a regression line of slope $^{176}\text{Lu}/^{177}\text{Hf} = 0.010$. A low $^{176}\text{Lu}/^{177}\text{Hf}$ ratio (i.e., 0.010) reflects evolution of felsic source reservoir with a mantle extraction age of c. 2.1 Ga. The c. 2.1 Ga crust-forming event is similar to the c. 2.1–2.3 Ga event observed in other Neoproterozoic sediments. Furthermore, three isolated zircons from this sample have either older ages or lower ϵ_{Hf} values (2.84 Ga and 4.1; 2.32 Ga and 0.4; 1.54 Ga and -9.2, respectively).

Two age groups occur in the arkose Lep-12A sample (Selsk Suite). The older group (1.72–1.89 Ga) ranges in ϵ_{Hf} from +2.3 to -1.6 ($n = 10$), and the younger group (1.42–1.67 Ga) ranges in ϵ_{Hf} from +5.3 to -5.4 ($n = 13$; Table 2; Fig. 7e). The large majority of the data plot along an evolution line of slope $^{176}\text{Lu}/^{177}\text{Hf} = 0.013$ indicating intermediate to felsic source and intercepting the new crust evolution line at c. 2.2 Ga, similar to the crust extraction age seen for the Volyn Series sediments.

Zircons from the lower Cambrian quartz arenite Kob-57 sample are extremely variable in terms of both their age (ranging from 3.41 Ga to 546 Ma) and Hf isotope composition (ϵ_{Hf} ranging from 5.1 to -20.0) (Table 2; Fig. 7f). Similarly, to sample Vilch-6A, such data scattering prevents distinguishing principal crust formation events with confidence.

5. Discussion

5.1. *Pre-Rodinia provenance signal*

The lower part of the sedimentary succession of the EEC consisting of the Pinsk and Orsha Suites, although not precisely dated, was deposited in a time interval of c. 1.32–1.0 Ga (Fig. 3). These sediments represent the time post-dating break-up of the Columbia/Nuna supercontinent (e.g., Rogers and Santosh, 2002; Zhao et al., 2002, 2004; Evans and Mitchell, 2011). According to most of currently accepted plate tectonic reconstructions the present-day EEC, a precursor of early Palaeozoic Baltica, was at that time attached to the Greenland margin of Laurentia, while both continents drifted together at low latitudes (Buchan et al., 2000; Ernst et al., 2000; Condie, 2002; Zhao et al., 2004; Pisarevsky et al., 2014).

Such reconstruction is consistent with our mineralogical data. The ratio of kaolinite to illite-smectite (originally a smectitic product of weathering; cf. Liivamägi et al., 2018) is proposed

here as a proxy for weathering intensity in the source areas (clay index; Table S1; Fig. 4). This value is not dependent on the percentage of primary minerals, used as a proxy for the grain size, thus it was not affected significantly by hydraulic sorting (cf. Środoń et al., 2014, their fig. 16). The ratio of quartz to all pre-weathering minerals can be considered as an alternative proxy for weathering intensity (primary minerals index; Table S1; Fig. 4). These indices offer some clues concerning the provenance of the Orsha Suite, where both weathering indices agree, indicating very intense kaolinitic-type weathering in a source area, implying warm and humid conditions.

The Pinsk Suite, with a current exposure of 150,000 km² (Makhnach et al., 2001), reveals nearly unimodal U-Pb age spectra in two samples analysed (c. 2.0 Ga; Fig. 6). Similar detrital age spectra have been reported from the Paleoproterozoic Ovruch Series in the Ukrainian Shield (dated as 1.76 Ga using zircons in the underlying rhyolites; Shumlyanskyy et al., 2017). However, the Ovruch Series can hardly be considered a source area for the Pinsk Suite sediments because of its rather minor extent (1000 km²) and much higher maturity of mineral composition (pyrophyllite-grade; Sinyakovskaya et al., 2005). Therefore, the Osnitsk-Mikashevychi Igneous Belt (northern Ukraine – southern Belarus), dated at c. 2.0 Ga (Shumlyanskyy et al., 2016 and references therein), is a plausible candidate for a source area, even though it might have been partly buried beneath younger sediments at the time of the Pinsk Suite deposition. Since the Proterozoic basins located on the Ukrainian Shield contain formations with similar 2.0–2.1 Ga zircon age patterns (Shumlyanskyy et al., 2015) a common, voluminous and widespread source terrain is suggested. Such a narrow detrital age spectrum in a sedimentary cover of a craton remains a rare phenomenon that can be best explained by erosion of an extensive volcanogenic cover and relatively short detritus transport that prevents mixing of zircons from various sources. Therefore, a continental arc

producing sediments with a relatively narrow age range can be an alternative solution to the Osnitsk-Mikashevychi Igneous Belt.

The Orsha Suite quartz arenite yielded a polymodal 1.3–3.2 Ga zircon age distribution, indicating a complex provenance for the Orsha Suite (Fig. 6). The detritus distributary systems and long-lasting weathering possibly lead to mixing and recycling of the material from numerous, potentially distant sources. Clearly, the catchment area changed in comparison to the Pinsk Suite.

5.2. Provenance of Rodinia-related sediments

Only the Vilchitsy Series, traditionally ascribed to Cryogenian (720–635 Ma; Fig. 3), can be correlated with the time, when the Rodinia supercontinent existed (1.0–0.63 Ma; e.g., Weil et al., 1998; Meert and Torsvik, 2003; Pisarevsky et al., 2003; Torsvik 2003; Li et al., 2008). The Rodinia reconstructions place the EEC (future Baltica) at high latitudes of the southern hemisphere until 900 Ma (Pisarevsky et al., 2003; Li et al., 2008). From 750 Ma onwards, the EEC occupied position at moderate latitudes until the break-up of Rodinia (630 Ma; e.g., Li et al., 2008).

The composition of primary (pre-weathering) minerals, detectable by XRD, can be used as a provenance indicator for the EEC sediments in Belarus. The Vilchitsy Series rocks are characterized by similar proportions of orthoclase to microcline and biotite to muscovite, like the Pinsk Suite (Fig. 4). These ratios, the high ratio of quartz to all pre-weathering minerals, along with low ratio of kaolinite to illite-smectite imply glacial erosion of the underlying sedimentary rocks, practically without chemical weathering.

The nearly continuous zircon age spectra (1.0–3.2 Ga; Fig. 6) from glacial sediments of the Vilchitsy Series are similar to those from the Orsha Suite, except for a c. 1.0–1.3 Ga cluster and more dominant 2.0 Ga peak in one of the Vilchitsy Series samples. These spectra indicate that the main source area were the underlying Pinsk and Orsha Suites, supplemented by a younger Grenvillian-age component. Such an interpretation is consistent with the mineral composition of the bulk rock, intermediate between the Pinsk and Orsha Suites and without measurable input of non-weathered material (Table S1). Since the maximum deposition age of the Vilchitsy Series is constrained by the zircon age spectra to c. 1.0 Ga (Fig. 6), and the oldest overlying basalts are dated at c. 570 Ma, the Vilchitsy tillites (Fig. 3) may represent any of the Cryogenian glaciations as well as the Ediacaran Gaskiers glaciation. The centre of glaciation must have been located SW from the glacial sediments of the Vilchitsy Series, as indicated by the lateral facies trends in the Volyn-Orsha Basin: the glacial sediments thin out towards the NE along the axis of the basin (Kheraskova et al., 2003). The glacial series was deposited on the continent covered by kaolinitic redbeds: products of intense weathering in hot and humid climate, *in situ* or redeposited (Orsha Suite). Therefore, the glacial character of the Vilchitsy Series implies a major climate change compared to the time of deposition of the Orsha Suite or, alternatively, a localised elevation of part of the craton. The former option is possible due to a large time gap between deposition of the Orsha Suite (c. 1.3–1.0 Ga) and the Vilchitsy Series. The latter interpretation is also reasonable since the addition of 1.0 Ga zircons may suggest some post-Grenvillian (post-Sveconorwegian) elevated topography. C. 1 Ga dates obtained by Shumlyanskyy et al. (2015) for the Ukrainian Polissya Series indicate delivery of the detritus from a comparable source terrain.

The Lu-Hf data show that the best-defined group of detrital zircons (Fig. 7a) with ages from 1.53 to 0.68 Ga and ϵ_{Hf} from 6.1 to -2.8 ($n = 8$) correspond to the average continental crust

with a model age of 1.8 Ga. This age represents a main crust-forming event in Fennoscandia implying a local character of the source terrain. The admixture of zircons dated at 1.0 Ga is notable, but these grains are characterized by only slightly positive ε_{Hf} values (0 to +2). Therefore, they do not match a clearly positive ε_{Hf} signature (+5 to +7) of magmatic zircon cores from the Grenvillian Oaxaquia Terrane (Weber et al., 2010).

5.3. Sedimentary record of Baltica

The sediments sampled that were laid down after the break-up of Rodinia are included into the Volyn and Valdai Series of the Ediacaran age (635–542 Ma) as well as the lower Cambrian succession (542–530 Ma; Fig. 3). They were deposited during a time interval, when Baltica was located at the equator (Popov et al., 2002; Li et al., 2008) or resided at moderate southern latitudes (Torsvik and Rehnström, 2001).

Since the Lu-Hf data for all the zircons from the Volyn and Valdai Series correspond to intermediate to felsic source with model ages of 2.1–2.3 Ga they suggest that the main catchment area was located within Sarmatia (present-day Ukraine, SW part of the EEC). Furthermore, the Mesoproterozoic zircons (c. 1.5 Ga) from the Volyn and Valdai Series reveal ε_{Hf} values in the range of +5.8 to -5.5 that are comparable to those in the granites and gneisses from the Danish island of Bornholm (Johansson et al., 2016) and rapakivi granites of SW Fennoscandia (Heinonen et al., 2010, 2014). Abundant zircons of similar age (c. 1.5 Ga) were documented in sedimentary rocks of the Ukrainian Shield and interpreted as detritus supplied from the Fennoscandian Shield (Shumlansky et al., 2015).

In the volcanoclastic sediments of the Volyn Series orthoclase dominates over microcline and they contain abundant biotite along with primary basalt minerals (Ca-plagioclase, pyroxene)

and their hydrothermal alteration products (trioctahedral clays and zeolites). This change reveals detritus derivation from sources comprising basalts and biotite-bearing rocks. Starting from the Redkino Horizon of the Valdai Series, the basaltic source is gradually diminished, whereas a biotite-rich source continues to supply material. Finally, contribution from a new source rich in muscovite continuously increases until early Cambrian (the youngest unit studied).

The Volyn Series mineral composition shows characteristics opposite to the Orsha Suite: both indices have the lowest values; clay index because of the lack of kaolinite (no weathering) and the primary mineral index because of low quartz content. Both mineral composition indices are the lowest in the area close to the centres of magmatic activity, where pure basalts or volcanoclastics occur. They increase in samples, where the admixture of non-volcanic material is the highest. The very low clay indices for the Volyn Series rocks with terrigenous addition indicate that they are approximate time equivalents to the basalts and tuffs, as they formed before the development of intense kaolinitic weathering of the top layer of basalts (Liivamägi et al., 2018).

The Redkino Horizon of the Valdai Series differs from the underlying Volyn Series by an abrupt increase of the clay index and a very small increase of the primary mineral index. Such relationships suggest that the Redkino Horizon contains a significant admixture of already weathered volcanic material. Indeed, in the Volyn region the Redkino Horizon sediments are deposited on kaolinitic palaeosols developed on basalts (Liivamägi et al., 2018). Above the Redkino Horizon, these indices evolve in reciprocal direction across the Ediacaran/Cambrian boundary: clay index decreases, accompanied by decrease of hematite, while primary mineral index increases. Such regularity seems to indicate a gradual decrease

of the contribution from the strongly weathered volcanic source (high in kaolinite and low in quartz).

The zircon U-Pb record (Fig. 6), in samples from the Volyn and Valdai Series deposited in the intraplate basin during c. 40 Ma of continuous sedimentation, shows a common discrete distribution of ages with prominent clusters of c. 1.8, and 1.5 Ga and 579–545 Ma. The latter cluster, occurring in the sediments of the Volyn and lower Valdai Series, is derived from the Volyn flood basalts (Fig. 8). Also, the disappearance of Ca-plagioclases (Table S1) indicates that the contribution of trap basalts to the volcano-sedimentary succession was terminated in the lower Valdai Series. The maximum deposition ages obtained for seven Volyn Series samples (Fig. 6; 579–545 Ma) document the sediment age decrease upward the profile and constrain the age of Volyn flood basalt province (Fig. 8), in general agreement with the previous age estimates of 573 ± 14 Ma for basalts, 571 ± 13 Ma for rhyolitic dacite (Shumlyanskyy et al., 2016), and 551 ± 4 Ma for a tuff (Compston et al., 1995).

The detrital age distribution in the Volyn and Valdai Series is markedly different from the underlying Vilchitsy Series (Fig. 6), probably reflecting a major reorganization of the sediment supply routes related to the break-up of Rodinia (Fig. 8). The bulk mineralogy change (Table S1) documents the same phenomenon. A potential source terrain can be found within the Precambrian basement of Baltica, where numerous igneous bodies with 1.5 or 1.8 Ga ages exist (e.g., Bogdanova et al., 2008, 2015; Shumlyanskyy et al., 2015; Krzemińska et al., 2017 and references therein). Narrow age spectra measured in the Ediacaran sediments (Fig. 6) suggest a short delivery route from a catchment area preventing mixing between detritus supplied by various crustal components. The sediment transport direction for the

Volyn and Valdai Series was from the SW (Fig. 8), as evidenced by basin geometry (Rozanov and Lydka, 1987) and sedimentary facies distribution (Paczeńska, 2010).

5.4. Ediacaran to Cambrian transition

At the end of the Ediacaran no abrupt change in bulk rock mineralogy can be detected by XRD: the mineral composition is gradually evolving, and only a decrease of the basaltic source can be deduced. Also, the bimodal distribution of zircon ages in the Kobryn profile continues into the rocks (sample Kob-54) that are interpreted as Cambrian based on trace fossils (Elena Golubkova, pers. comm.).

Sample Kob-57, taken 15 m above, presents a completely different age spectrum, including a broad 500–700 Ma Neoproterozoic cluster (Fig. 6). Similar major provenance shifts from the bimodal (1.5 and 1.8 Ga) to polymodal distribution with a Neoproterozoic cluster were reported from Estonia (Isozaki et al., 2014), the Russian part of the Baltic Monoclise (Kuznetsov et al., 2011; Ivleva et al., 2016) and Scandinavia (lower Cambrian in Lorentzen et al., 2017 vs. middle-upper Cambrian in Sláma and Pedersen, 2015; Sláma, 2016). Similarly, the middle Cambrian sediments of the Okuniew IG-1 borehole (Podlasie Depression Poland, SW part of the EEC; Valverde-Vaquero et al., 2000) and of the Syczyn OU1 borehole (Lublin Basin; Porębski et al., 2019) contain a Neoproterozoic zircon cluster.

The complex age spectrum of sample Kob-57 with a dominant Neoproterozoic cluster seems to herald the advance of a Neoproterozoic orogen at the margin of Baltica. There are at least two possible orogenic sources of the Neoproterozoic zircons. The first is the Timanide belt along the northern edge of Baltica (cf. Kuznetsov et al., 2011; Isozaki et al., 2014; Sláma and Pedersen, 2015; Ivleva et al., 2016; Sláma, 2016). The second possible source terrain is

located around the SW corner of the present-day EEC and it is related to a peri-Gondwanan Neoproterozoic terrane (Scythia) docked to the Baltica margin (Fig. 9) and giving rise to the pre-Scythides orogen (Kheraskova et al., 2015). The latter option appears the most plausible in the light of subsidence analysis published by Poprawa et al. (2018). Their study shows that the majority of the SW Baltica margin remained relatively stable in the latest Ediacaran and early Cambrian, whereas the Baltica's southern section, adjacent to the Scythian Platform, noted rapid subsidence in the latest Ediacaran. The subsidence curves show shapes indicative of a flexural basin, suggesting the Baltica continental margin being overridden by a collisional orogen.

5.5. Crustal evolution constrained by Hf isotopes

Combined Hf zircon data from investigated samples suggest at least four episodes of new continental crust generation at c. 1.8, 2.1–2.3, 2.8 and 3.3 Ga (Fig. 10). The intermediate character of the source reservoirs with average composition of the continental crust dominates, although more felsic components are tentatively identified as well. Considerable mixing of the crustal reservoirs occurred at c. 1.8 Ga and 550–600 Ma. The data from Belarus are similar to recent age-Hf isotope data from the Ukrainian, SW part of the EEC that constrained four main crustal growth events at 1.5, 2.0–2.2, 3.15–3.20 and 3.75 Ga and a minor 2.4–2.5 Ga event (Shumlyanskyy et al., 2015). The main difference is the timing of the youngest crust-forming event, i.e., 1.8 Ga in Belarus versus 1.5 Ga in Ukraine.

A characteristic feature of samples analysed is their reasonable similarity to each other with a main crust-forming event defined at 2.1–2.3 Ga and an evolution line corresponding to a $^{176}\text{Lu}/^{177}\text{Hf}$ ratio of 0.010–0.016 (Figs. 7, 10). The latter points to crustal reservoirs of intermediate composition, i.e. average composition of continental crust with some felsic

components. An exception makes more shallow apparent crustal evolution line in sample Vilch-6A with a $^{176}\text{Lu}/^{177}\text{Hf}$ ratio of 0.019 (Fig. 7a), suggesting of an intermediate to mafic crustal reservoir, representing a discrete crust-forming events at c. 3.3 Ga. However, this should be taken with caution due to limited data. This collectively suggests a relatively uniform source terrain throughout the Neoproterozoic that were located within the crust of the present-day EEC. These sources experienced subsequent reworking of crust at c. 1.8 Ga and 550–600 Ma. A stark contrast from the common characteristics is sample Kob-57 collected from rocks representing the uppermost Ediacaran or lower Cambrian. The lack of any trends or clustering within the data (Fig. 7f) may suggest insufficient number of measurements but also sedimentary mixing of zircons derived from exotic source terrains. The latter explanation appears plausible considering a possible derivation of Neoproterozoic zircons from the basement of the peri-Gondwanan Scythian Platform that was docked to the SW corner of Baltica in the latest Ediacaran (see above; Kheraskova et al., 2015).

6. Conclusions

The provenance record from the Meso- and Neoproterozoic sediments covering the Belarusian sector of the EEC reveals fairly uniform sources of sediments located on Paleoproterozoic crust typical of the EEC. An additional source was provided by Neoproterozoic intraplate volcanic rocks (Volyn volcanic province). Analysed samples show reasonable similarity to each other with a main crust-forming event defined at 2.1–2.3 Ga and an evolution line corresponding to crustal reservoirs of average composition of continental crust with some felsic components. An important change of detritus provenance is noted only at the transition from the Ediacaran to Cambrian or in the early Cambrian. This is shown by

significant input of late Neoproterozoic zircons derived from an orogenic source. The latter was probably related to docking of an exotic terrane to the SW corner of Baltica.

Acknowledgements: Financial support for this project came from the Polish National Science Centre MAESTRO grant 2013/10/A/ST10/00050. Hf isotope analyses were funded by the Natural Environment Research Council [NERC grant NE/K008862/1 to B.D.]. Jiří Sláma was supported by the Academy of Sciences of the Czech Republic institutional support to the Institute of Geology, ASCR, RVO 67985831. State Enterprise “Scientific and Industrial Centre for Geology” from Minsk, Belarus made available all core material used in this study. Oksana Kuzmenkova, Alla Lapceovich, and Sergei Mankevich are thanked for their help with the borehole selection and sampling. Izabela Kocjan is acknowledged for the zircon separation and Zuzanna Ciesielska for the XRD measurements. Andrzej Łaptaś and Monika Plech are thanked for graphical support. Comments from Associate Editor Tony Kemp, and Reviewers Bernard Bingen and Anonymous are greatly appreciated and significantly improved this article.

7. References

- Bogdanova, S., Paskevich, I.K., Gorbatshev, R., Oryluk, M.I., 1996. Riphean rifting and major Palaeoproterozoic crustal boundaries in the basement of the East European Craton: Geology and geophysics. *Tectonophysics* 268, 1–21.
- Bogdanova, S.V., Page, L.M., Skridlaite, G., Taran, L.N., 2001. Proterozoic tectonothermal history in the western part of the East European Craton: $^{40}\text{Ar}/^{39}\text{Ar}$ geochronological constraints. *Tectonophysics* 339, 39–66.

696 Bogdanova, S.V., Bingen, B., Gorbatshev, R., Kheraskova, T.N., Kozlov, V.I., Puchkov,
 697 V.N., Volozh, Y.A., 2008. The East European Craton (Baltica) before and during the
 698 assembly of Rodinia. *Precambrian Research* 160, 23–45.

699 Bogdanova, S., Gorbatshev, R., Skridlaite, G., Soesoo, A., Taran, L., Kurlovich, D., 2015.
 700 Trans-Baltic Palaeoproterozoic correlations towards the reconstruction of
 701 supercontinent Columbia/Nuna. *Precambrian Research* 259, 5–33.

702 Bouvier, A., Vervoort, J.D., Patchett, P.J., 2008. The Lu-Hf and Sm-Nd isotopic composition
 703 of CHUR: constraints from unequilibrated chondrites and implications for the bulk
 704 composition of terrestrial planets. *Earth and Planetary Science Letters* 273, 48–57.

705 Buchan, K.L., Mertanen, S., Park, R.G., Pesonen, L.J., Elming, S.Å., Abrahamsen, N.,
 706 Bylund, G., 2000. Comparing the drift of Laurentia and Baltica in the Proterozoic: the
 707 importance of key palaeomagnetic poles. *Tectonophysics* 319 (3), 167–198.

708 Chebanenko, I.I., Vyshnyakov, I.B., Vlasov, B.I., 1990. Geotectonics of the Volyno-Podolian
 709 area. Naukova Dumka publisher, 244 pp. (in Russian).

710 Chumakov, N.M., Semikhatov, M.A., 1981. Riphean and Vendian of the USSR. *Precambrian*
 711 *Research* 15 (3–4), 229–253.

712 Chumakov, N.M., 2010. Precambrian Glaciations and Associated Biospheric Events.
 713 *Stratigraphy and Geological Correlation* 18 (5), 467–479.

714 Chumakov, N.M., 2015. The role of glaciations in the biosphere. *Russian Geology and*
 715 *Geophysics* 56, 541–548.

716 Claesson, S., Bogdanova, S.V., Bibikova, E.V., Gorbatshev, R., 2001. Isotopic evidence for
 717 Palaeoproterozoic accretion in the basement of the East European Craton.
 718 *Tectonophysics* 339, 1–18.

719 Compston, W., Sambridge, M.S., Reinfrank, R.F., Moczyłowska, M., Vidal, G., Claesson, S.,
720 1995. Numerical ages of volcanic rocks and the earliest faunal zone within the Late
721 Precambrian of east Poland. *Journal of the Geological Society* 152, 599–611.

722 Condie, K.C., 2002. Breakup of a Paleoproterozoic supercontinent. *Gondwana Research* 5(1),
723 41–43.

724 Dhuime, B., Hawkesworth, Ch., Cawood, P., 2011. When Continents Formed. *Science* 331,
725 154–155.

726 Dickinson, W.R., Gehrels, G.E., 2009. Use of U–Pb ages of detrital zircons to infer
727 maximum depositional ages of strata: A test against a Colorado Plateau Mesozoic
728 database. *Earth and Planetary Science Letters* 288, 115–125.

729 Elming, S.-Å., Mikhailova, N.P., Kravchenko, S.N., 1998. The consolidation of the East
730 European Craton: a palaeomagnetic analysis of Proterozoic rocks from the Ukrainian
731 Shield and tectonic reconstruction versus Fennoscandia. *Geophysical Journal* 20, 71–
732 74.

733 Ernst, R.E., Buchan, K.L., Hamilton, M.A., Okrugin, A.V., Tomshin, M.D., 2000. Integrated
734 paleomagnetism and U–Pb geochronology of mafic dikes of the eastern Anabar Shield
735 region, Siberia: Implications for Mesoproterozoic paleolatitude of Siberia and
736 comparison with Laurentia. *The Journal of Geology* 108 (4), 381–401.

737 Evans, D.A.D., Mitchell, R.N., 2011. Assembly and breakup of the core of
738 Palaeoproterozoic–Mesoproterozoic supercontinent Nuna. *Geology* 39, 443–446.

739 Gardiner, N. J., Johnson, T. E., Kirkland, C. L., Smithies, R. H., 2018. Melting controls on
740 the lutetium–hafnium evolution of Archaean crust. *Precambrian Research* 305, 479–
741 488.

742 Goryl, M., Marynowski, L., Brocks, J.J., Bobrovskiy, I., Derkowski, A., 2018. Exceptional
 743 preservation of hopanoid and steroid biomarkers in Ediacaran sedimentary rocks of the
 744 East European Craton. *Precambrian Research* 316, 38–47.

745 Heinonen, A.P., Andersen, T., Rämö, O.T., 2010. Re-evaluation of rapakivi petrogenesis:
 746 Source constraints from the Hf isotope composition of zircon in the rapakivi granites
 747 and associated mafic rocks of southern Finland. *Journal of Petrology* 51 (8), 1687–
 748 1709.

749 Heinonen, A., Andersen, T., Rämö, O.T., Whitehouse, M., 2015. The source of Proterozoic
 750 anorthosite and rapakivi granite magmatism: evidence from combined in situ Hf–O
 751 isotopes of zircon in the Ahvenisto complex, southeastern Finland. *Journal of the*
 752 *Geological Society* 172 (1), 103–112.

753 Hoskin, P.W.O., Black, L.P., 2000. Metamorphic zircon formation by solid-state
 754 recrystallization of protolith igneous zircon. *Journal of Metamorphic Geology* 18, 423–
 755 439.

756 Isozaki, Y., Põldvere, A., Bauert, H., Nakahata, H., Aoki, K., Sakata, S., Hirata, T., 2014.
 757 Provenance shift in Cambrian mid-Baltica: detrital zircon chronology of Ediacaran-
 758 Cambrian sandstones in Estonia. *Estonian Journal of Earth Sciences* 63 (4), 251–256.

759 Ivleva, A.S., Podkovyrov, V.N., Ershova, V.B., Anfinson, O.A., Khudoley, A.K., Fedorov,
 760 P.V., Maslov, A.V., Zdobin, D.Yu., 2016. Results of U–Pb LA–ICP–MS dating of
 761 detrital zircons from Ediacaran–Early Cambrian deposits of the Eastern part of the
 762 Baltic Monocline. *Doklady Earth Sciences* 468, 593–597.

763 Johansson, Å., Waight, T., Andersen, T., Simonsen, S.L., 2016. Geochemistry and
 764 petrogenesis of Mesoproterozoic A-type granitoids from the Danish island of
 765 Bornholm, southern Fennoscandia. *Lithos* 244, 94–108.

766 Kelly, N.M., Harley, S.L., 2005. An integrated microtextural and chemical approach to zircon
767 geochronology: refining the Archaean history of the Napier Complex, east Antarctica.
768 Contributions to Mineralogy and Petrology 149, 57–84.

769 Kheraskova, T.N., Didenko, A.N., Bush, V.A., 2003. The Vendian-Early Paleozoic history of
770 the continental margin of eastern Paleogondwana, Paleoasian Ocean, and Central Asian
771 foldbelt. Russian Journal of Earth Sciences 5 (3), 165–184.

772 Kheraskova, T. N., Volozh, Yu. A., Antipov, M. P., Bykadorov, V. A., Sapozhnikov, R. B.,
773 2015. Correlation of Late Precambrian and Paleozoic events in the East European
774 Platform and the adjacent paleoceanic domains. Geotectonics 49, 27–52.

775 Krzemińska, E., Krzemiński, L., Petecki, Z., Wiszniewska, J., Salwa, S., Żaba, J., Gaidzik,
776 K., Williams, I.S., Rosowiecka, O., Taran, L., Johansson, Å., Pécskay, Z., Demaiffe,
777 D., Grabowski, J., Zieliński, G., 2017. Geological Map of Crystalline Basement in the
778 Polish part of the East European Platform 1:1 000 000. Państwowy Instytut
779 Geologiczny. Warszawa.

780 Kuzmenkova, O.F., Nosova, A.A., Shumlyansky, L.V., 2010. Comparison of Neoproterozoic
781 Volyn-Brest magmatic province with large world continental plate basalt provinces, the
782 nature of low- and high-Ti basite magmatism. Lithosphere 33, 3–16 (in Russian)

783 Kuzmenkova, O.F., Shumlyansky, L.V., Nosova, A.A., Voskoboynikova, T.V., Grakovich,
784 I.Yu., 2011. Petrology and correlation of trap formations of the Vendian in the adjacent
785 areas of Belarus and Ukraine. Litasfera 2 (35), 3–11.

786 Kuzmenkova, O.F., Laptsevich, A.G., Mankevich, S.S., 2016. Perspectives of the diamond
787 content of Vendian deposits of the Polesye Saddle of Belarus. Litosfera 44, 38–50 (in
788 Russian).

789 Kuznetsov, N.B., Orlov, S.Y., Miller, E.L., Shatsillo, A.V., Dronov, A.V., Soboleva, A.A.,
790 Udoratina, O.V., Gehrels, G.E., 2011. First U/Pb age results for detrital zircons from

791 Early Paleozoic and Devonian sandstones, South Priladozhje. Doklady of Earth
792 Sciences 438, 1–7.

793 Li, Z.X., Bogdanova, S.V., Collins, A.S., Davidson, A., De Waele, B., Ernst, R.E.,
794 Fitzsimons, I.C.W., Fuck, R.A., Gladkochub, D.P., Jacobs, J., Karlstrom, K.E., Lu, S.,
795 Natapov, L.M., Pease, V., Pisarevsky, S.A., Thrane, K., Vernikovsky, V., 2008.
796 Assembly, configuration, and break-up history of Rodinia: a synthesis. Precambrian
797 research 160 (1–2), 179–210.

798 Liivamägi, S., Środoń, J., Bojanowski, M., Gerdes, A., Stanek, J.J., Williams, L., Szczerba,
799 M., 2018. Paleosols on the Ediacaran basalts of the East European Craton: A unique
800 record of paleoweathering with minimum diagenetic overprint. Precambrian Research
801 316, 66–82.

802 Lorentzen, S., Augustsson, C., Nystuen, J.P., Berndt, J., Jahren, J., Schovsbo, N.H., 2017.
803 Provenance and sedimentary processes controlling the formation of lower Cambrian
804 quartz arenite along the southwestern margin of Baltica. Sedimentary Geology 375,
805 203–217.

806 Lubnina, N.V., Bogdanova, S.V., Shumlyanskyy, L.V., 2009. The East European Craton in
807 the Palaeoproterozoic: new paleomagnetic data on magmatic complexes in the
808 Ukrainian Shield. Geofizika 5, 56–64 (in Russian).

809 Makhnach, A.S., Veretennikov, N.V., Shkuratov, V.I., Bordon, V.E., 1976. Riphean and
810 Vendian of Belarus. Nauka i Tekhnika publisher, 360 pp. (in Russian).

811 Makhnach, A.S., Garetskiy, R.G., Matveev, A.V., Anoshko, Ya.I., 2001. Geology of Belarus.
812 Minsk, Institute of Geological Sciences, 815 pp. (in Russian).

813 Makhnach, A.S., Veretennikov, N.V., Shkuratov, V.I., Laptsevich, A.G., Piskun, L.V., 2005.
814 Stratigraphic chart of Vendian deposits of Belarus. Litasfera 22, 36–44 (in Russian).

815 Meert, J.G., Torsvik, T.H., 2003. The making and unmaking of a supercontinent: Rodinia
816 revisited. *Tectonophysics* 375 (1–4), 261–288.

817 Nechaev, S.V., 1974. Geochronology of the Late Precambrian deposits of the south-western
818 slope of the Russian platform. Abstract volume of the Conference on the Late
819 Precambrian (Riphean) of the Russian platform. Nauka publisher, pp. 40–47. (in
820 Russian).

821 Nosova, A.A., Kuzmenkova, O.F., Veretennikov, N.V., Petrova, L.G., Levskiy, L.K., 2008.
822 Neoproterozoic Volyn-Brest magmatic province on western margin of the East
823 European Craton: Peculiarities of intracratonic magmatism in the area of ancient suture
824 zone. *Petrologia* 16, 115–147 (in Russian).

825 Paczeńska, J., 2010. The evolution of late Ediacaran riverine-estuarine system in the Lublin-
826 Podlasie slope of the East European Craton, southeastern Poland. *Polish Geological*
827 *Institute Special Papers* 27, 1–96.

828 Pehr, K., Love, G.D., Kuznetsov, A., Podkovyrov, V., Junium, C.K., Shumlyanskyy, L.,
829 Sokur, T., Bekker, A., 2018. Ediacaran fauna flourished in oligotrophic and bacterially
830 dominated marine environments. *Nature communications* 9, 1807.

831 Pisarevsky, S.A., Wingate, M.T., Powell, C.M., Johnson, S., Evans, D.A., 2003. Models of
832 Rodinia assembly and fragmentation. Geological Society, London, Special Publications
833 206 (1), 35–55.

834 Pisarevsky, S.A., Elming, S.-Å., Pesonen, L.J., Li, Z.-X., 2014. Mesoproterozoic
835 paleogeography: supercontinent and beyond. *Precambrian Research* 244, 207–225.

836 Popov, V., Iosifidi, A., Khramov, A., Tait, J., Bachtadse, V., 2002. Paleomagnetism of Upper
837 Vendian sediments from the Winter Coast, White Sea region, Russia: implications for
838 the paleogeography of Baltica during Neoproterozoic times. *Journal of Geophysical*
839 *Research* 107 (B11), 1–0EPM10; 1–8.

840 Poprawa, P., Radkovets, N., Rauball, J., 2018. Ediacaran-Paleozoic subsidence history of the
841 Volyn-Podillya-Moldavia Basin (W and SW Ukraine, Moldova, NE Romania).
842 Geological Quarterly 62 (3), 459–486.

843 Porębski, S.J., Anczkiewicz, R., Paszkowski, M., Skompski, S., Kędzior, A., Mazur, S.,
844 Szczepański, S., Buniak, A., Mikołajewski, Z., 2019. Hirnantian icebergs in the
845 subtropical shelf of Baltica: Evidence from sedimentology and detrital zircon
846 provenance. Geology 47, 284–288.

847 Rogers, J.J., Santosh, M., 2002. Configuration of Columbia, a Mesoproterozoic
848 supercontinent. Gondwana Research 5 (1), 5–22.

849 Rozanov, A.Yu., Łydka, K., 1987. Paleogeography and Lithology of the Vendian and
850 Cambrian of the western East European Platform. Wydawnictwa Geologiczne,
851 Warsaw. 114 pp.

852 Rubatto, D., 2017. Zircon: The Metamorphic Mineral. Reviews in Mineralogy &
853 Geochemistry 83, 261–295.

854 Rundqvist, D.V., Mitrofanov, F.P., 1993. Precambrian Geology of the USSR, in:
855 Developments in Precambrian Geology, Windley, B.F. (Ed.), Elsevier, Amsterdam-
856 New York-London-Tokyo, 1440 pp.

857 Shumlyanskyy, L., 2012. Evolution of the Vendian flood basalt magmatism in the Volyn
858 region. Mineralogical Journal (Ukraine) 34 (4), 50–68 (in Ukrainian).

859 Shumlyanskyy, L., 2014. Geochemistry of the Osnitsk-Mikashevichy volcanoplutonic
860 complex of the Ukrainian shield. Geochemistry International 52, 912–924.

861 Shumlyanskyy, L., Hawkesworth, C., Dhuime, B., Billström, K., Claesson, S., Storey, C.,
862 2015. $^{207}\text{Pb}/^{206}\text{Pb}$ ages and Hf isotope composition of zircons from sedimentary rocks
863 of the Ukrainian shield: crustal growth of the south-western part of East European
864 craton from Archaean to Neoproterozoic. Precambrian Research 260, 39–54.

865 Shumlyanskyy, L., Nosova, A., Billström, K., Söderlund, U., Andréasson, P.-G.,
 866 Kuzmenkova, O., 2016. The U-Pb zircon and baddeleyite ages of the Neoproterozoic
 867 Volyn Large Igneous Province: implication for the age of the magmatism and the
 868 nature of a crustal contaminant. *GFF* 138, 17–30.

869 Shumlyanskyy, L., Hawkesworth, C., Billström, K., Bogdanova, S., Mytrokhyn, O., Romer,
 870 R., Dhuime, B., Claesson, S., Ernst, R., Whitehouse, M., Bilan, O., 2017. The origin of
 871 the Palaeoproterozoic AMCG complexes in the Ukrainian Shield: new U-Pb ages and
 872 Hf isotopes in zircon. *Precambrian Research* 292, 216–239.

873 Sinyakovskaya, I., Zaykov V., Kitagawa R., 2005. Types of Pyrophyllite Deposits in
 874 Foldbelts. *Resource Geology* 55 (4), 405–418.

875 Sláma, J., Pedersen, R.B., 2015. Zircon provenance of SW Caledonian phyllites reveals a
 876 distant Timanian sediment source. *Journal of the Geological Society* 172, 465–478.

877 Sláma, J., 2016. Rare late Neoproterozoic detritus in SW Scandinavia as a response to distant
 878 tectonic processes. *Terra Nova* 28, 394–401.

879 Środoń, J., Drits, V.A., McCarty, D.K., Hsieh, J.C.C., Eberl, D.D., 2001. Quantitative XRD
 880 analysis of clay-rich rocks from random preparations. *Clays & Clay Minerals* 49, 514–
 881 528.

882 Środoń, J., Szulc, J., Anczkiewicz, A., Jewuła, K., Banaś, M., Marynowski, L., 2014.
 883 Weathering, sedimentary, and diagenetic controls of mineral and geochemical
 884 characteristics of the vertebrate-bearing Silesian Keuper. *Clay Minerals* 49, 569–594.

885 Šliaupa, S., Fokin, P., Lazauskiene, J., Stephenson, R., 2006. The Vendian-Early Palaeozoic
 886 sedimentary basins of the East European craton. In: Gee, D.G., Stephenson, R.A. (Eds.)
 887 European lithosphere dynamics. *Geological Society Memoir* 32, 449–462.

888 Torsvik, T.H., Smethurst, M.A., Van der Voo, R., Trench, A., Abrahamsen, N., Halvorsen, E.,
889 1992. Baltica A synopsis of Vendian-Permian palaeomagnetic data and their
890 palaeotectonic implications. *Earth-Science Reviews* 33 (2), 133–152.

891 Torsvik, T.H., Smethurst, M.A., Meert, J.G., Van der Voo, R., McKerrow, W.S., Brasier,
892 M.D., Sturt, B.A., Walderhaug, H.J., 1996. Continental break-up and collision in the
893 Neoproterozoic and Palaeozoic – a tale of Baltica and Laurentia. *Earth-Science*
894 *Reviews* 40 (3–4), 229–258

895 Torsvik, T.H., Rehnström, E.F., 2001. Cambrian palaeomagnetic data from Baltica:
896 implications for true polar wander and Cambrian palaeogeography. *Journal of the*
897 *Geological Society* 158 (2), 321–329.

898 Torsvik, T.H., 2003. The Rodinia jigsaw puzzle. *Science* 300 (5624), 1379–1381.

899 Valverde-Vaquero, P., Dörr, W., Belka, Z., Franke, W., Wiszniewska, J., Schastok, J., 2000.
900 U–Pb single-grain dating of detrital zircon in the Cambrian of central Poland:
901 implications for Gondwana versus Baltica provenance studies. *Earth and Planetary*
902 *Science Letters* 184, 225–240.

903 Weber, B., Scherer, E.E., Schulze, C., Valencia, V.A., Montecinos, P., Mezger, K., Ruiz, J.,
904 2010. U–Pb and Lu–Hf isotope systematics of lower crust from central-southern
905 Mexico–Geodynamic significance of Oaxaquia in a Rodinia Realm. *Precambrian*
906 *Research* 182 (1–2), 149–162.

907 Weil, A.B., Van der Voo, R., Mac Niocaill, C., Meert, J.G., 1998. The Proterozoic
908 supercontinent Rodinia: paleomagnetically derived reconstructions for 1100 to 800 Ma.
909 *Earth and Planetary Science Letters* 154 (1–4), 13–24.

910 Zhao, G., Cawood, P.A., Wilde, S.A., Sun, M., 2002. Review of global 2.1–1.8 Ga orogens:
911 implications for a pre-Rodinia supercontinent. *Earth-Science Reviews* 59 (1–4), 125–
912 162.

913 Zhao, G., Sun, M., Wilde, S.A., Li, S., 2004. A Paleo-Mesoproterozoic supercontinent:
914 assembly, growth and breakup. *Earth-Sciences Reviews* 67, 91–123.
915

Figure captions

Fig. 1. (a) The main structural elements of pre-Ediacaran Baltica (modified from Johansson et al., 2009; Bogdanova et al., 2015). (b) Present day maximum extent of the Ediacaran sediments (Kotlin) on investigated part of Baltica, the extent of underlying Volyn sediments and volcanics (in worm's eye map manner; modified from Rozanov and Łydka, 1987; Nosova et al., 2008; Kuzmenkova et al., 2010, 2016), and Rapakivi granites (after Isozaki et al. 2014; Bogdanova et al., 2015; Krzemińska et al. 2015), and of the boreholes sampled in this study. The borehole geographic coordinates: Vil'chytsy – 53°47'N, 30°21'E; Bogushevsk – 54°50'N, 30°12'E; Lepel – 54°53'N, 28°42'E; Kobryn – 52°13'N, 24°23'E; Pinsk – 52°07'N, 26°10'E.

Fig. 2. Correlation of the drilled sections with marked depths of studied samples. Maximum depositional ages estimated in this study are given when applicable.

Fig. 3. Composite stratigraphic chart for the western part of Belarus. Compiled from Chumakov and Semikhatov (1981), Rundqvist and Mitrofanov (1993), Makhnach et al. (2005) and Paczeńska (2010).

Fig. 4. Quantitative mineral composition of the subsequent rock series, averaged for all investigated profiles: (a) quartz and weathering indices: kaolinite/dioctahedral 2:1 clay (left) and quartz/sum primary minerals (right); (b) other primary minerals, including sum of basaltic minerals (Ca-plagioclase, pyroxene, aluminoceladonite, saponite, chlorite, chlorite-smectite, analcime, and clinoptilolite); (c) weathering (anatase, hematite, kaolinite, and dioctahedral 2:1 clay) and authigenic (goethite, pyrite, apatite, siderite, dolomites, berthierine, gypsum, jarosite, barite) minerals.

Fig. 5. Representative cathodoluminescence (CL) images of the analysed zircons including spot number, U-Pb age with $\pm 2\sigma$ error (Ma) and ϵ_{Hf} with $\pm 2\sigma$ error (in italic).

Fig. 6. Probability density plots presenting U-Pb age data yielded by zircons from Belarus, combined for A and B groups of zircons (see text for explanation).

Fig. 7. ϵ_{Hf} vs. time plots presenting results for each sample investigated. $^{206}\text{Pb}/^{238}\text{U}$ age for data <1000 Ma and $^{207}\text{Pb}/^{206}\text{Pb}$ age for data >1000 Ma. New crust evolution line according to Dhuime et al. (2011).

Fig. 8. Paleogeographic reconstruction of the Baltica paleocontinent during eruptions of the Volynian traps at c. 570 Ma. Detritus derivation from the SW margin of Baltica and Volynian trap basalts.

Fig. 9. Paleogeographic reconstruction of the Baltica paleocontinent during deposition of lower and middle Cambrian (Terreneuvian, c. 532 Ma) partly based on Šliaupa et al. (2006). Sourcing from an orogen/magmatic arc (Scythian orogen) approaching the SW Baltica edge.

Fig. 10. ϵ_{Hf} vs. time plot summarizing results for all samples. $^{206}\text{Pb}/^{238}\text{U}$ age for data <1000 Ma and $^{207}\text{Pb}/^{206}\text{Pb}$ age for data >1000 Ma. New crust evolution line according to Dhuime et al. (2011).

Table captions:

Table 1. Samples used for isotopic measurements of zircons.

Table 2. U-Pb ages and Hf isotope composition in investigated zircons.

Supplementary Data (online only)

Supplementary Data 1 (SD1). Detailed description of analytical methods.

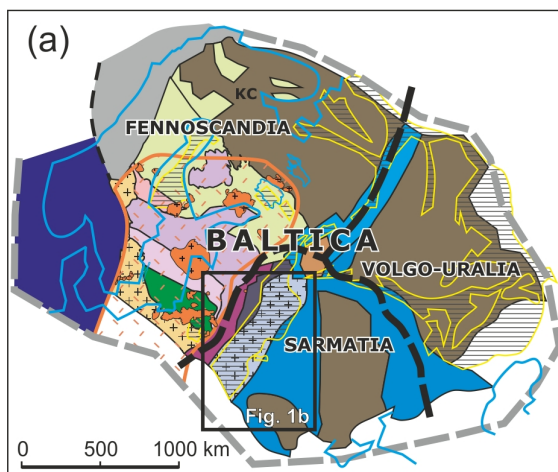
Supplementary Data 2 (SD2). U-Pb zircon standards data.

Supplementary Data 3 (SD3). Hf zircon standards data.

Supplementary Data 4 (SD4). Summary of LA-ICP-MS U-Pb age data.

965 **Table S1.** Average quantitative XRD mineral composition of mudstones from different
966 stratigraphic units in five studied Belarussian wells. Weathering indices used in the text
967 are presented in the two columns on the right.

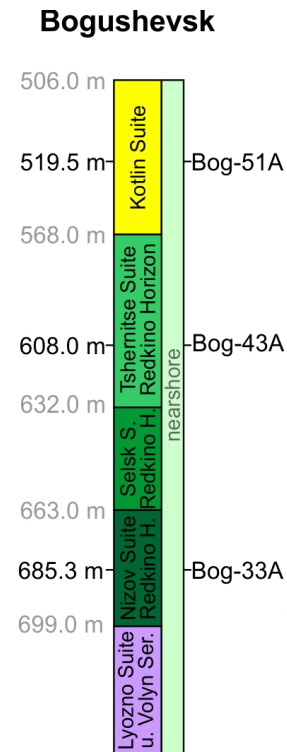
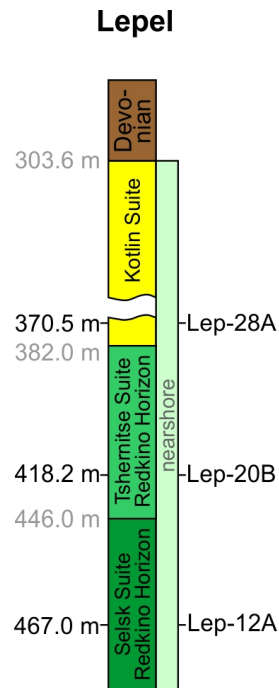
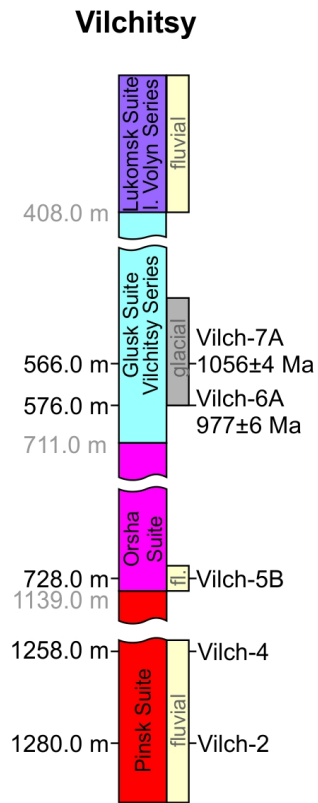
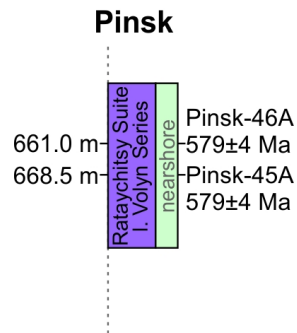
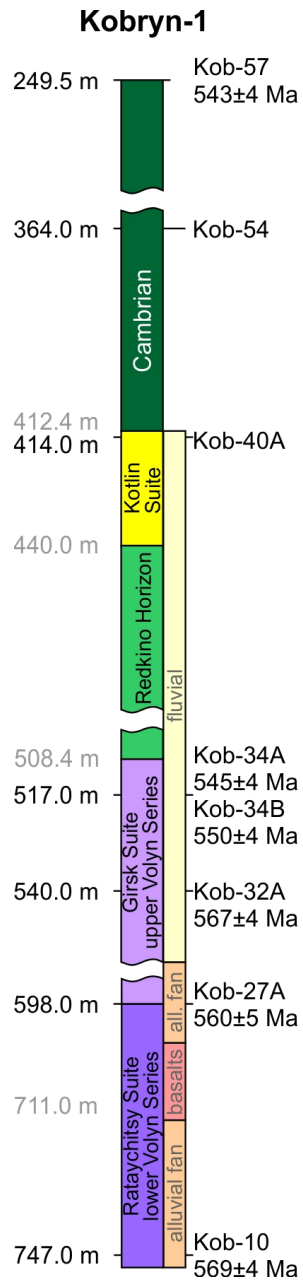
968 **Table S2.** Results of the U-Pb analyses of zircons.



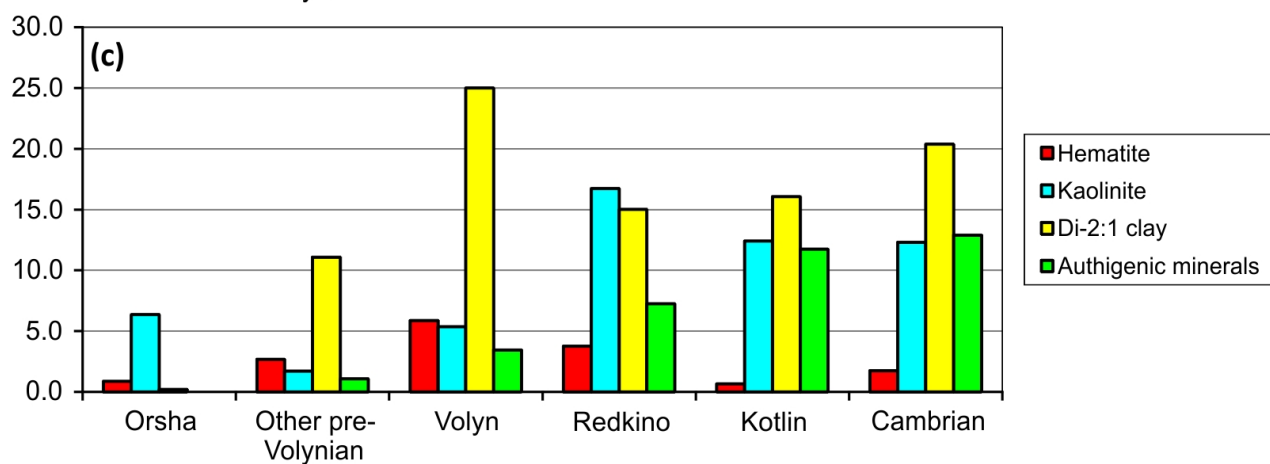
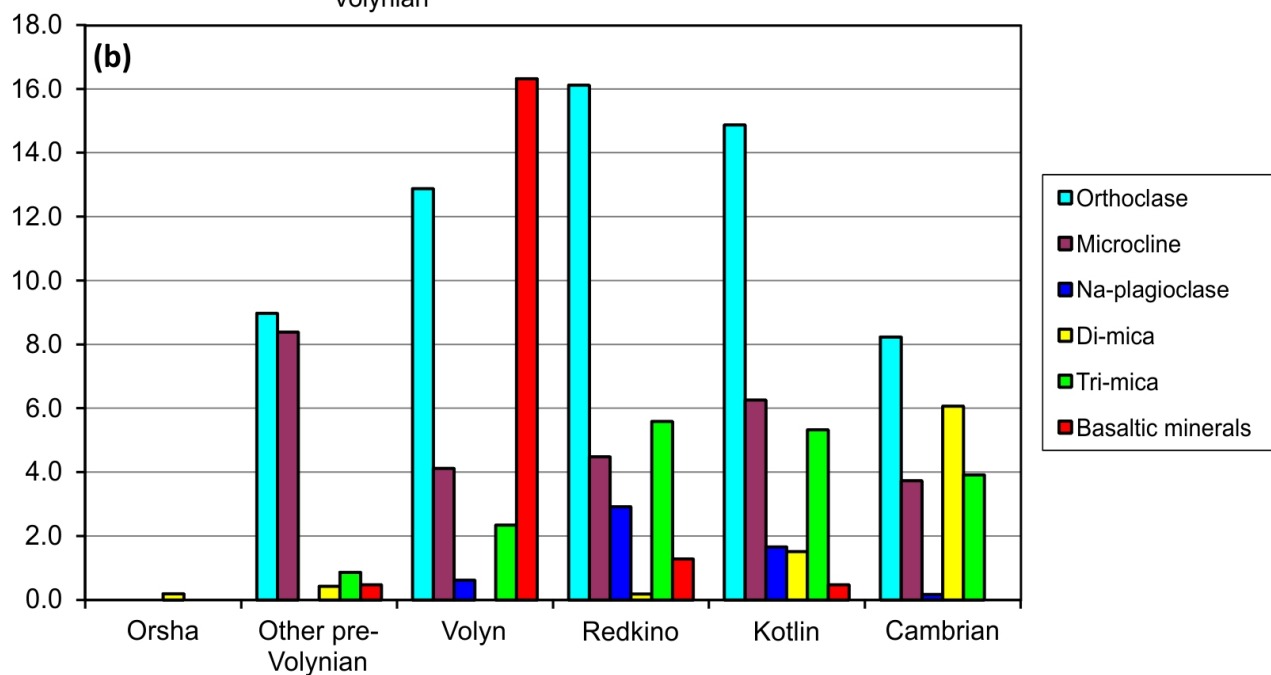
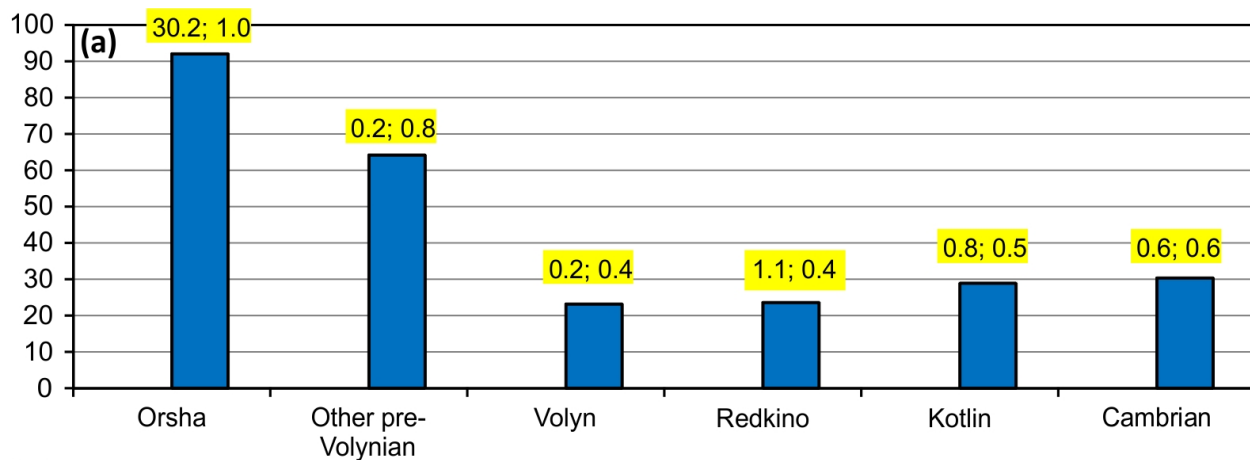
- Archean cratonic nuclei (>2.5 Ga)
- Central Finland Arc Complex (1.89 Ga)
- Bergslagen - Livonia (1.89-1.87 Ga)
- Ljusdal (1.87-1.84 Ga)
- Mid-Baltic Belt (1.86-1.84 Ga)
- Amberland (1.84-1.81 Ga)
- Archean and Paleoproterozoic crust reworked at 1.8-1.6 Ga
- Orogenic belts (2.2-1.95 Ga)
- TIB 0-2 (1.81-1.70 Ga)
- Osnitsk-Mikashevichi Igneous Belt (1.98-1.95 Ga)
- Okolovo / Belarus-Podlasie granulite belt (1.90 Ga)
- Presumable western fringe of Baltica crust
- Mesoproterozoic Rapakivi effusives (ca 1.3-1.6 Ga)
- Sveconorwegian/Grenvillian/Telemarkian crust (ca 0.9-1.3 Ga)
- Presumable extent of Mesoproterozoic Rapakivi effusives
- Maximum presumable extent of Paleo- to Mesoproterozoic (Riphean) undeformed sedimentary cover
- Recent shorelines & lakes
- Borders of main Baltica crust domains

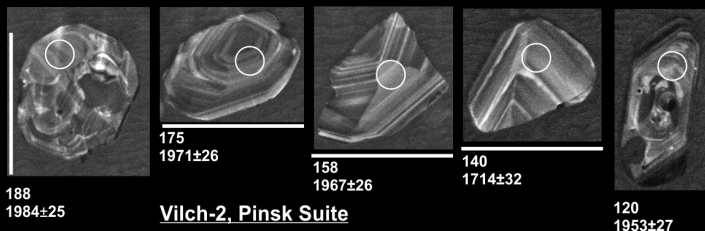


- | | |
|---|--|
| Eroded land on Baltica | Upper Ediacaran deposits outside of Volynian effusives |
| Examined boreholes | Lower basalts and pyroclastics |
| State border | Tholeiitic basalts of Upper Series (lower to high-Ti) |
| Towns | Volcanoclastics |
| Pripjat Through | Rapakivi granites |
| Rift shoulder | Felsic and intermediate volcanics |
| Łukov-Ratno Horst | BB Brest Basin |
| | OB Orsha Basin |

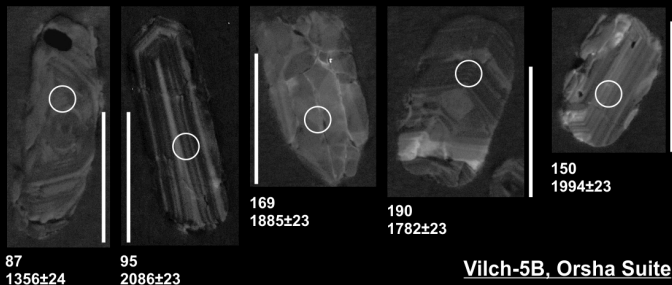


 stratigraphic gap[illegible]

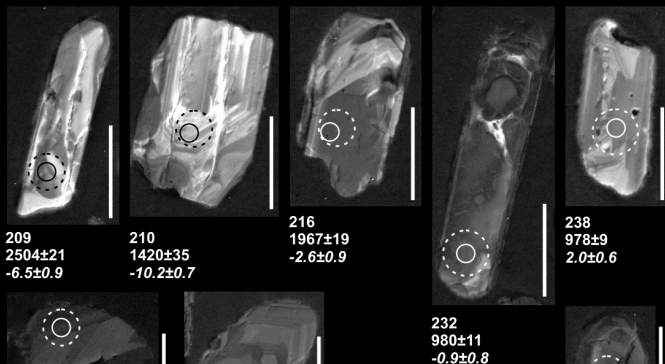




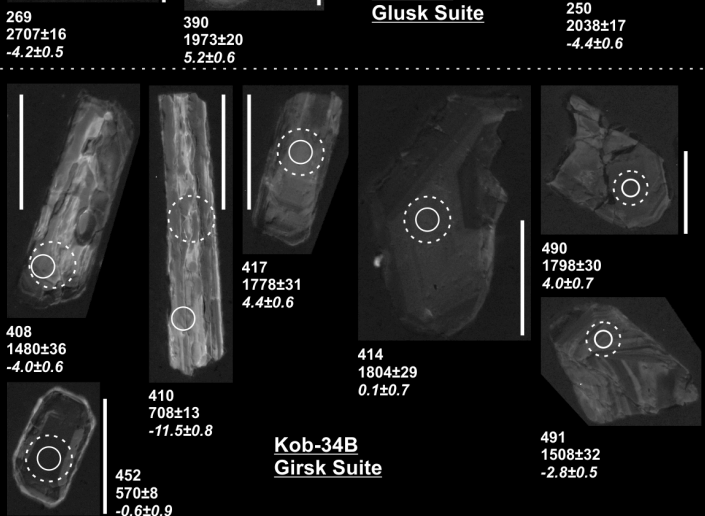
Vilch-2, Pinsk Suite



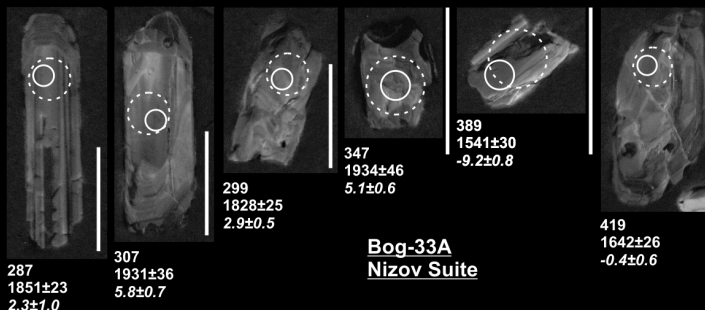
Vilch-5B, Orsha Suite



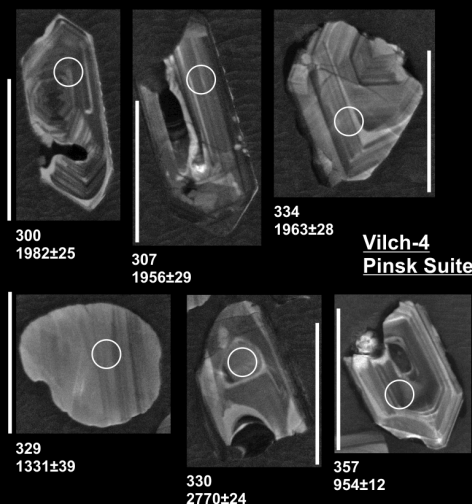
**Vilch-6A
Glusk Suite**



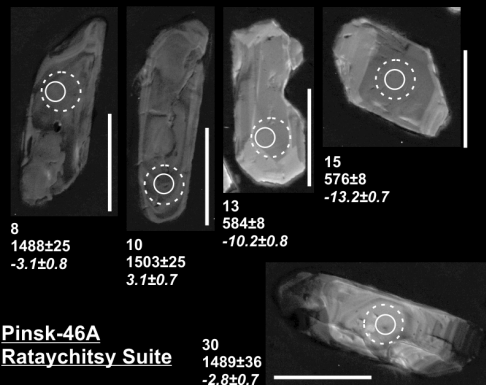
**Kob-34B
Girsk Suite**



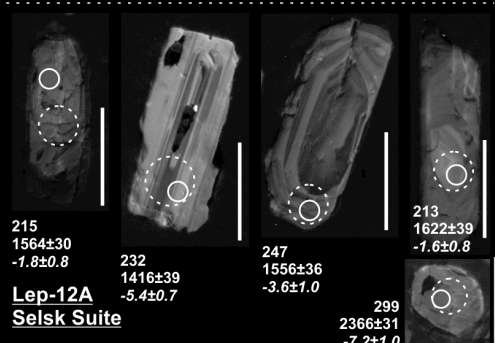
**Bog-33A
Nizov Suite**



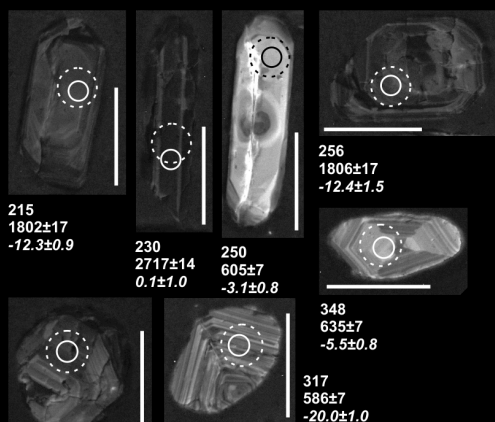
**Vilch-4
Pinsk Suite**



**Pinsk-46A
Rataychitsy Suite**

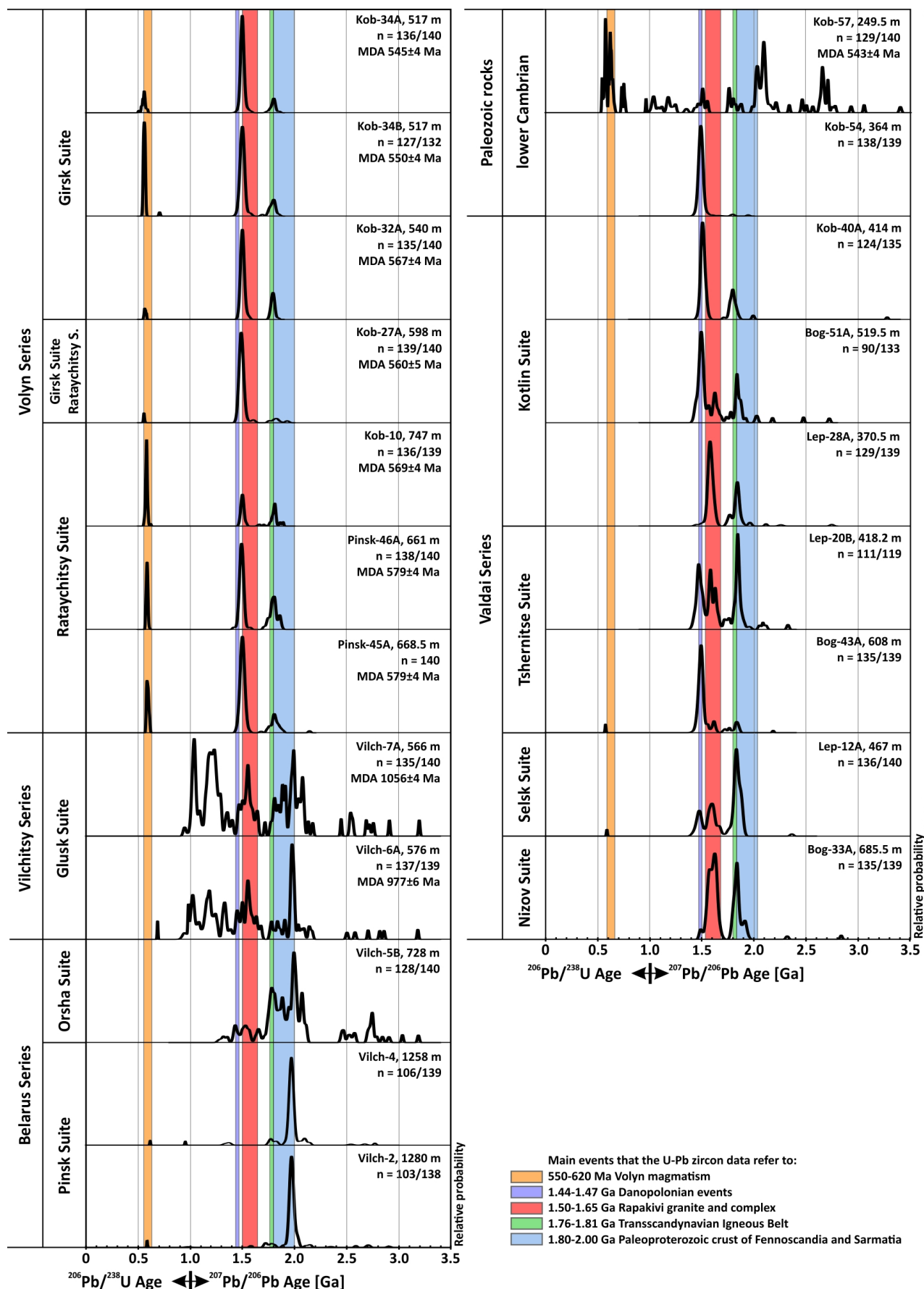


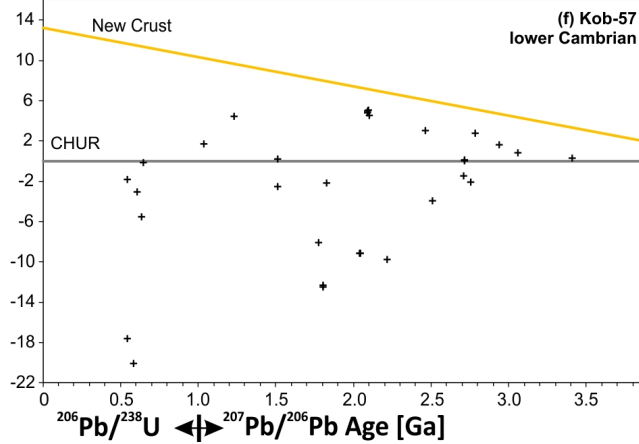
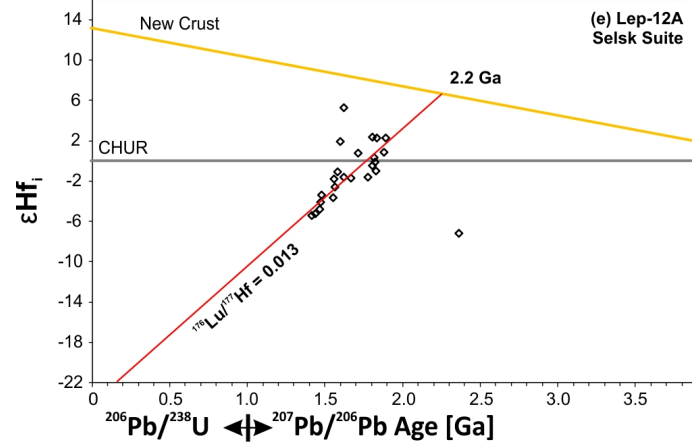
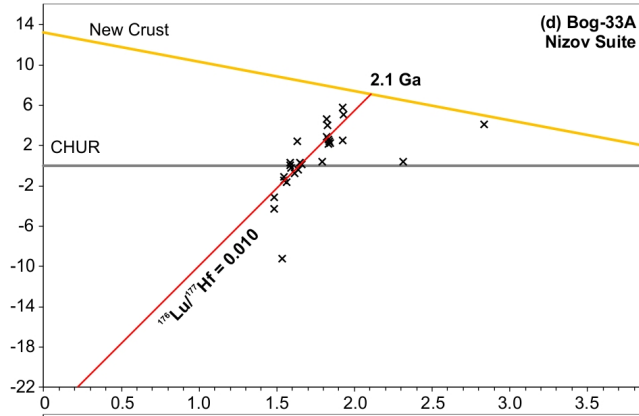
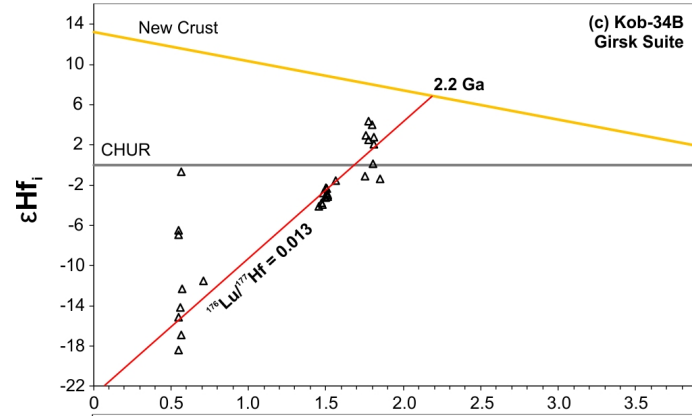
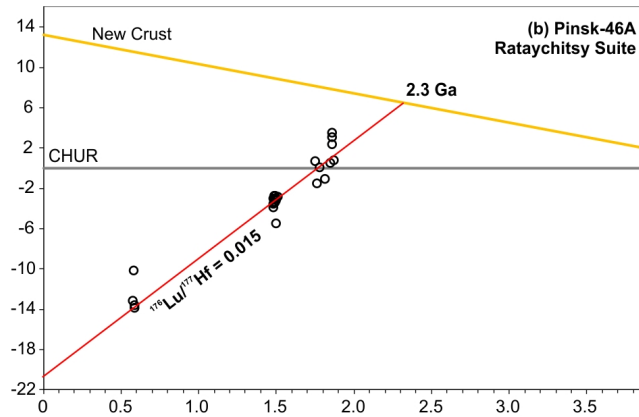
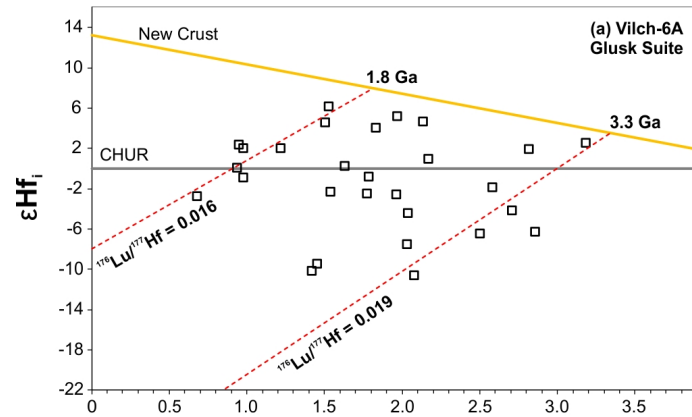
**Lep-12A
Selsk Suite**

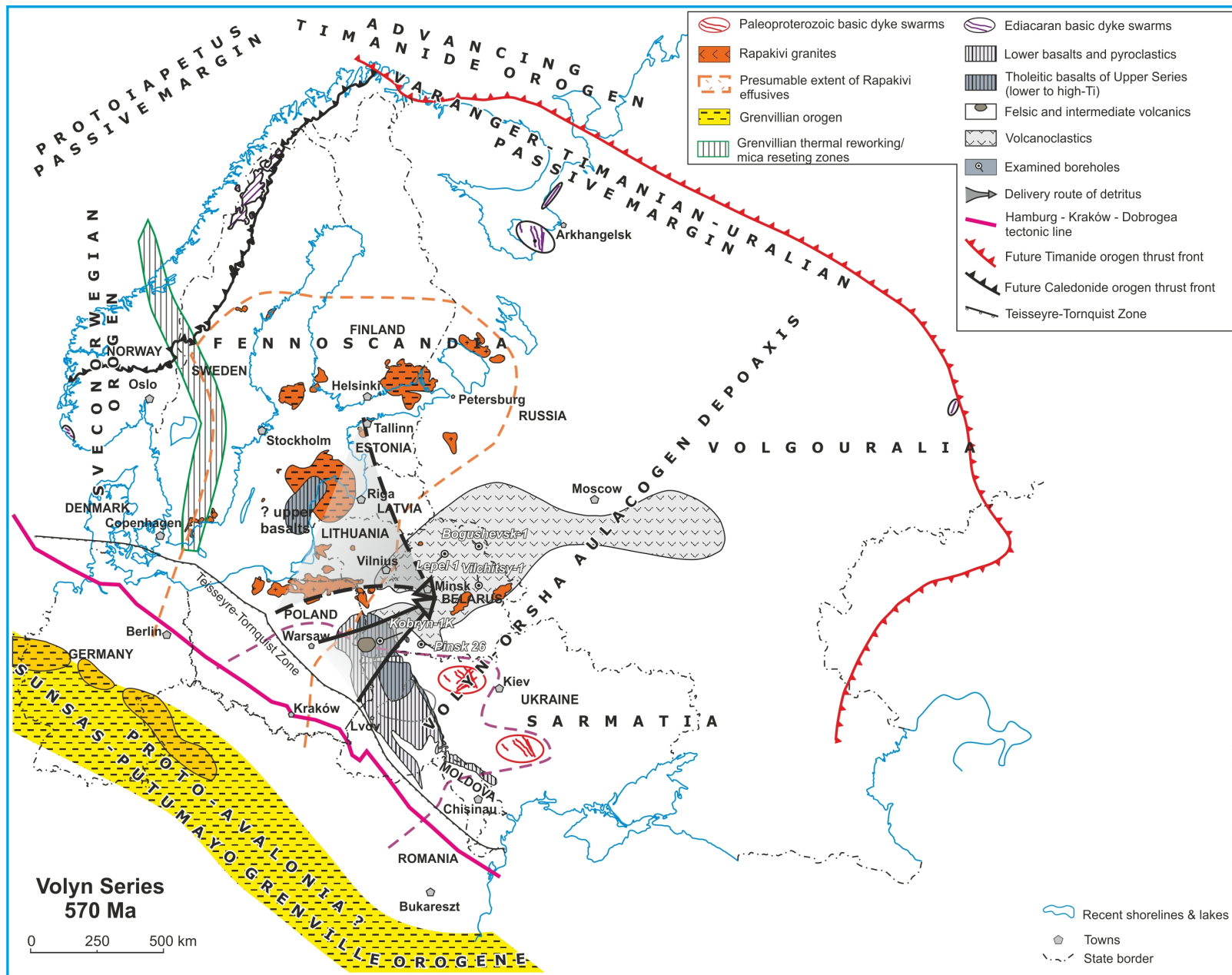


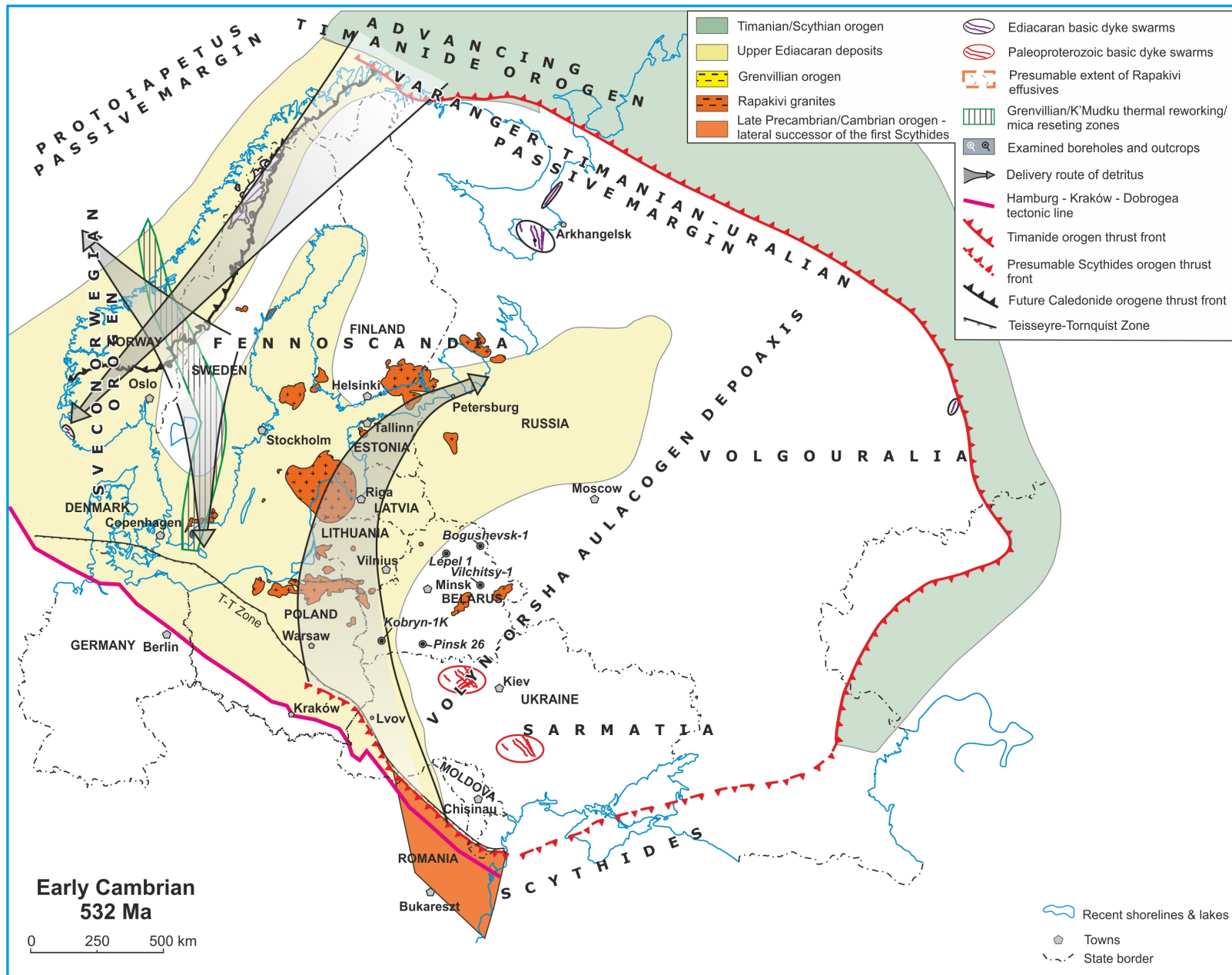
**Kob-57
lower Cambrian**

○ $^{206}\text{Pb}/^{238}\text{U}$ or $^{207}\text{Pb}/^{209}\text{Bi}$ age $\pm 2\text{SE}$
 ○ $\epsilon\text{Hf} \pm 2\text{SE}$
 scale bars 100 μm









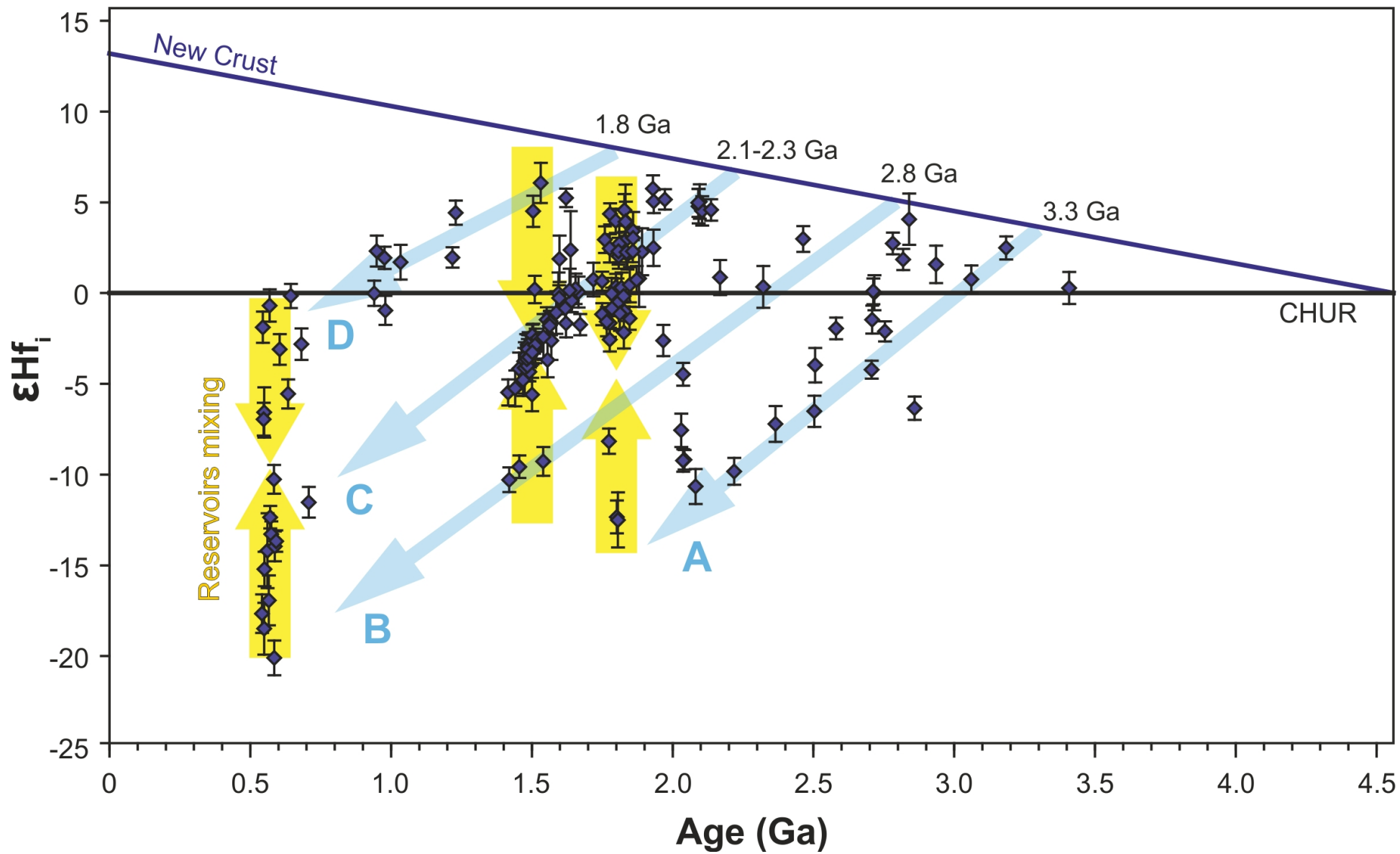


Table 1. Samples used for isotopic measurements of zircons.

Abbreviation	Borehole name	Depth [m]	Lithology	Stratigraphic interval
Kob-57	Kobryn-1	249.5	coarse-grained sandstone	lower Cambrian
Kob-54	Kobryn-1	364.0	glauconite-bearing quartz arenite	lower Cambrian
Kob-40A	Kobryn-1	414.0	subarkose	Kotlin Suite
Kob-34A	Kobryn-1	517.0	tuff	Girsk Suite
Kob-34B	Kobryn-1	517.0	arkose	Girsk Suite
Kob-32A	Kobryn-1	540.0	arkose/wacke	Girsk Suite
Kob-27A	Kobryn-1	598.0	soft brown tuff	Girsk Suite / Rataychitsy Suite
Kob-10	Kobryn-1	747.0	volcanogenic sandstone	Rataychitsy Suite
Pinsk-46A	Pinsk	661.0	tuffite	Rataychitsy Suite
Pinsk-45A	Pinsk	668.5	sandy tuffite	Rataychitsy Suite
Vilch-7A	Vilchitsy	566.0	tillite	Glusk Suite
Vilch-6A	Vilchitsy	576.0	tillite	Glusk Suite
Vilch-5B	Vilchitsy	728.0	quartz arenite	Orsha Suite
Vilch-4	Vilchitsy	1258.0	sandstone	Pinsk Suite
Vilch-2	Vilchitsy	1280.0	sandstone	Pinsk Suite
Lep-28A	Lepel	370.5	arkosic sandstone	Kotlin Suite
Lep-20B	Lepel	418.2	subarkose	Tshernitse Suite
Lep-12A	Lepel	467.0	arkose	Selsk Suite
Bog-51A	Bogushevsk	519.5	arkose	Kotlin Suite
Bog-43A	Bogushevsk	608.0	arkose/wacke	Tshernitse Suite
Bog-33A	Bogushevsk	685.3	quartz arenite/subarkose	Nizov Suite

Supplementary Data SD1. Detailed description of analytical methods.

U-Pb measurements

The sample selection was primarily based on the presence of zircons that may constrain timing of volcanic activity coeval with sedimentation, in addition to the detrital zircons, present in all separated zircon populations and dated for provenance. All selected samples contained euhedral zircons, including needle-shaped acicular crystals typical for rapidly crystallized, porphyritic, sub-volcanic intrusions or high-level granites (cf. Corfu et al., 2003), that potentially may constrain maximum depositional ages of Riphean and Ediacaran sediments. Analytical strategy included selecting c. 40 most euhedral grains with sharp edges (named group A), whenever possible, and c. 100 grains representing random detrital population for provenance analysis (named group B), particularly in terms of geotectonic setting of the potential source terrains.

Zircons were separated by routine methods including crushing and sieving, followed by electromagnetic and heavy liquids separations. Zircons were mounted on adhesive tape and carbon-coated for imaging of the morphology by using Scanning Electron Microscopy at the Institute of Petrology and Structural Geology, Charles University in Prague. Then zircons were mounted in epoxy resin and polished for CL imaging prior to U-Pb measurements.

A Thermo Scientific Element 2 sector field ICP-MS coupled to a 193 nm ArF excimer laser (Teledyne Cetac Analyte Excite laser) at the Institute of Geology of the Czech Academy of Sciences, Prague, Czech Republic, was used to measure the Pb/U and Pb isotopic ratios in zircons. The laser was fired at a repetition rate of 5 Hz and fluence of 3.17–3.66 J/cm² with 20–25-micron spot size, depending on the zircon grain size. The carrier gas was flushed through the two-volume ablation cell at a flow rate of 0.7 L/min and mixed with 0.66 L/min Ar and 0.004 L/min N prior to introduction into the ICP. The in-house glass signal homogenizer (design of Tunheng and Hirata, 2004) was used for mixing all the gases and aerosol resulting in smooth, spike-free signal. The signal was tuned for maximum sensitivity of Pb and U, Th/U ratio close to unity and low oxide level, commonly below 0.2 %. Typical acquisitions consisted of 15 second of blank measurement followed by measurement of U, Th and Pb signals from the ablated zircon for another 35 seconds. The total of 420 mass scans data were acquired in time resolved – peak jumping – pulse counting / analogue mode with 1 point measured per peak for masses ²⁰⁴Pb + Hg, ²⁰⁶Pb, ²⁰⁷Pb, ²⁰⁸Pb, ²³²Th, ²³⁵U, and ²³⁸U. Due

to a non-linear transition between the counting and analogue acquisition modes of the ICP instrument, the raw data were pre-processed using a purpose-made Excel macro. As a result, the intensities of ^{238}U were left unchanged if measured in a counting mode and recalculated from ^{235}U intensities if the ^{238}U was acquired in analogue mode. Data reduction was then carried out off-line using the Iolite data reduction package version 3.4 with VizualAge utility (Petrus and Kamber, 2012). Full details of the data reduction methodology can be found in Paton et al. (2010). The data reduction included correction for gas blank, laser-induced elemental fractionation of Pb and U and instrument mass bias. For the data presented here, blank intensities and instrumental bias were interpolated using an automatic spline function while down-hole inter-element fractionation was corrected using an exponential function. No common Pb correction was applied to the data due to the high Hg contamination of the commercially available He carrier gas, which precludes accurate correction of the interfering ^{204}Hg on the very small signal of ^{204}Pb (common lead).

Residual elemental fractionation and instrumental mass bias were corrected by normalization to the natural zircon reference material Plešovice (Sláma et al., 2008). The excess variance (Paton et al., 2010) of Plešovice zircon was calculated in Isoplot and quadratically added to the measurement uncertainties of all unknowns including validation zircon reference materials GJ-1 {nr. 63} (Jackson et al., 2004) and 91500 (Wiedenbeck et al., 1995). These two were periodically analysed during the measurement for quality control. The values obtained from analyses performed over many days (discordant GJ-1: mean concordia age of 600 ± 3 Ma (2σ), mean $^{207}\text{Pb}/^{206}\text{Pb}$ age of 608 ± 2 Ma (2σ); near-concordant 91500: mean concordia age of 1065 ± 5 Ma (2σ); see the STD data and plots in the electronic supplementary material) correspond perfectly and are less than 1% accurate within the published reference values (GJ-1: $^{206}\text{Pb}/^{238}\text{U}$ age of 600.5 ± 0.4 Ma, Schaltegger et al., 2015 and $^{207}\text{Pb}/^{206}\text{Pb}$ age of 608.53 ± 0.4 Ma, Jackson et al., 2004 respectively; 91500: $^{207}\text{Pb}/^{206}\text{Pb}$ age of 1065.4 ± 0.3 Ma, Wiedenbeck et al., 1995). The zircon U–Pb ages are presented as concordia (pooled) age and probability density plots generated with the ISOPLOT program v. 4.16 (Ludwig, 2008).

Maximum depositional ages were calculated using from 2 to 5 youngest zircons following Dickinson and Gehrels (2009). These are presented as concordia ages calculated from the youngest zircons with <2.0 % discordance.

Lu-Hf measurements

The Lu-Hf analyses were performed at the University of Bristol (Bristol Isotope Group) using a ThermoFinnigan Neptune plus multicollector inductively-coupled plasma mass spectrometer (MC-ICP-MS) coupled with a Photon-Machine Analyte G2 Excimer laser (193 nm wavelength). Ablation was performed using 50 μm and 40 μm spot sizes, a laser frequency of 4 Hz, and the energy density of the laser beam was c. 5.5 J/cm². A typical analysis was 90 seconds, including a 30 seconds background measurement and a 60 seconds ablation period. Correction for the interferences and mass bias followed the Bristol routine procedure (Hawkesworth and Kemp, 2006; Kemp et al., 2009). The correction for the isobaric interference of Yb and Lu on ¹⁷⁶Hf was made following a method detailed in Fisher et al. (2011). For Yb, the interference-free ¹⁷¹Yb was corrected for mass bias effects using an exponential law and ¹⁷³Yb/¹⁷¹Yb = 1.132685 (Chu et al., 2002). The mass bias-corrected ¹⁷¹Yb was monitored during the run and the magnitude of the ¹⁷⁶Yb interference on ¹⁷⁶Hf was calculated using ¹⁷⁶Yb/¹⁷¹Yb = 0.901864 (Chu et al., 2002). For Lu, the interference-free ¹⁷⁵Lu was corrected for mass bias effects assuming $\beta_{\text{Lu}} = \beta_{\text{Yb}}$ and using an exponential law. The mass bias-corrected ¹⁷⁶Lu was monitored during the run and the magnitude of the ¹⁷⁶Lu interference on ¹⁷⁶Hf was calculated using ¹⁷⁶Lu/¹⁷⁵Lu = 0.02655 (Vervoort et al., 2004). Interference-corrected ¹⁷⁶Hf/¹⁷⁷Hf were corrected for mass bias using an exponential law and ¹⁷⁹Hf/¹⁷⁷Hf = 0.7325 (Patchett et al., 1981). To facilitate data comparison between labs, a final correction was applied to ¹⁷⁶Hf/¹⁷⁷Hf ratios to account for the ca. 80 ppm difference between the JMC-475 solution value measured in Bristol (0.282137±6) and the accepted value of 0.282160 for this standard (Blichert-Toft et al., 1997). ¹⁷⁶Hf/¹⁷⁷Hf initial values were calculated using the ¹⁷⁶Lu decay constant of Söderlund et al. (2004) and the U-Pb crystallisation ages of the zircons. Uncertainties over crystallisation ages were taken into account for the calculation of initial Hf isotope ratios. The accuracy and long-term reproducibility of the measurements were gauged by analyzing three zircon reference standards: Plešovice (¹⁷⁶Hf/¹⁷⁷Hf = 0.282478±23, n = 21), Mud Tank (¹⁷⁶Hf/¹⁷⁷Hf = 0.282506±19, n = 21) and TEMORA 2 (¹⁷⁶Hf/¹⁷⁷Hf = 0.282683±22, n = 8). All errors are given at 2 s.d. level. ¹⁷⁶Hf/¹⁷⁷Hf initial values were calculated using the ¹⁷⁶Lu decay constant of Söderlund et al. (2004). New crust evolution curve of Dhuime et al. (2011), and chondritic values from Bouvier et al. (2008) were used for model age calculations.

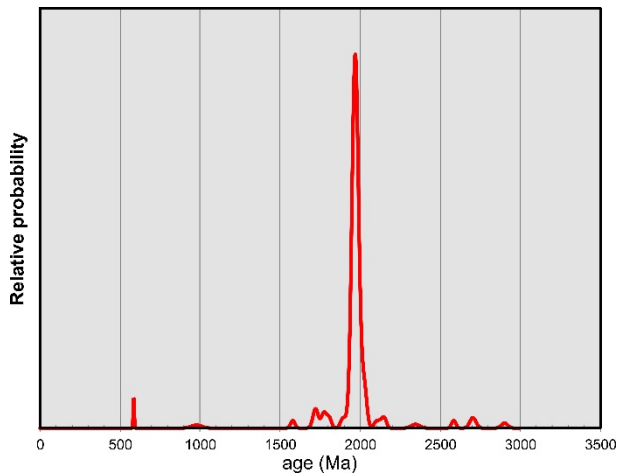
References

- Blichert-Toft, J., Chauvel, C., Albarède, F., 1997. Separation of Hf and Lu for high-precision isotope analysis of rock samples by magnetic sector-multiple collector ICP-MS. *Contributions to Mineralogy and Petrology* 127, 248–260.
- Bouvier, A., Vervoort, J.D., Patchett, P.J., 2008. The Lu-Hf and Sm-Nd isotopic composition of CHUR: constraints from unequilibrated chondrites and implications for the bulk composition of terrestrial planets. *Earth and Planetary Science Letters* 273, 48–57.
- Chu, N.-Ch., Taylor, R.N., Chavagnac, V., Nesbitt, R.W., Boella, R.M., Milton, J.A., German, Ch.R., Bayon, G., Burton, K., 2002. Hf isotope ratio analysis using multi-collector inductively coupled plasma mass spectrometry: an evaluation of isobaric interference corrections. *Journal of Analytical Atomic Spectrometry* 17, 1567–1574.
- Corfu, F., Hanchar, J.M., Hoskin, P.W.O., Kinny, P., 2003. Atlas of zircon textures. In: Hanchar, J.M., Hoskin, P.W.P. (eds.) *Zircon*. Mineralogical Society of America. *Reviews in Mineralogy and Geochemistry* 53, pp. 469–500.
- Dhuime, B., Hawkesworth, Ch., Cawood, P., 2011. When Continents Formed. *Science* 331, 154–155.
- Dickinson, W.R., Gehrels, G.E., 2009. Use of U–Pb ages of detrital zircons to infer maximum depositional ages of strata: A test against a Colorado Plateau Mesozoic database. *Earth and Planetary Science Letters* 288, 115–125.
- Fisher, Ch.M., Hanchar, J.M., Samson, S.D., Dhuime, B.D., Blichert-Toft, J., Vervoort, J.D., Lam, R., 2011. Synthetic zircon doped with hafnium and rare earth elements: A reference material for in situ hafnium isotope analysis. *Chemical Geology* 286, 32–47.
- Hawkesworth, C.J., Kemp, A.I.S., 2006. Using hafnium and oxygen isotopes in zircons to unravel the record of crustal evolution. *Chemical Geology* 226, 144–162.
- Jackson, S.E., Pearson, N.J., Griffin, W.L., Belousova, E.A., 2004. The application of laser ablation-inductively coupled plasma-mass spectrometry to in situ U-Pb zircon geochronology. *Chemical Geology* 211, 47–69.
- Kemp, A.I.S., Foster, G.L., Scherstén, A., Whitehouse, M.J., Darling, J., Storey, C., 2009. Concurrent Pb–Hf isotope analysis of zircon by laser ablation multi-collector ICP-MS, with implications for the crustal evolution of Greenland and the Himalayas. *Chemical Geology* 261, 244–260.

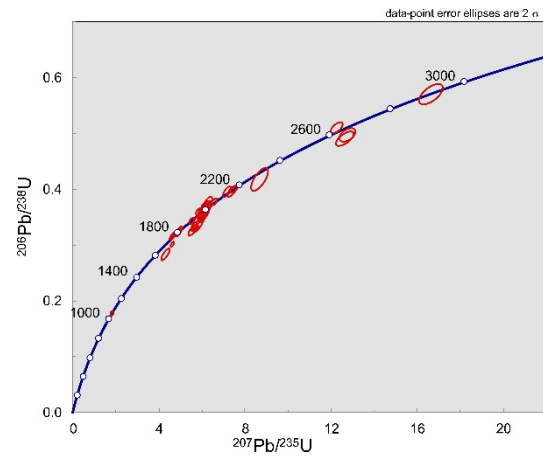
- Ludwig, K.R., 2008. Isoplot 3.70. A geochronological toolkit for Microsoft Excel. Berkley Geochronology Center Special Publication No. 4.
- Patchett, P.J., Tatsumoto, M., 1981. A routine high-precision method for Lu-Hf isotope geochemistry and chronology. *Contributions to Mineralogy and Petrology* 75, 263–267.
- Paton, C., Woodhead, J.D., Hellstrom, J.C., Hergt, J.M., Greig, A., Maas, R., 2010. Improved laser ablation u-pb zircon geochronology through robust downhole fractionation correction. *Geochemistry Geophysics Geosystems*, 11.
- Petrus, J.A., Kamber, B.S., 2012. VizualAge: A Novel Approach to Laser Ablation ICP-MS U-Pb Geochronology Data Reduction. *Geostandards and Geoanalytical Research* 36, 247–270.
- Schaltegger, U., Schmitt, A.K., Horstwood, M.S.A., 2015. U–Th–Pb zircon geochronology by ID-TIMS, SIMS, and laser ablation ICP-MS: Recipes, interpretations, and opportunities. *Chemical Geology* 402, 89–110.
- Sláma, J., Kosler, J., Condon, D.J., Crowley, J.L., Gerdes, A., Hanchar, J.M., Horstwood, M.S.A., Morris, G.A., Nasdala, L., Norberg, N., Schaltegger, U., Schoene, B., Tubrett, M.N., Whitehouse, M.J., 2008. Plesovice zircon – a new natural reference material for U-Pb and Hf isotopic microanalysis. *Chemical Geology* 249, 1–35.
- Söderlund, U., Patchett, J.P., Vervoort, J.D., Isachsen, C.E., 2004. The ^{176}Lu decay constant determined by Lu–Hf and U–Pb isotope systematics of Precambrian mafic intrusions. *Earth and Planetary Science Letters* 219, 311–324.
- Tunheng, A., Hirata, T., 2004. Development of signal smoothing device for precise elemental analysis using laser ablation-ICP-mass spectrometry. *Journal of Analytical Atomic Spectrometry* 19, 932.
- Vervoort, J. D., Patchett, P.J., Söderlund, U., Baker, M., 2004. Isotopic composition of Yb and the determination of Lu concentrations and Lu/Hf ratios by isotope dilution using MC-ICPMS. *Geochemistry, Geophysics, Geosystems*, 5, Q11002, doi: 10.1029/2004GC000721
- Wiedenbeck, M., Alle, P., Corfu, F., Griffin, W.L., Meier, M., Oberli, F., Vonquadt, A., Roddick, J.C., Spiegel, W., 1995. 3 natural zircon standards for U-Th-Pb, Lu-Hf, trace-element and REE analyses. *Geostandards Newsletter* 19, 1–23.

Supplementary Data SD4. Summary of LA-ICP-MS U-Pb age data.

1. Sandstone Vilch-2 (Vilchitsy borehole, depth 1280 m); Belarus Series, Pinsk Suite

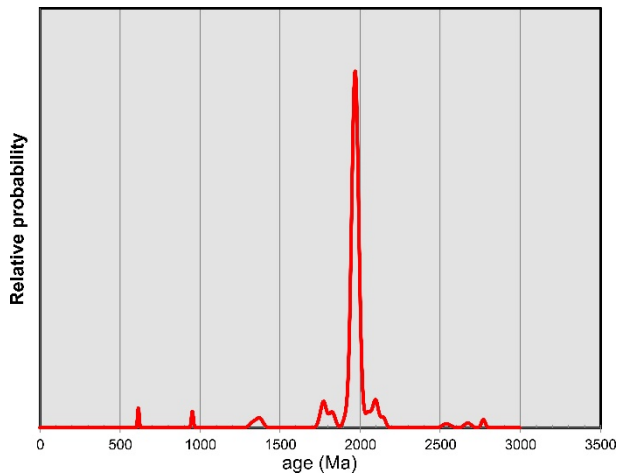


Detrital zircon age spectrum (probability density plot) (n = 103) for the Vilch-2 sample.

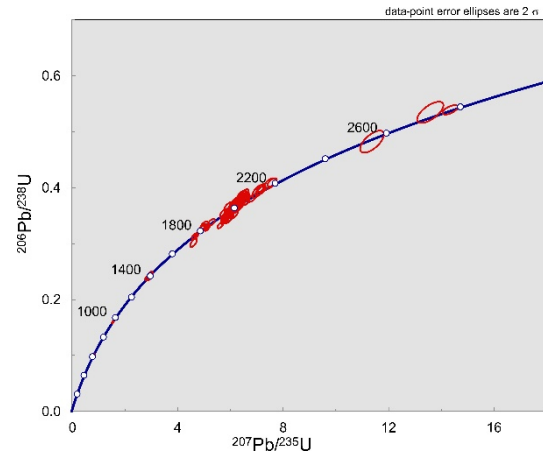


U-Pb isotopic data obtained from the detrital zircon population from the Vilch-2 sample.

2. Sandstone Vilch-4 (Vilchitsy borehole, depth 1258 m); Belarus Series, Pinsk Suite

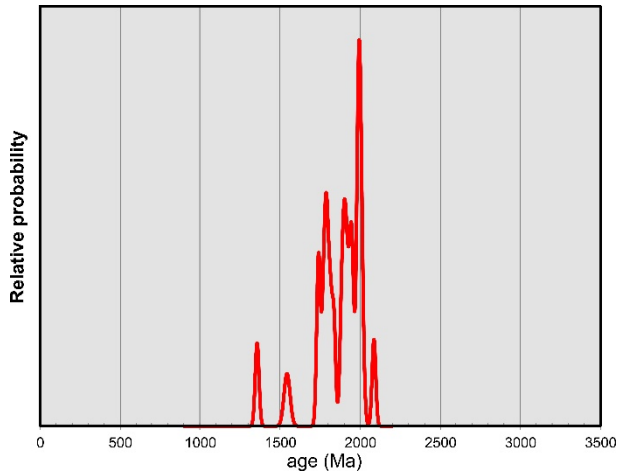


Detrital zircon age spectrum (n = 106) for the Vilch-4 sample.

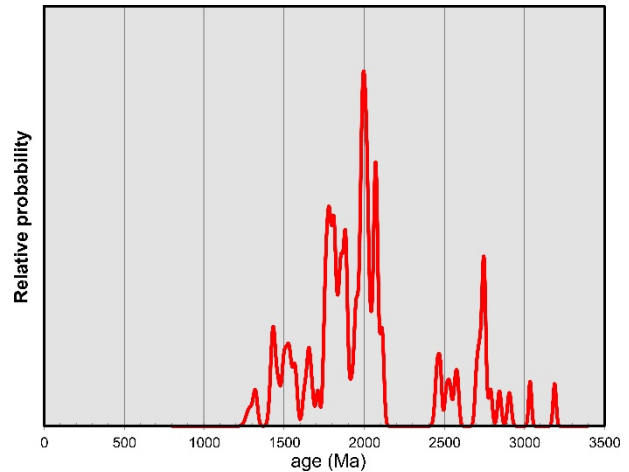


U-Pb isotopic data obtained from the detrital zircon population from the Vilch-4 sample.

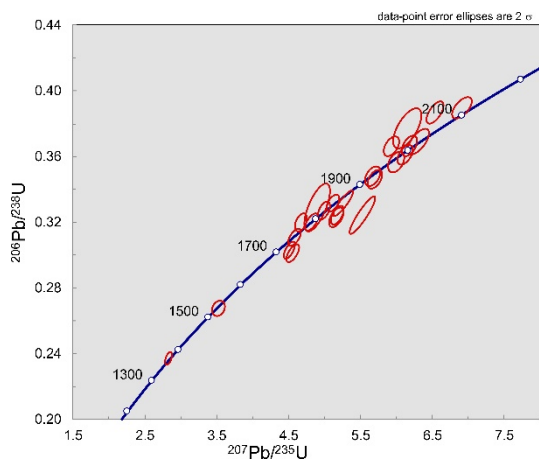
3. Quartz arenite Vilch-5B (Vilchitsy borehole, depth 728 m); Belarus Series, Orsha Suite



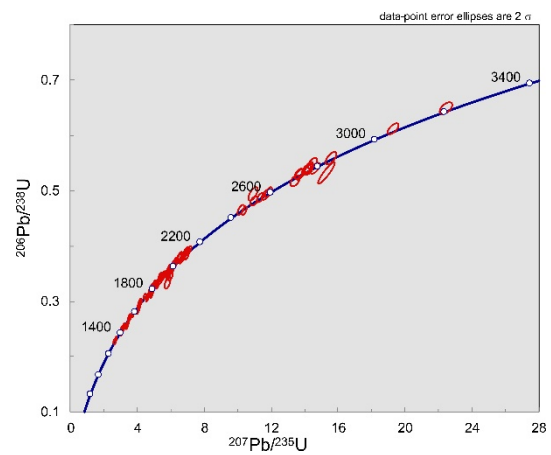
Detrital zircon age spectrum (n = 24) for the group A zircons from the Vilch-5B sample.



Detrital zircon age spectrum (n = 104) for the group B zircons from the Vilch-5B sample

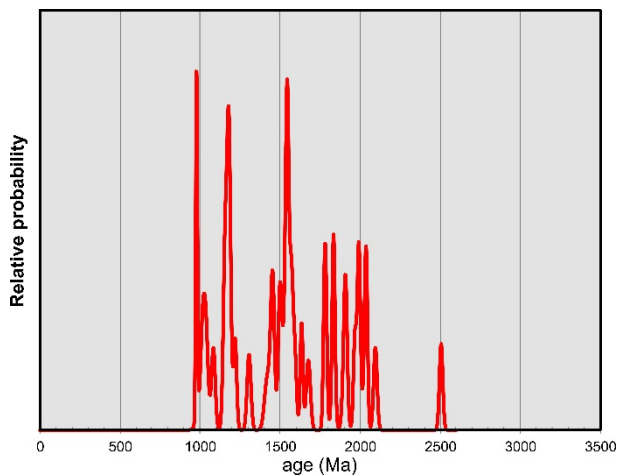


U-Pb isotopic data obtained from the detrital zircon population of the group A in the Vilch-5B sample.

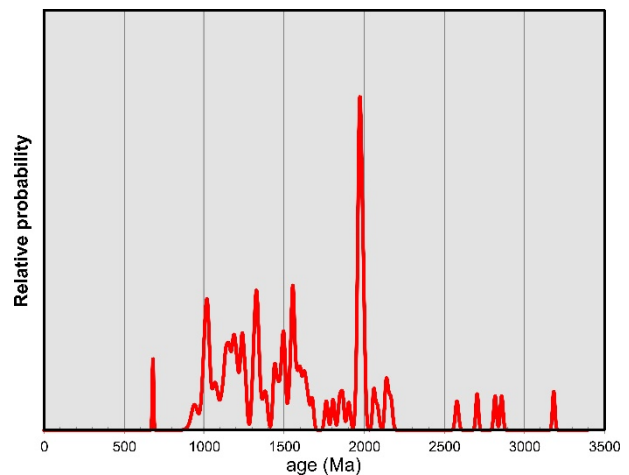


U-Pb isotopic data obtained from the detrital zircon population of the group B in the Vilch-5B sample.

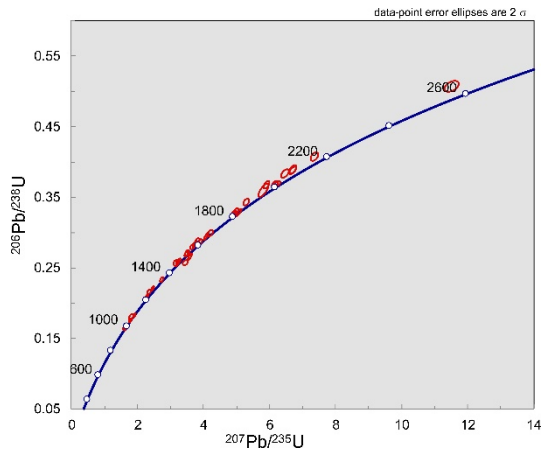
4. Tillite Vilch-6A (Vilchitsy borehole, depth 576.0 m); Vilchitsy Series, Glusk Suite



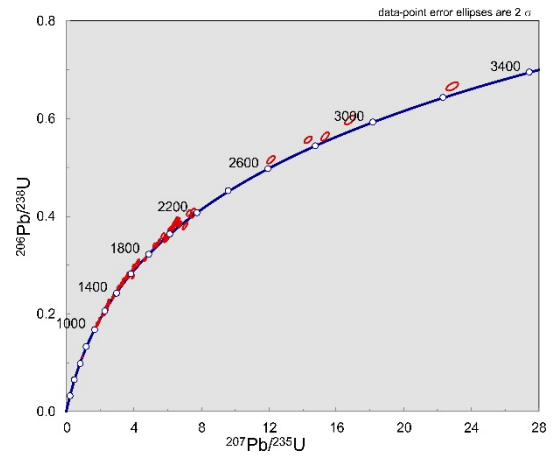
Detrital zircon age spectrum (n = 41) for the group A zircons from the Vilch-6A sample.



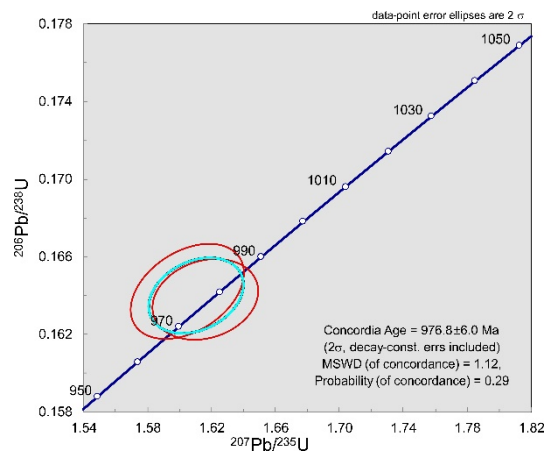
Detrital zircon age spectrum (n = 96) for the group B zircons from the Vilch-6A sample.



U-Pb isotopic data obtained from the detrital zircon population of the group A in the Vilch-6A sample.

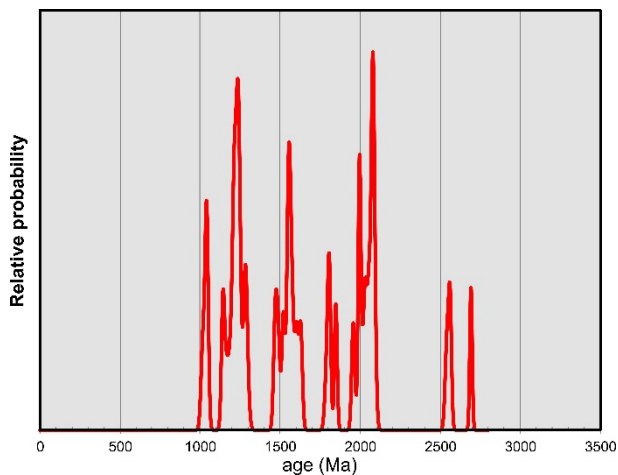


U-Pb isotopic data obtained from the detrital zircon population of the group B in the Vilch-6A sample.

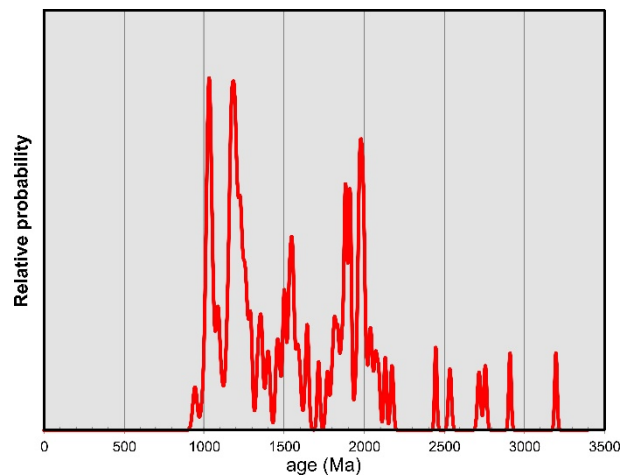


U-Pb isotopic data obtained from the youngest detrital zircons, constraining maximum depositional age for the Vilch-6A sample.

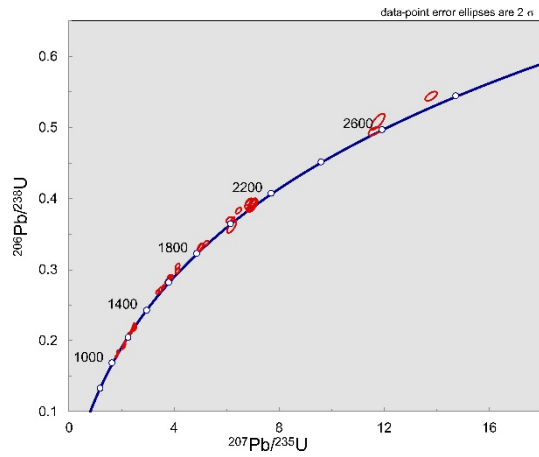
5. Tillite Vilch-7A (Vilchitsy borehole, depth 566.0 m); Vilchitsy Series, Glusk Suite



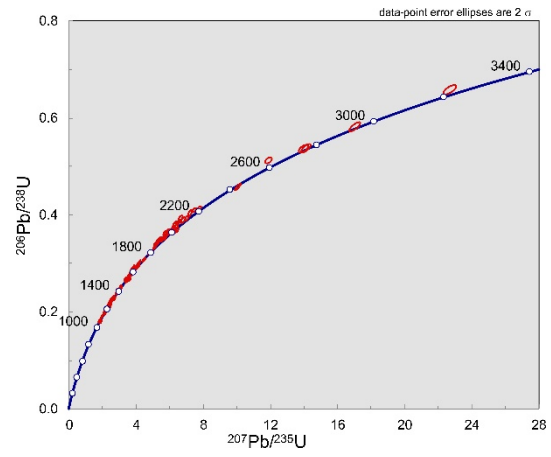
Detrital zircon age spectrum ($n = 39$) for the group A zircons from the Vilch-7A sample.



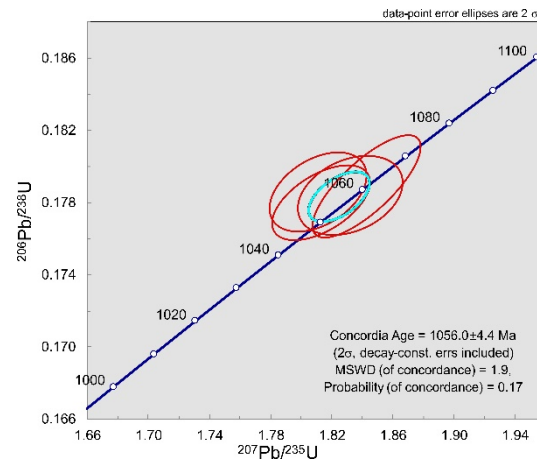
Detrital zircon age spectrum ($n = 96$) for the group B zircons from the Vilch-7A sample.



U-Pb isotopic data obtained from the detrital zircon population of the group A in the Vilch-7A sample.

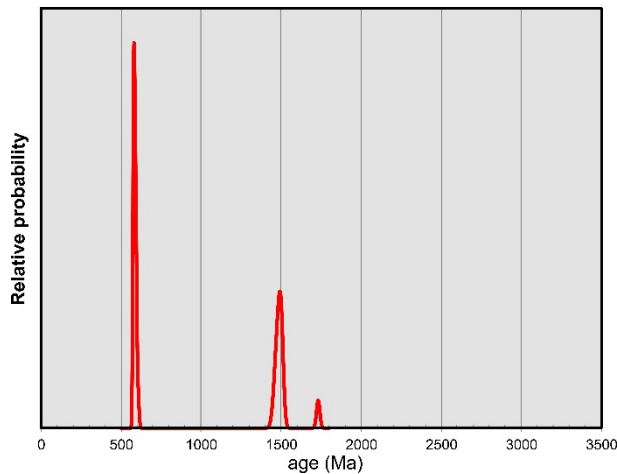


U-Pb isotopic data obtained from the detrital zircon population of the group B in the Vilch-7A sample.

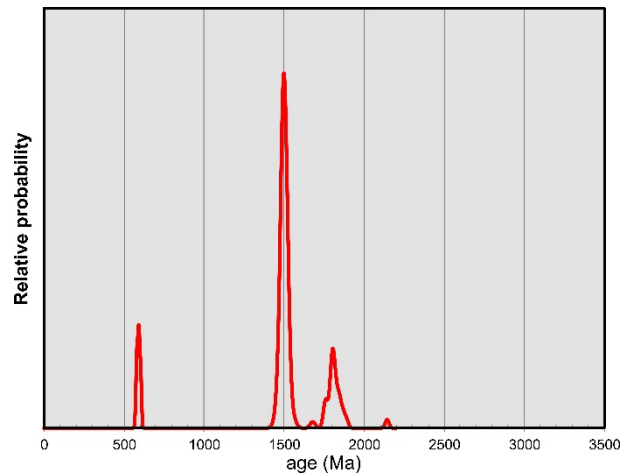


U-Pb isotopic data obtained from the youngest detrital zircons, constraining maximum depositional age for the Vilch-7A sample.

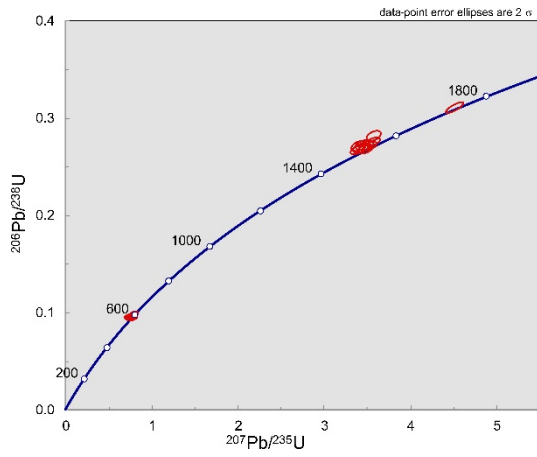
6. Sandy tuffite Pinsk-45A (Pinsk borehole, depth 668.5 m); Volyn Series, Rataychitsy Suite



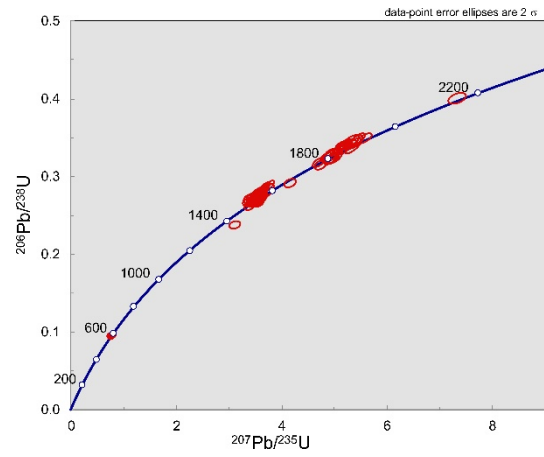
Detrital zircon age spectrum ($n = 12$) for the group A zircons from the Pinsk-45A sample.



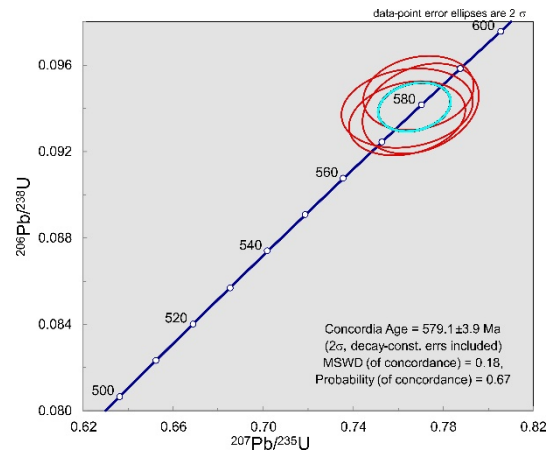
Detrital zircon age spectrum ($n = 117$) for the group B zircons from the Pinsk-45A sample.



U-Pb isotopic data obtained from the detrital zircon population of the group A in the Pinsk-45A sample.

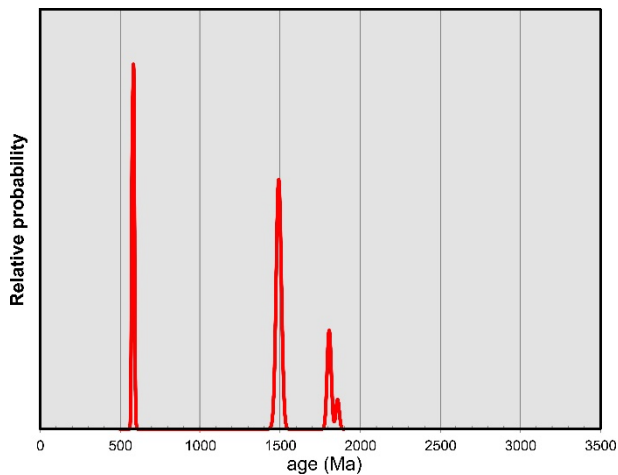


U-Pb isotopic data obtained from the detrital zircon population of the group B in the Pinsk-45A sample.

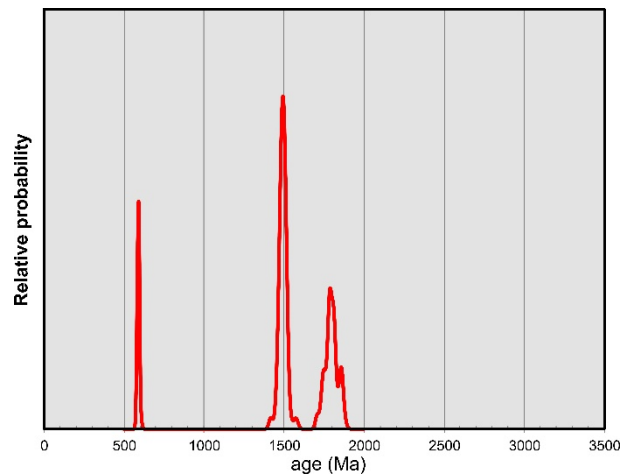


U-Pb isotopic data obtained from the youngest detrital zircons, constraining maximum depositional age for the Pinsk-45A sample.

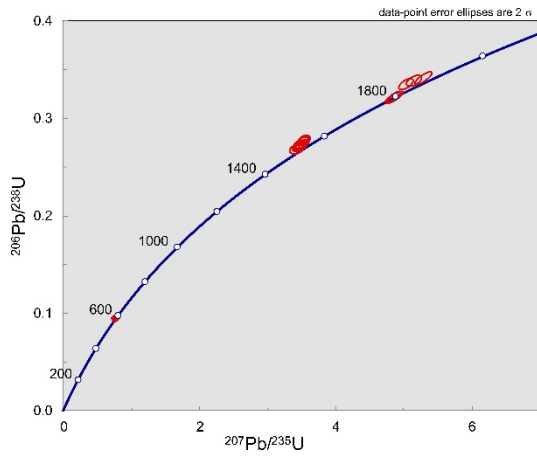
7. Tuffite Pinsk-46A (Pinsk borehole, depth 661 m); Volyn Series, Rataychitsy Suite



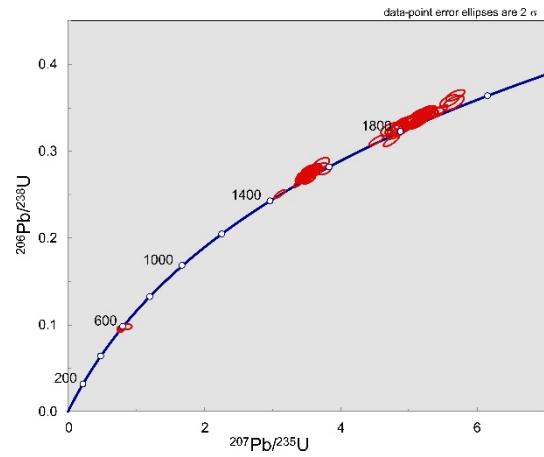
Detrital zircon age spectrum ($n = 27$) for the group A zircons from the Pinsk-46A sample.



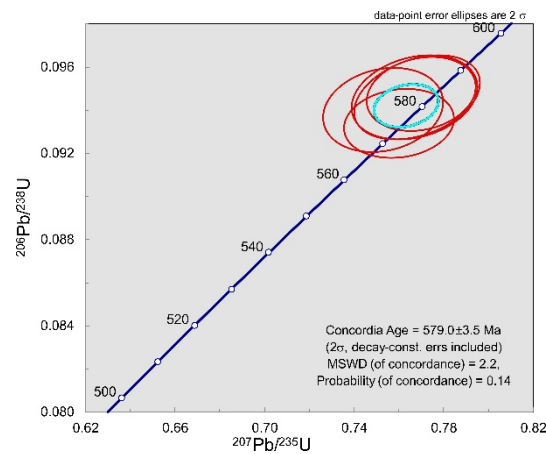
Detrital zircon age spectrum ($n = 111$) for the group B zircons from the Pinsk-46A sample.



U-Pb isotopic data obtained from the detrital zircon population of the group A in the Pinsk-46A sample.

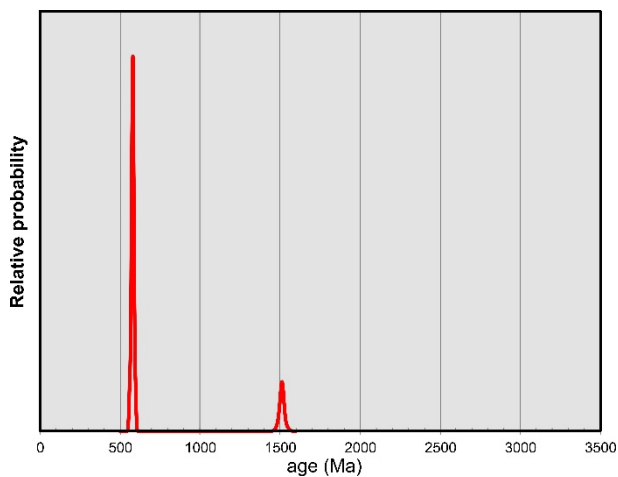


U-Pb isotopic data obtained from the detrital zircon population of the group B in the Pinsk-46A sample.

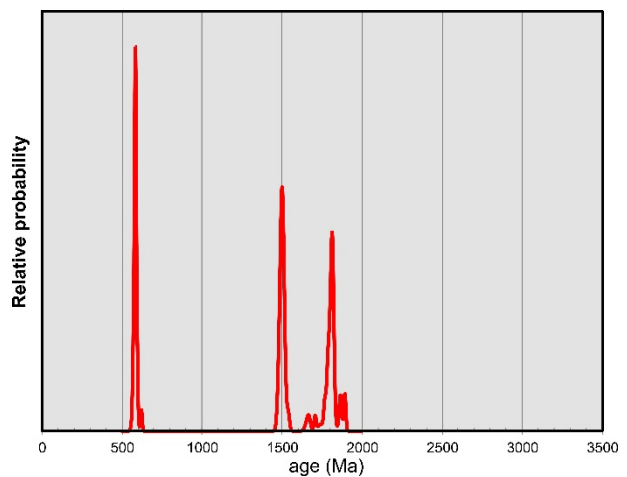


U-Pb isotopic data obtained from the youngest detrital zircons, constraining maximum depositional age for the Pinsk-46A.

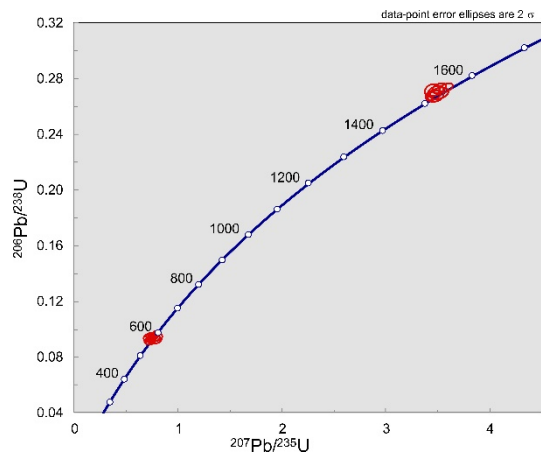
8. Volcanogenic sandstone Kob-10 (Kobryn borehole, depth 747 m); Volyn Series, Rataychitsy Suite



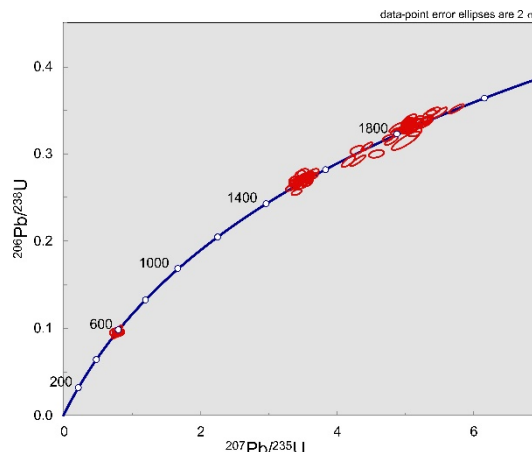
Detrital zircon age spectrum ($n = 37$) for the group A zircons from the Kob-10 sample.



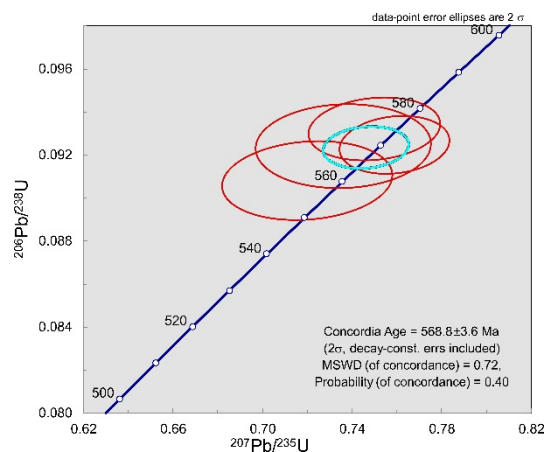
Detrital zircon age spectrum ($n = 99$) for the group B zircons from the Kob-10 sample.



U-Pb isotopic data obtained from the detrital zircon population of the group A in the Kob-10 sample.

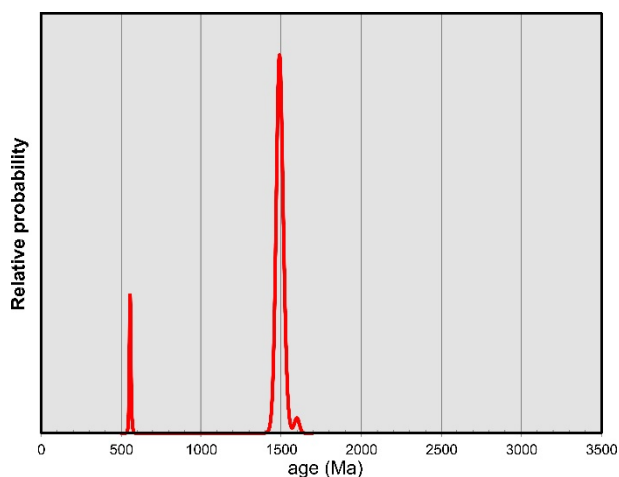


U-Pb isotopic data obtained from the detrital zircon population of the group B in the Kob-10 sample.

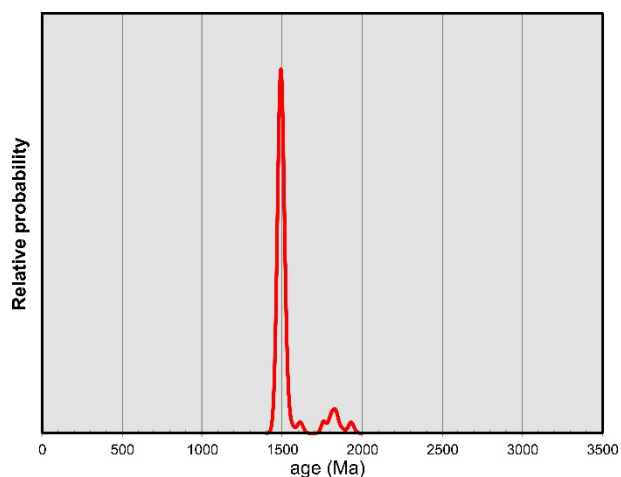


U-Pb isotopic data obtained from the youngest detrital zircons, constraining maximum depositional age for the Kob-10 sample.

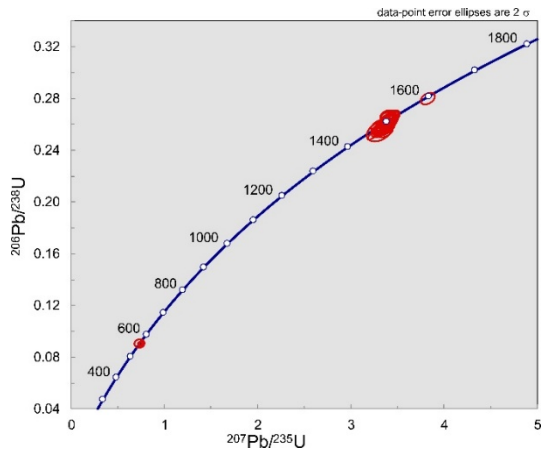
9. Soft brown tuff Kob-27A (Kobryn borehole, depth 598 m); Volyn Series, Girska Suite / Rataychitsy Suite



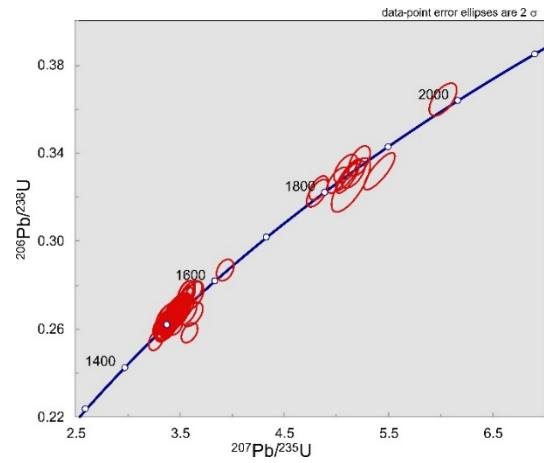
Detrital zircon age spectrum ($n = 40$) for the group A zircons from the Kob-27A sample.



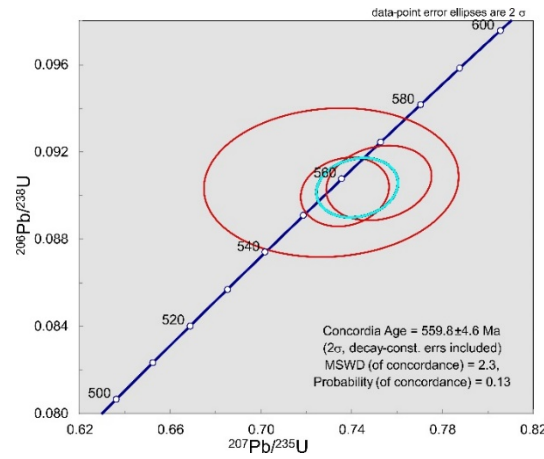
Detrital zircon age spectrum ($n = 99$) for the group B zircons from the Kob-27A sample.



U-Pb isotopic data obtained from the detrital zircon population of the group A in the Kob-27A sample.

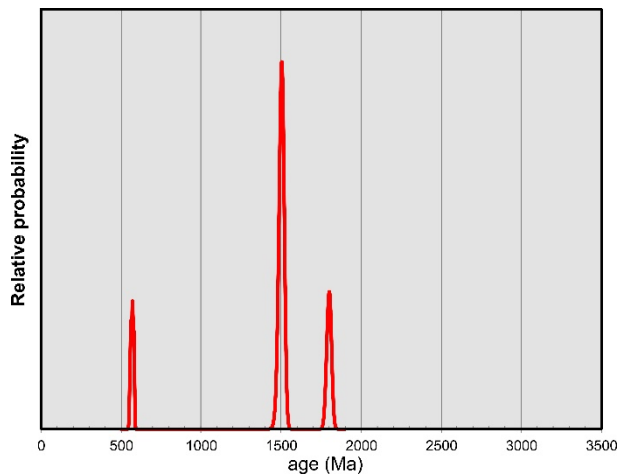


U-Pb isotopic data obtained from the detrital zircon population of the group B in the Kob-27A sample.

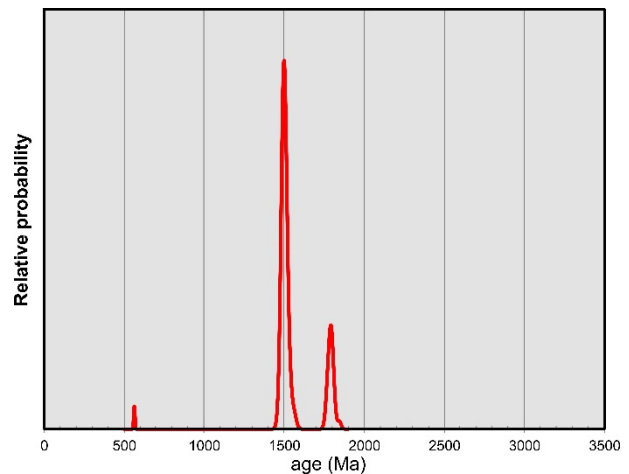


U-Pb isotopic data obtained from the youngest detrital zircons, constraining maximum depositional age for the Kob-27A sample.

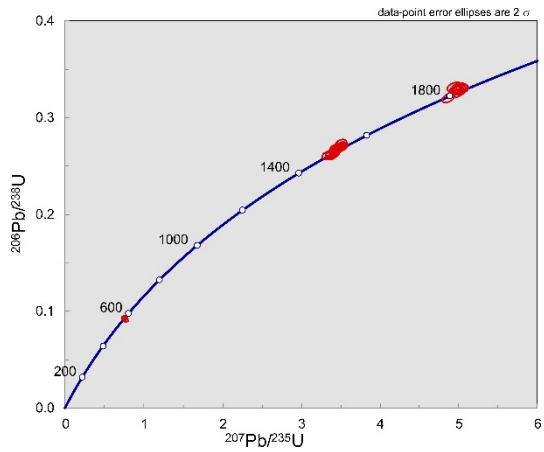
10. Arkose/wacke Kob-32A (Kobryn borehole, depth 540 m); Volyn Series, Girsk Suite



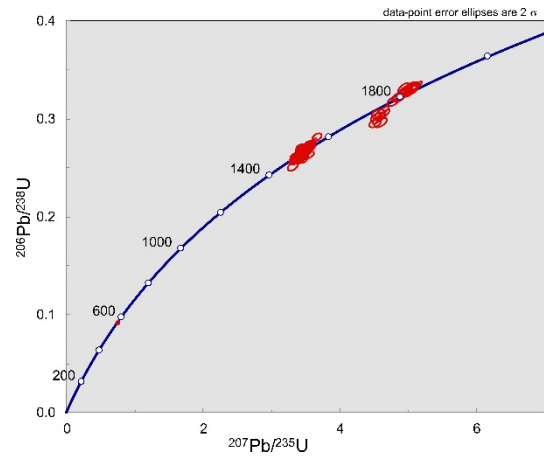
Detrital zircon age spectrum (n = 36) for the group A zircons from the Kob-32A sample.



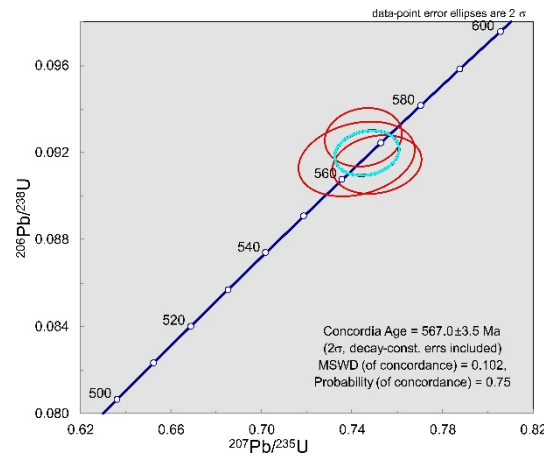
Detrital zircon age spectrum (n = 99) for the group B zircons from the Kob-32A sample.



U-Pb isotopic data obtained from the detrital zircon population of the group A in the Kob-32A sample.

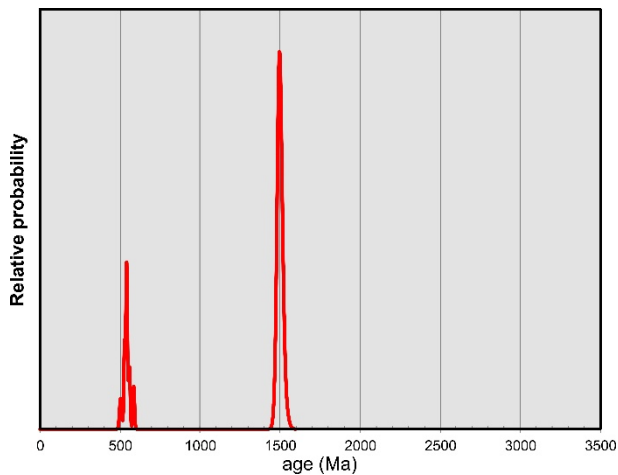


U-Pb isotopic data obtained from the detrital zircon population of the group B in the Kob-32A sample.

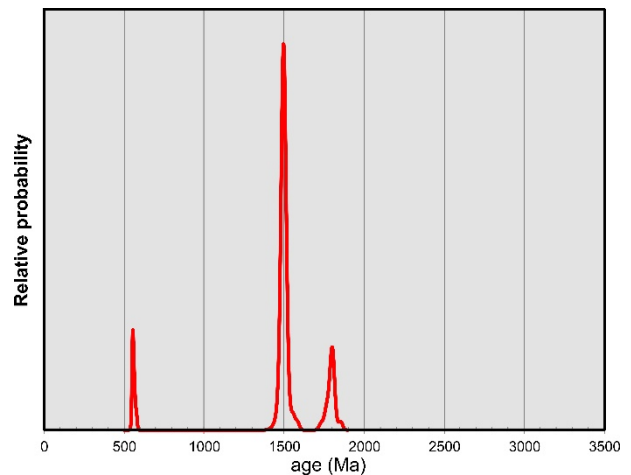


U-Pb isotopic data obtained from the youngest detrital zircons, constraining maximum depositional age for the Kob-32A sample.

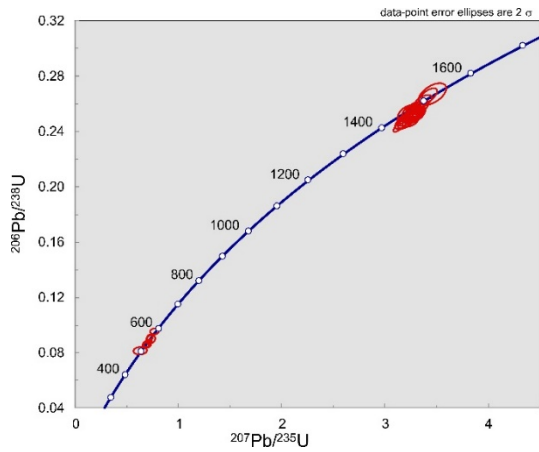
11. Tuff Kob-34A (Kobryn borehole, depth 517 m); Volyn Series, Girska Suite



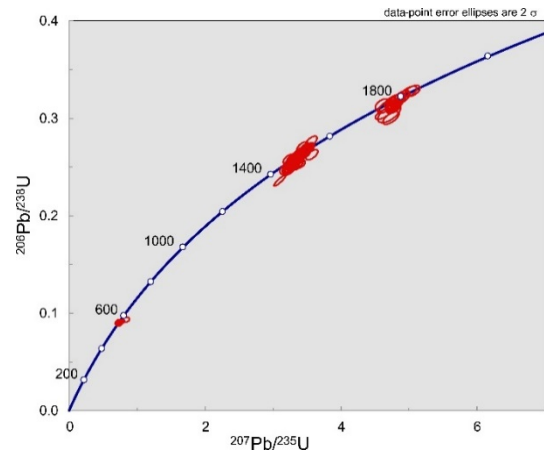
Detrital zircon age spectrum ($n = 39$) for the group A zircons from the Kob-34A sample.



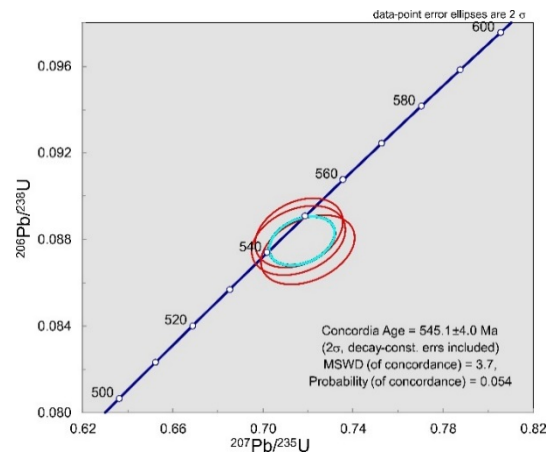
Detrital zircon age spectrum ($n = 97$) for the group B zircons from the Kob-34A sample.



U-Pb isotopic data obtained from the detrital zircon population of the group A in the Kob-34A sample.

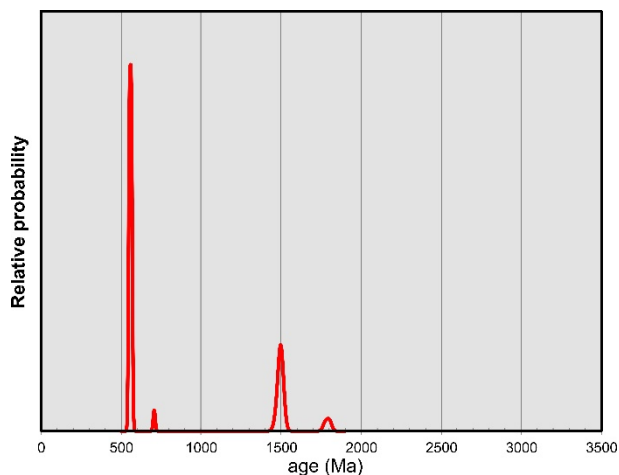


U-Pb isotopic data obtained from the detrital zircon population of the group B in the Kob-34A sample.

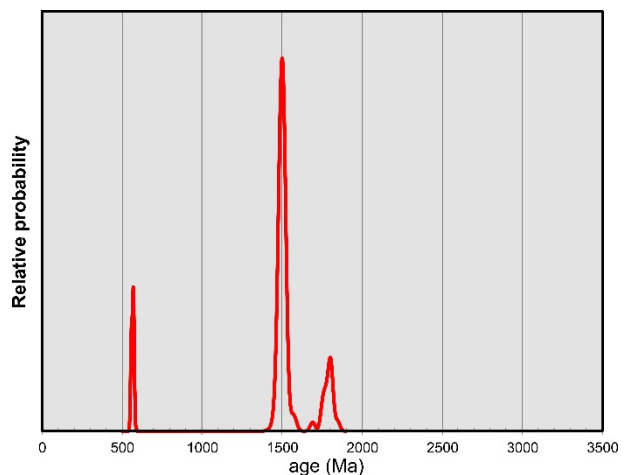


U-Pb isotopic data obtained from the youngest detrital zircons, constraining maximum depositional age for the Kob-34A sample.

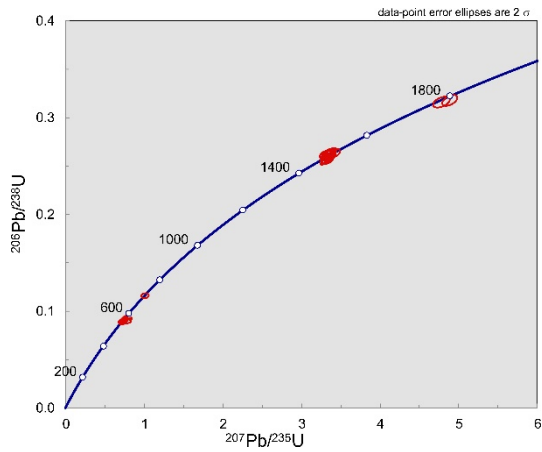
12. Arkose Kob-34B (Kobryn borehole, depth 517 m); Volyn Series, Girsk Suite



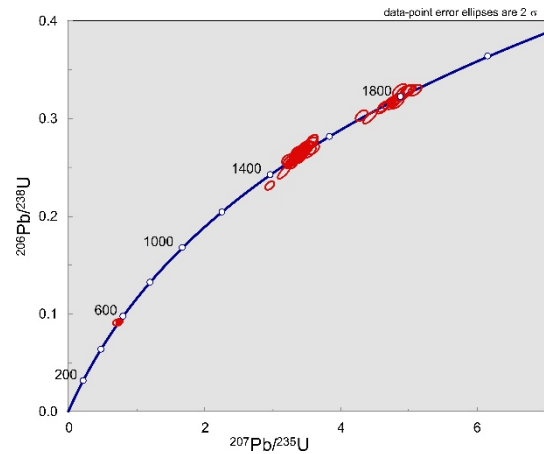
Detrital zircon age spectrum ($n = 41$) for the group A zircons from the Kob-34B sample.



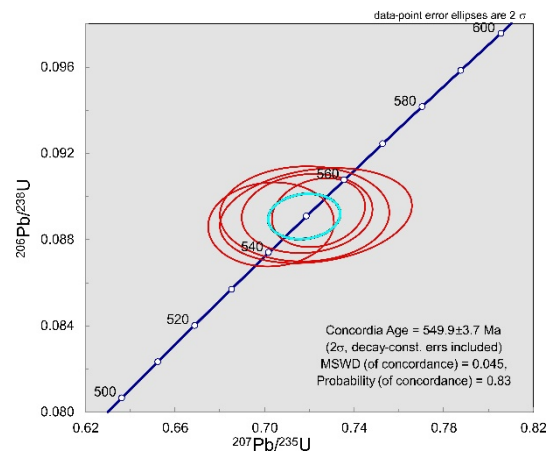
Detrital zircon age spectrum ($n = 86$) for the group B zircons from the Kob-34B sample.



U-Pb isotopic data obtained from the detrital zircon population of the group A in the Kob-34B sample.

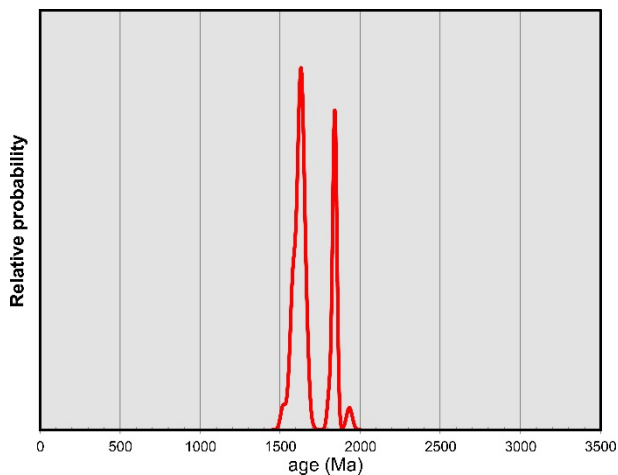


U-Pb isotopic data obtained from the detrital zircon population of the group B in the Kob-34B sample.

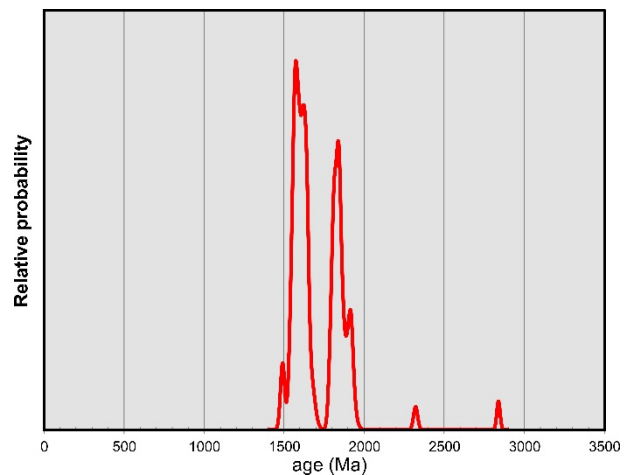


U-Pb isotopic data obtained from the youngest detrital zircons, constraining maximum depositional age for the Kob-34B sample.

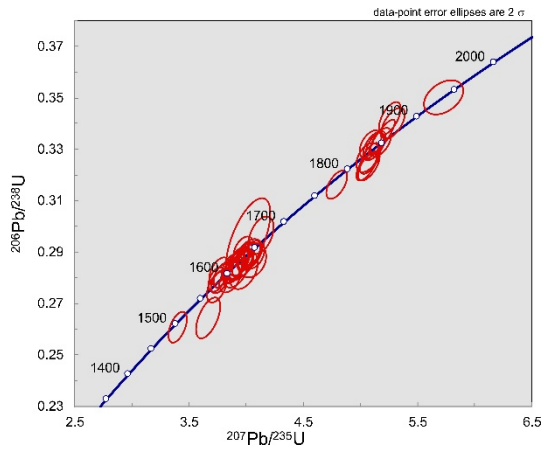
13. Quartz arenite/subarkose Bog-33A (Bogushevsk borehole, depth 685.3 m); Valdai Series, Nizov Suite.



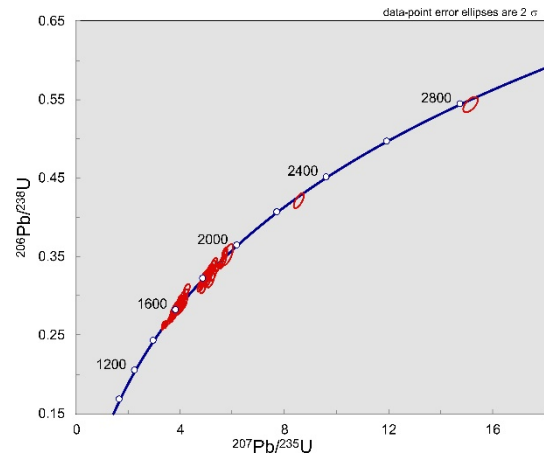
Detrital zircon age spectrum (n = 42) for the group A zircons from the Bog-33A sample.



Detrital zircon age spectrum (n = 93) for the group B zircons from the Bog-33A sample.

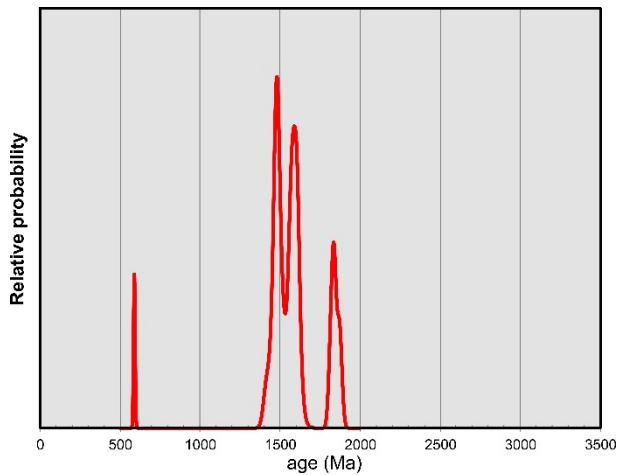


U-Pb isotopic data obtained from the detrital zircon population of the group A in the Bog-33A sample.

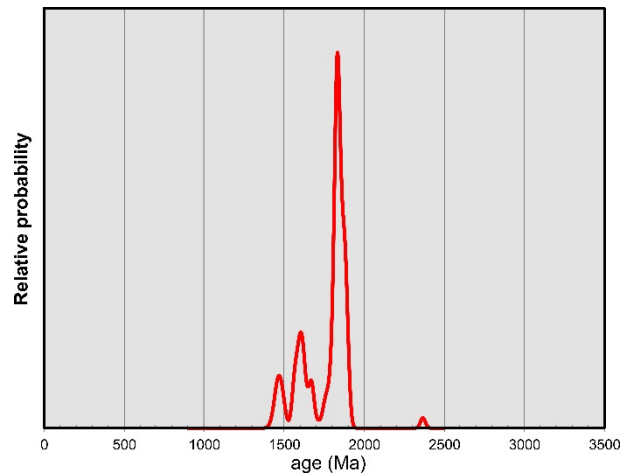


U-Pb isotopic data obtained from the detrital zircon population of the group B in the Bog-33A sample.

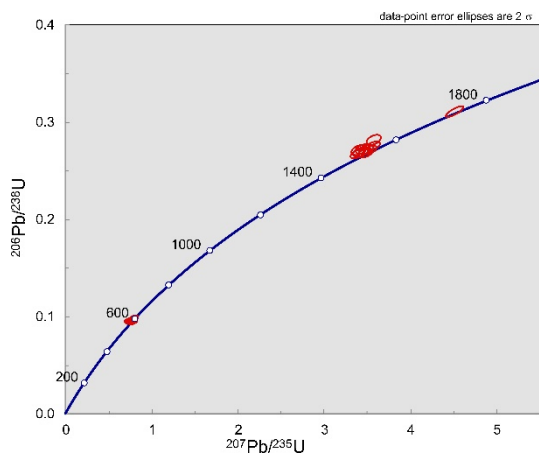
14. Arkose Lep-12A (Lepel borehole, depth 467 m); Valdai Series, Selsk Suite.



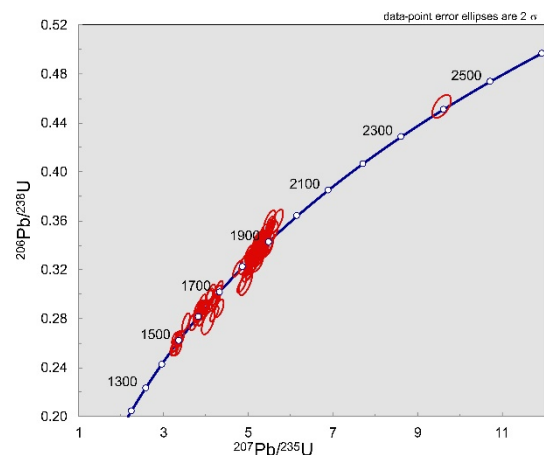
Detrital zircon age spectrum (n = 31) for the group A zircons from the Lep-12A sample.



Detrital zircon age spectrum (n = 105) for the group B zircons from the Lep-12A sample.

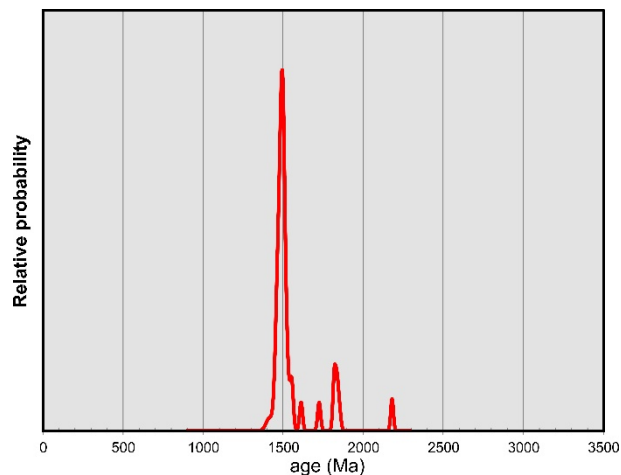


U-Pb isotopic data obtained from the detrital zircon population of the group A in the Lep-12A sample.

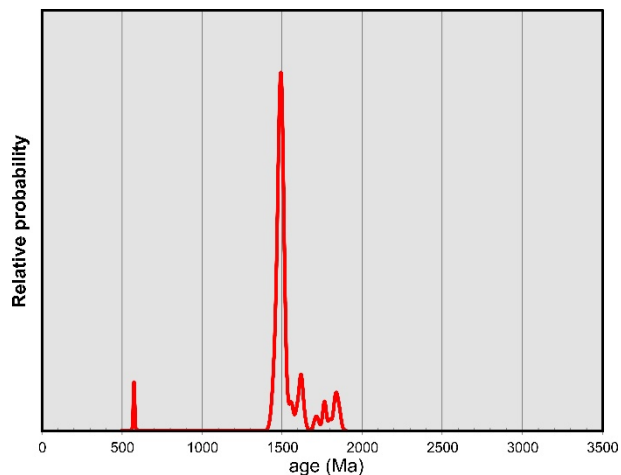


U-Pb isotopic data obtained from the detrital zircon population of the group B in the Lep-12A sample.

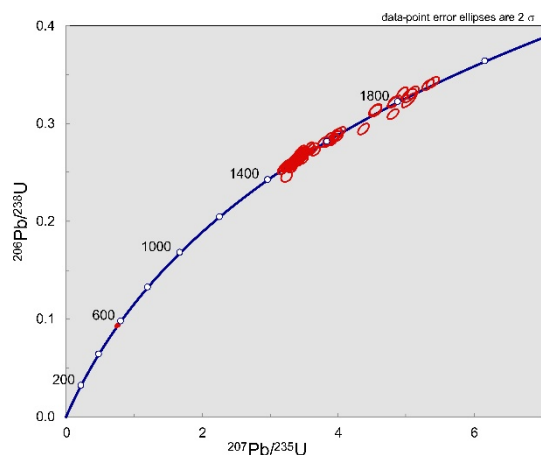
15. Arkose/wacke Bog-43A (Bogushevsk borehole, depth 608 m); Valdai Series, Tshernitse Suite.



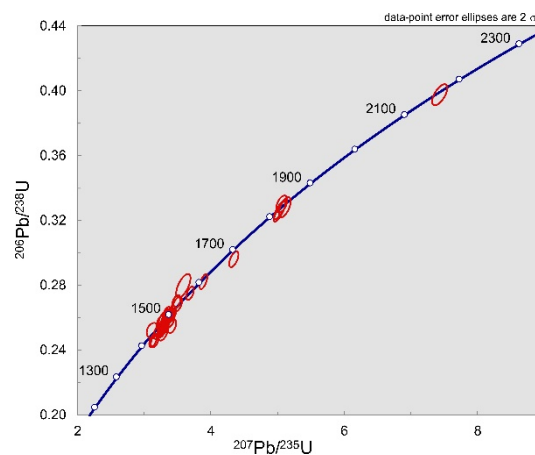
Detrital zircon age spectrum (n = 39) for the group A zircons from the Bog-43A sample.



Detrital zircon age spectrum (n = 96) for the group B zircons from the Bog-43A sample.

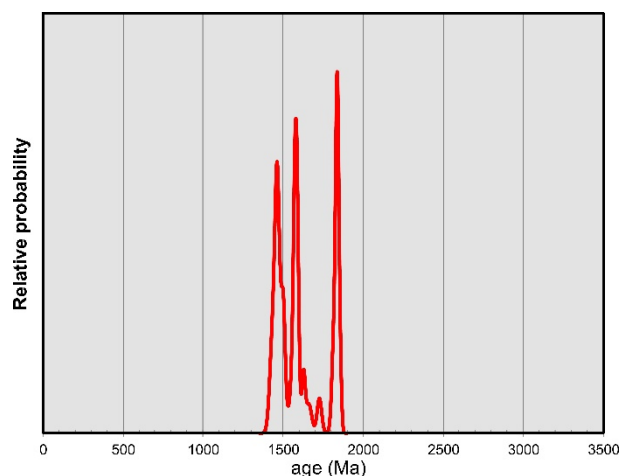


U-Pb isotopic data obtained from the detrital zircon population of the group A in the Bog-43A sample.

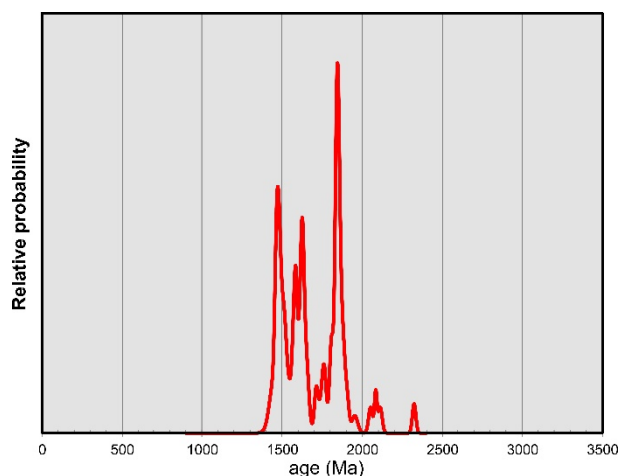


U-Pb isotopic data obtained from the detrital zircon population of the group B in the Bog-43A sample.

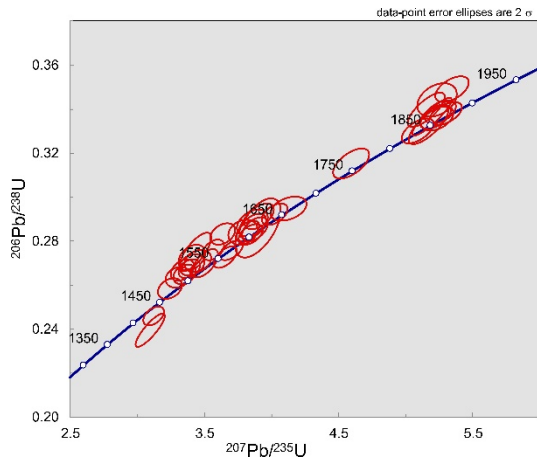
16. Subarkose Lep-20B (Lepel borehole, depth 418.2 m); Valdai Series, Tshernitse Suite.



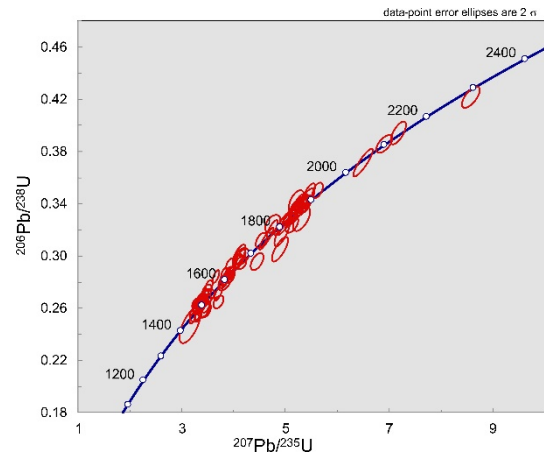
Detrital zircon age spectrum (n = 37) for the group A zircons from the Lep-20B sample.



Detrital zircon age spectrum (n = 74) for the group B zircons from the Lep-20B sample.

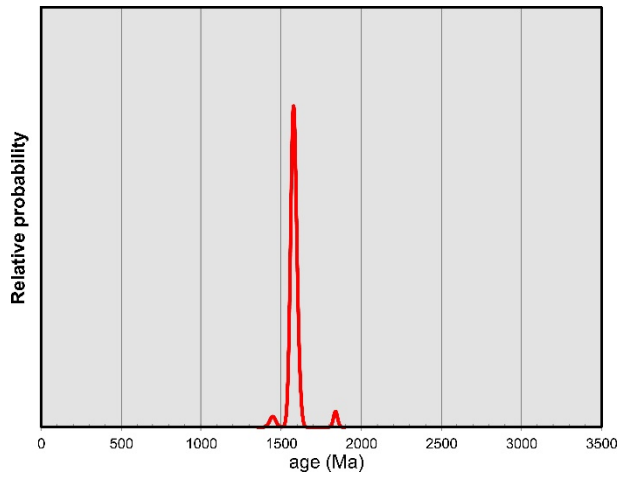


U-Pb isotopic data obtained from the detrital zircon population of the group A in the Lep-20B sample.

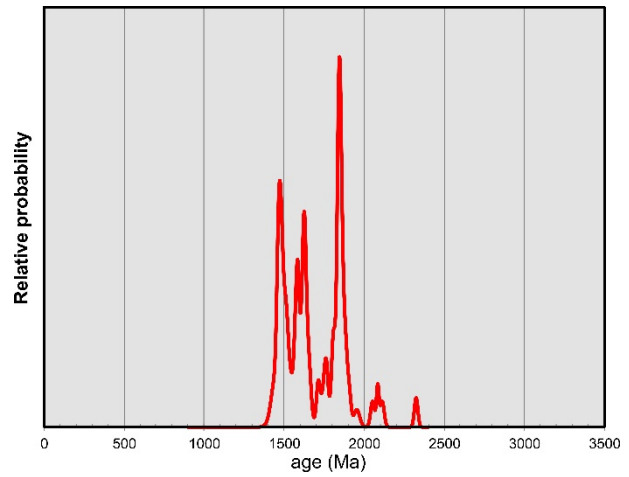


U-Pb isotopic data obtained from the detrital zircon population of the group B in the Lep-20B sample.

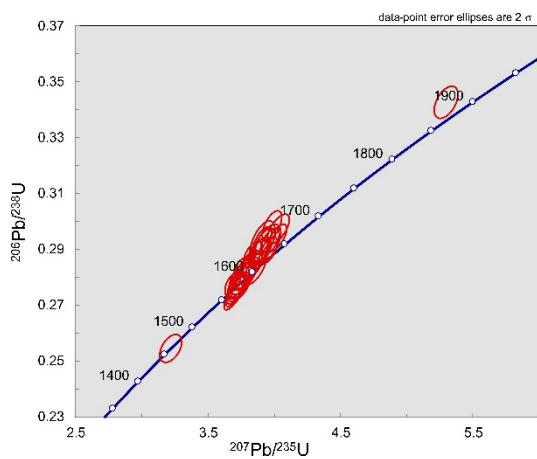
17. Arkosic sandstone Lep-28A (Lepel borehole, depth 370.5 m); Valdai Series, Kotlin Suite.



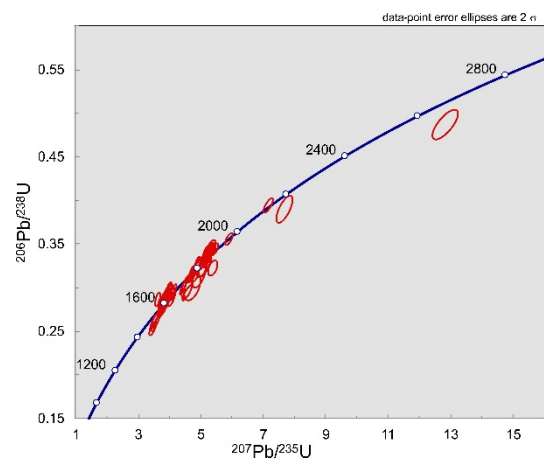
Detrital zircon age spectrum (n = 33) for the group A zircons from the Lep-28A sample.



Detrital zircon age spectrum (n = 96) for the group B zircons from the Lep-28A sample.

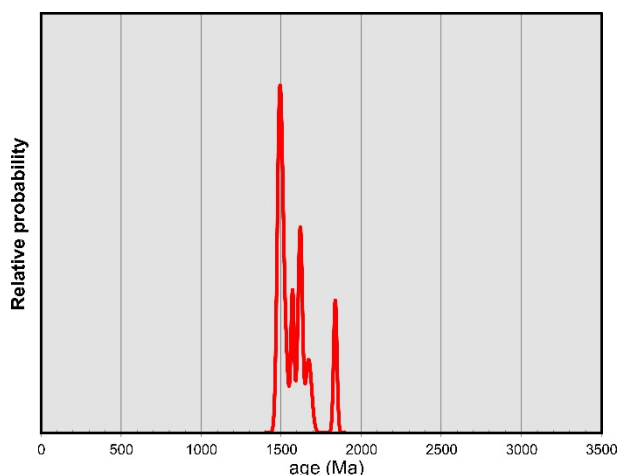


U-Pb isotopic data obtained from the detrital zircon population of the group A in the Lep-28A sample.

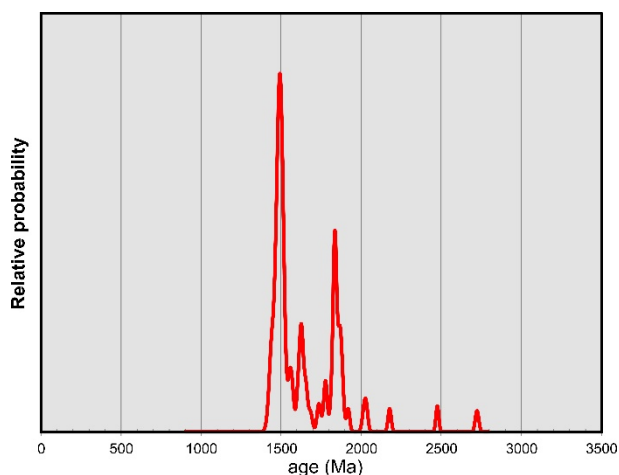


U-Pb isotopic data obtained from the detrital zircon population of the group B in the Lep-28A sample.

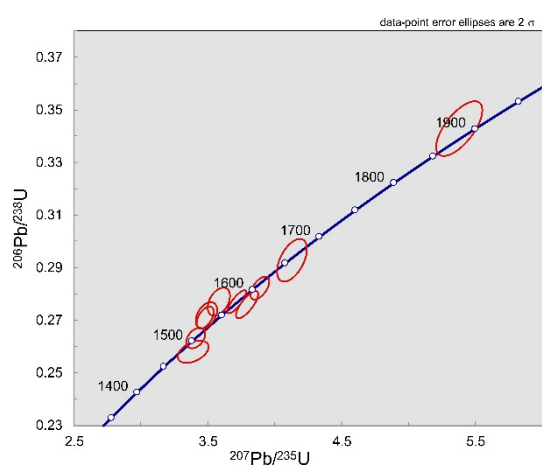
18. Arkose Bog-51A (Bogushevsk borehole, depth 519.5 m); Valdai Series, Kotlin Suite.



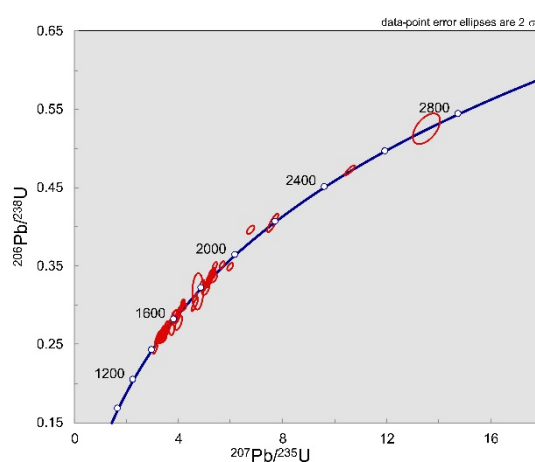
Detrital zircon age spectrum (n = 10) for the group A zircons from the Bog-51A sample.



Detrital zircon age spectrum (n = 80) for the group B zircons from the Bog-51A sample.

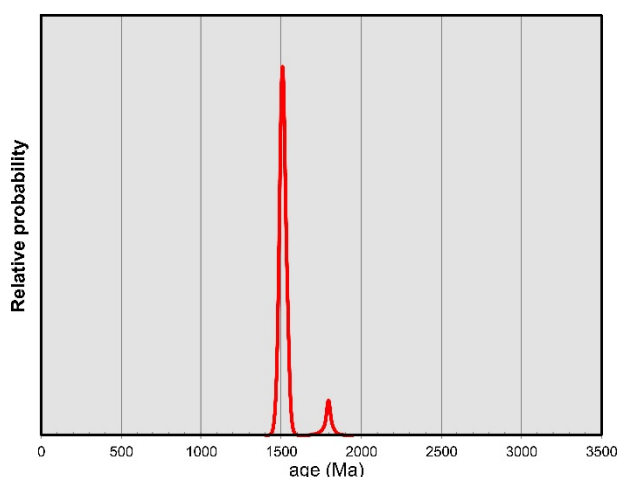


U-Pb isotopic data obtained from the detrital zircon population of the group A in the Bog-51A sample.

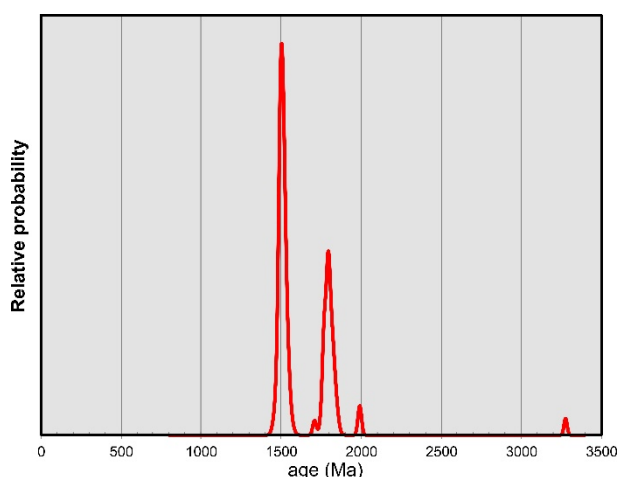


U-Pb isotopic data obtained from the detrital zircon population of the group B in the Bog-51A sample.

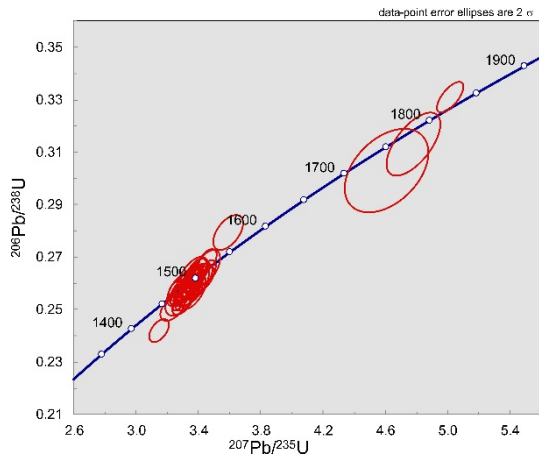
19. Subarkose Kob-40A (Kobryn borehole, depth 414 m); Valdai Series, Kotlin Suite.



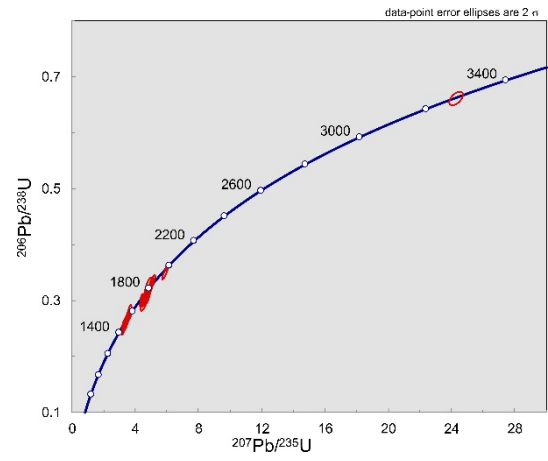
Detrital zircon age spectrum (n = 40) for the group A zircons from the Kob-40A sample.



Detrital zircon age spectrum (n = 84) for the group B zircons from the Kob-40A sample.

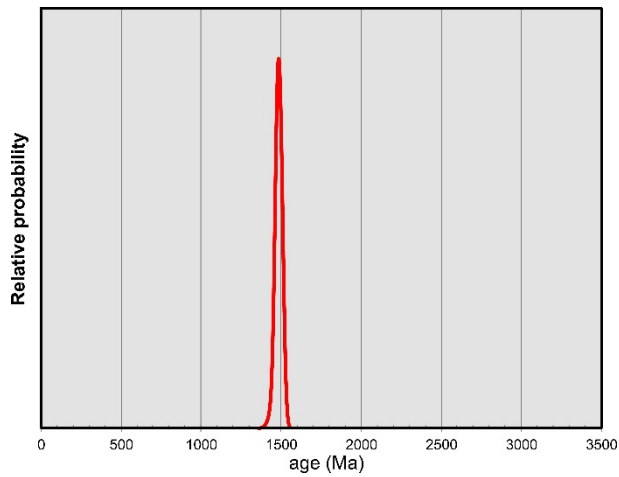


U-Pb isotopic data obtained from the detrital zircon population of the group A in the Kob-40A sample.

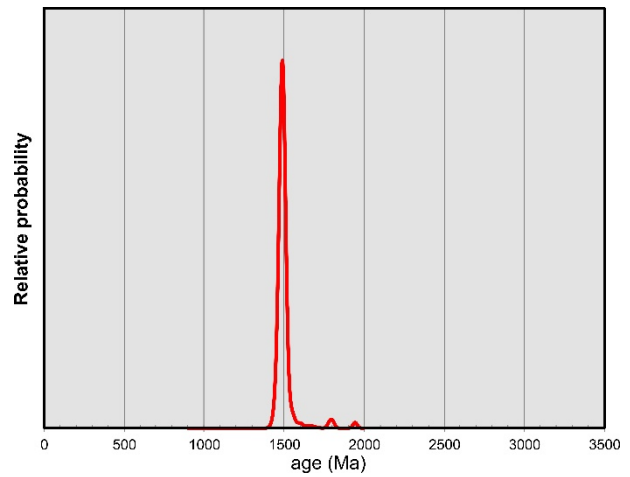


U-Pb isotopic data obtained from the detrital zircon population of the group B in the Kob-40A sample.

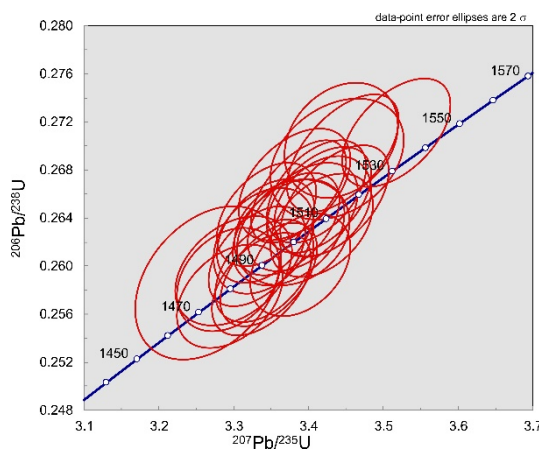
20. Glauconite-bearing quartz arenite Kob-54 (Kobryn borehole, depth 364 m), Early Cambrian



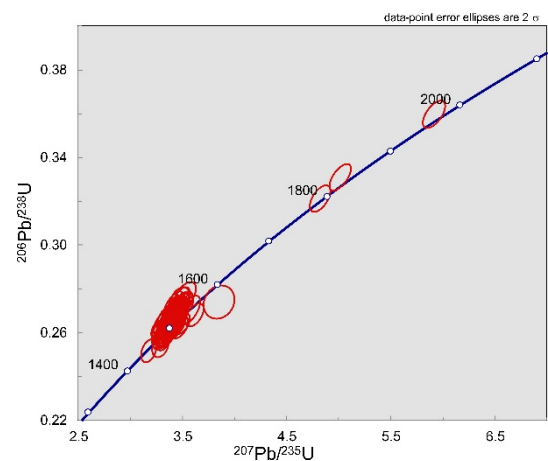
Detrital zircon age spectrum ($n = 27$) for the group A zircons from the Kob-54 sample.



Detrital zircon age spectrum ($n = 111$) for the group B zircons from the Kob-54 sample.

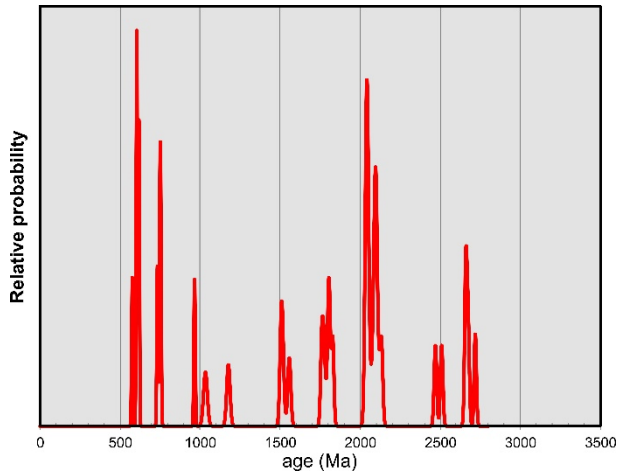


U-Pb isotopic data obtained from the detrital zircon population of the group A in the Kob-54 sample.

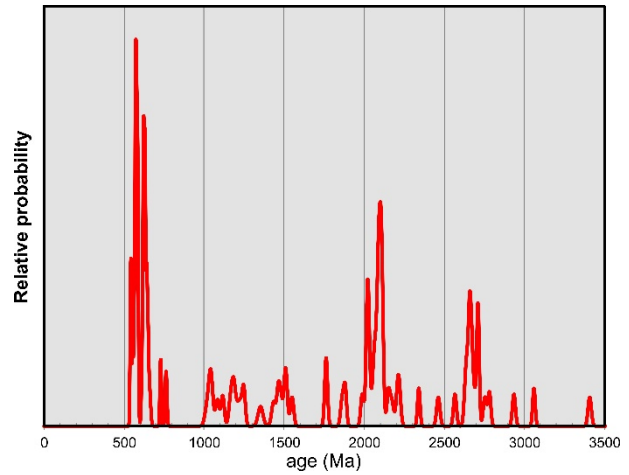


U-Pb isotopic data obtained from the detrital zircon population of the group B in the Kob-54 sample.

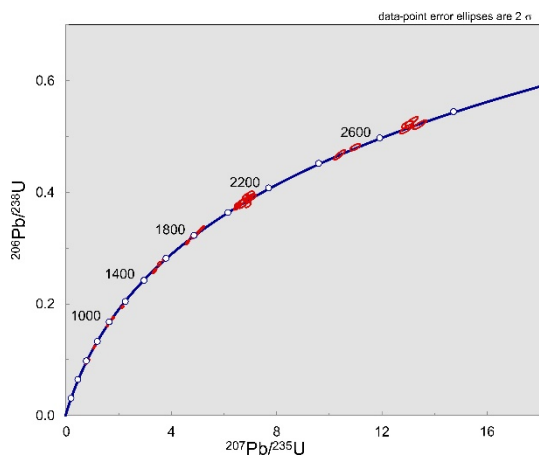
21. Coarse-grained sandstone Kob-57 (Kobryn borehole, depth 249.5 m), Early Cambrian



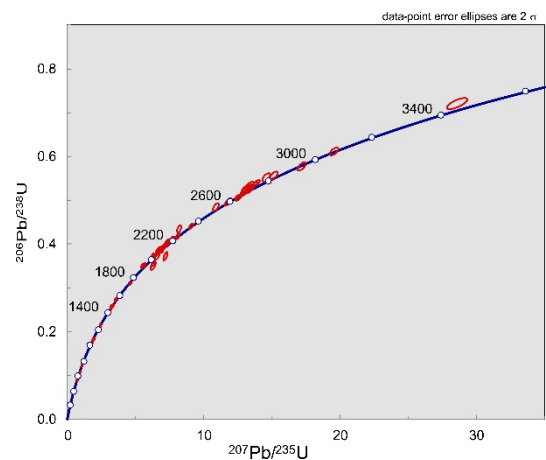
Detrital zircon age spectrum (n = 37) for the group A zircons from the Kob-57 sample.



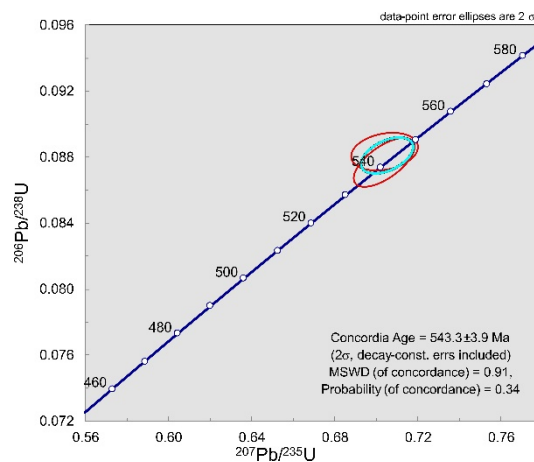
Detrital zircon age spectrum (n = 92) for the group B zircons from the Kob-57 sample.



U-Pb isotopic data obtained from the detrital zircon population of the group A in the Kob-57 sample.



U-Pb isotopic data obtained from the detrital zircon population of the group B in the Kob-57 sample.



U-Pb isotopic data obtained from the youngest detrital zircons, constraining maximum depositional age for the Kob-57 sample.